

**FLOOD MITIGATION MODELLING IN THE RIVER NZOIA BASIN
THROUGH STORAGE RESERVOIRS**

RICHARD RUTTO

Grad. Eng., B.Sc (Hons.) AGEN (Egerton University)

**A Thesis Submitted in Partial Fulfilment of the Requirements of Master of
Science in Water Engineering of the Department of Civil and Structural
Engineering, School of Engineering of Moi University**

2013

DECLARATION

DECLARATION BY THE CANDIDATE

This thesis is my own original work and has not been presented for a degree in any other University. No part of this thesis may be reproduced without the prior written permission of the author and /or Moi University.

.....

.....

Richard Rutto (TEC/PGCS/02/08)

Date

DECLARATION BY THE SUPERVISORS

This thesis has been submitted for examination with our approval as University supervisors.

.....

.....

Dr. Joel K. Kibiiy,

Date

Department of Civil and Structural Engineering,

Moi University,

.....

.....

Eng. Prof. Stanley M. Shitote,

Date

Department of Civil and Structural Engineering,

Moi University.

.....

.....

Prof. Patrick Willems,

Date

Department of Civil and Structural Engineering,

Katholieke University-Leuven, Belgium.

ABSTRACT

Nzoia River in Western Kenya is prone to frequent floods particularly in the flood plains of Budalangi. These floods result in displacement of people and destruction of property. The implementation of flood control works through the rehabilitation of dykes and river training has remained a challenge because these dykes are constantly breached due to inadequate capacity of the river channel to contain high flows. To mitigate this problem three dams have been proposed: Anyiko/Rambula (42A), Rongai (34B) and Kipkaren (35). The aim of this study was to evaluate the effectiveness of the proposed reservoirs as a flood mitigation measure in the Nzoia River basin using MIKE 11 model. MIKE 11 is a software package for simulation of one dimensional fully dynamic wave flow in rivers. It has the ability to simulate different flood mitigation scenarios before and after dam construction. The overall methodology involved rainfall-runoff modelling for each of the reservoir catchments using NAM module in MIKE 11, and MIKE 11 HD model for river flow simulation. Good results, with a coefficient of determination above 0.85, were obtained for both calibration and verification. The calibrated model was evaluated on its ability to predict extreme events, and the performance was satisfactory based on graphical probability plots. In order to quantify the flood magnitude for each return period for the scenarios with and without reservoirs, flood frequency analysis was undertaken. In the scenario investigation, the reservoirs were analyzed individually and the flood effect based on the dam implemented was evaluated at Rwambwa (1EF01), a downstream river gauging station. With the implementation of dam 42A, 34B and 35 the simulated peak flows were $320\text{m}^3/\text{s}$, $491\text{m}^3/\text{s}$ and $601\text{m}^3/\text{s}$ respectively. Based on flood thresholds of $298\text{m}^3/\text{s}$ and $568\text{m}^3/\text{s}$ for overtopping the river banks and the dykes respectively, it was evident that even after flood regulation, dam 35 was least effective in controlling the floods. The flood peak from dam 42A will overtop the river bank but is not sufficient to overtop the dykes. From the flood frequency analysis it was observed that implementation of the individual dams reduced the incidence of flooding significantly. The return period of the dyke crest level flood improved from 1.7 years for no dam to 13 years when either dam 35 or 34B was implemented, but increased to 31 years when dam 42A was implemented. Among the proposed dams, dam 42A was found to be more effective in flood mitigation. It is recommended that it is constructed with gates to control the outflow from the reservoir.

TABLE OF CONTENTS

DECLARATION.....	i
ABSTRACT.....	ii
LIST OF TABLES.....	vii
LIST OF FIGURES.....	viii
LIST OF NOTATIONS.....	xiii
LIST OF ABBREVIATIONS AND ACRONYMS.....	xiv
ACKNOWLEDGEMENT.....	xvi
DEDICATION.....	xvii
CHAPTER ONE.....	1
INTRODUCTION.....	1
1.1 BACKGROUND OF STUDY.....	1
1.2 SIGNIFICANCE AND JUSTIFICATION OF THE STUDY.....	2
1.3 STATEMENT OF THE PROBLEM.....	2
1.4 RESEARCH OBJECTIVES.....	3
1.4.1 The Main Objective.....	3
1.4.2 The Specific Objectives.....	3
1.5 STUDY AREA.....	4
1.5.1 The Hydrology of River Nzoia Basin.....	4
1.5.2 History of Budalangi Floods and Dykes.....	5
CHAPTER TWO.....	7
LITERATURE REVIEW.....	7
2.0 INTRODUCTION.....	7
2.1 FLOOD MITIGATION RESERVOIRS.....	8
2.2 RESERVOIR STORAGE ZONES.....	9
2.2.1 Ideal Reservoir Operation for Flood Control.....	10
2.2.2 Operation of a Multipurpose Reservoir System.....	12
2.3 FLOOD MODELLING: NEED FOR MODELLING FLOODS.....	13
2.4 MIKE 11 MODEL.....	14
2.4.1 Solution Scheme.....	16
2.4.2 Courant Condition.....	18
2.5 NAM MODEL.....	19
2.5.1 Model Structure.....	20
2.5.2 Basic NAM Modelling Components.....	21
2.6 HYDROLOGICAL TIME SERIES ANALYSIS.....	26
2.6.1 Subflow Separation and Filtering.....	27

2.6.2 Selection of Peak-Over-Threshold (POT) In the Discharge Series.....	29
2.6.3 Extreme Value Analysis.....	30
2.6.4 The Return Period for the Extreme Events.....	32
2.7 HYDROLOGICAL AND METEOROLOGICAL DATA.....	33
2.7.1 Errors in hydrological/ meteorological data.....	33
2.7.2 Data Quality Control.....	34
2.7.3 Determination of Areal Rainfall.....	35
2.8 ASSESSMENT OF MODEL PERFORMANCE.....	37
2.8.1 The Coefficient of Determination (R^2).....	37
2.8.2 Mean Error (ME).....	38
2.8.3 Root Mean Square Error (RMSE).....	39
2.8.4 Squared Standard Deviation of Model Residuals.....	39
2.8.5 Bias of Residuals.....	39
2.8.6 Graphical Goodness-of-Fit Plots.....	40
2.8.7 Model Calibration.....	41
2.8.8 Model Verification/Validation.....	41
CHAPTER THREE.....	43
MATERIALS AND METHODS.....	43
3.1 INTRODUCTION.....	43
3.2 DATA COLLECTION.....	43
3.2.1 Weather Data.....	43
3.2.2 Stream Flow Data.....	44
3.2.3 Proposed Reservoirs.....	45
3.3 DATA PROCESSING AND QUALITY CONTROL.....	45
3.3.1 Filling Data Gaps.....	46
3.3.2 Density of Rain Gauges.....	47
3.3.3 Consistency of Rainfall Data.....	49
3.3.4 Catchment Delineation.....	49
3.3.5 Computation of Mean Areal Rainfall (MAR).....	51
3.4 SET-UP OF THE NAM MODULE.....	52
3.4.1 NAM Models for the Sub-Basins.....	52
3.4.2 NAM Calibration.....	53
3.4.3 NAM Validation/Verification.....	56
3.5 SET-UP OF MIKE 11 HYDRODYNAMIC MODEL.....	57
3.5.1 Network Setup.....	58
3.5.2 Boundary Conditions.....	59

3.5.3 Hydrodynamic Modelling.....	61
3.5.4 Simulation.....	62
3.5.5 MIKE 11 Model Calibrations and Validation.....	63
3.6 MODEL PERFORMANCE EVALUATION.....	63
3.6.1 Extreme Value Analysis.....	63
3.7 SCENARIO ANALYSIS.....	65
3.7.1 Simulation of Model with Reservoirs.....	65
3.7.2 Reservoir Flood Mitigation Analysis.....	66
CHAPTER FOUR.....	68
RESULTS AND DISCUSSION.....	68
4.1 INTRODUCTION.....	68
4.2 RAINFALL-RUNOFF MODELLING.....	68
4.2.1 Mean Areal Rainfall (MAR) Estimation.....	69
4.2.2 Subflow Separation of Observed River Flow.....	70
4.2.3 Calibration and Validation of NAM Model.....	73
4.3. MIKE 11 MODEL RESULTS: HYDRAULIC MODELLING.....	80
4.3.1 Definition of the River Network.....	80
4.3.2 Model Calibration.....	82
4.3.3 MIKE 11 Model Validation.....	84
4.3.4 MIKE 11 Simulation Results.....	88
4.4 FLOOD MITIGATION THROUGH THE RESERVOIRS.....	89
4.4.1 Flow Regulation at the Reservoirs for Flood Control.....	90
4.4.2 Comparison of the Two Scenarios (With and Without Reservoirs).....	96
4.5 HIGH FLOW FREQUENCY ANALYSIS.....	98
4.5.1. Peak-Over-Threshold Selection.....	99
4.5.2 Extreme Value Analysis.....	102
CHAPTER FIVE.....	109
CONCLUSIONS AND RECOMMENDATIONS.....	109
5.1. CONCLUSIONS.....	109
5.2. RECOMMENDATIONS.....	110
REFERENCES.....	112
APPENDICES.....	117
APPENDIX A: WEATHER DATA AND RESERVOIR PARAMETERS.....	117
APPENDIX B: THIESSEN POLYGON WEIGHTS.....	120
APPENDIX C: NAM CALIBRATION AND VALIDATION.....	125
APPENDIX D: LOCATION OF THE PROPOSED RESERVOIRS.....	128

<i>APPENDIX E: PEAK-OVER – THRESHOLDS</i>	130
<i>APPENDIX F: RESERVOIR FLOWS EXTREME VALUE ANALYSIS</i>	134
<i>APPENDIX G: RETURN PERIOD</i>	140

LIST OF TABLES

Table 3.1: Flood Threshold water levels and discharges at Rwambwa	<u>62</u>
Table 4.1: Thiessen polygon weights for Kipkaren sub basin	<u>65</u>
Table 4.2: Summary of Subflow separation results	<u>67</u>
Table 4.3: Calibrated NAM parameters	<u>70</u>
Table 4.4: The hydrodynamic variables involved in the model setup	<u>78</u>
Table 4.5: Excel Logical statement for flow regulation at dam 42A, 34B and 35	<u>87</u>
Table 4.6: Peak flow selection Parameters for the independency criterion	<u>94</u>
Table 4. 7: Theoretical Extreme value distribution parameters	<u>102</u>
Table 4.8: Summary of recurrence interval for the flood threshold levels	<u>103</u>
Table A 1: Nzoia catchment rain gauging stations and their coordinates	<u>111</u>
<i>Table A 2: Evaporation data for Nzoia weather stations</i>	<u>112</u>
Table A 3: Stream flow data (RGS) in the Nzoia basin	<u>112</u>
Table A 4: Elevation–Area–Volume Relationships of the 3 Dam Sites	<u>112</u>
Table B 1: Thiessen polygon weights for Webuye (Sub basin C)	<u>114</u>
Table B 2: Thiessen polygon weights for Nzoia Market (Sub basin B)	<u>115</u>
Table B 3: Thiessen polygon weights for Nzoia Market (Sub basin B)	<u>118</u>
Table C1: NAM Calibration parameters and default hypercube search space	<u>119</u>
Table E1: Peak-Over-Threshold flows for no dams	<u>124</u>
Table E 2: Peak-Over-Threshold flows after implementing dam 42A	<u>125</u>
Table E3: Peak-Over- Threshold results after implementing dam 34B:	<u>125</u>
Table E4: Peak-Over- Threshold flows after implementing dam 35	<u>126</u>

LIST OF FIGURES

Figure 1.1: Map of Study Area.....	4
Figure 1.2: The main drainage rivers and the river gauging stations (RGS).....	6
Figure 2.1: Reservoir operation levels in flood mitigation (Bhawan, 1999).....	10
Figure 2.2: Ideal operation of a reservoir for flood control (After Bhawan, 1999)....	11
Figure 2.3: Normal mode of flood control reservoir operation (After Bhawan, 1999)12	
Figure 2.4: Channel section with computational grid.....	16
Figure 2.5: Centred 6-point Abbott scheme.....	17
Figure 2.6: Centering of continuity equation in 6-point Abbot Schemes.....	17
Figure 2.7: Centering of momentum equation in 6-point Abbott scheme.....	18
Figure 2.8: Lumped conceptual rainfall-runoff modelling.....	19
Figure 2.9: Structure of the NAM model (DHI, 2007).....	21
Figure 2.10: Input and output series of a linear reservoir model.....	27
Figure 2.11: Generalization of the Chapman-filter.....	28
Figure 2.12: Parameters used in the criteria to select independent POT values.....	30
(After Willems, 2009).....	30
Figure 3.1: Rain gauge network in and around the Nzoia Catchment.....	44
Figure 3.2: The River gauging stations and the proposed reservoirs.....	45
Figure 3.3: The River Nzoia sub basins.....	51
Figure 3.4: Thiessen Polygons constructed for Nzoia sub basins.....	52
Figure 3.5: NAM calibration process flow diagram.....	54
Figure 3.6: Dam catchments and NAM rainfall- runoff link to MIKE 11.....	58
Figure 3.7: Nzoia River Basin Network Setup.....	59
Figure 3.8 a: Hydrodynamic boundary data Setup window.....	60
Figure 3.8 b: NAM runoff time Series upstream boundary window.....	60
Figure 3.8 c: Water level time series at downstream boundary window.....	61
Figure 3.9: Hydrodynamic initial parameters window.....	61

Figure 3.10: Simulation input setup window.....	62
Figure 4.1: Thiessen polygon map for Kipkaren sub basin D.....	70
Figure 4. 2: Subflow filter results for daily river flow series of RGS 1CE01.....	72
Figure 4. 3: Assessment of the baseflow recession constant for RGS 1CE01.....	72
Figure 4. 4: Assessment of the interflow recession constant for RGS 1CE01.....	73
Figure 4.5: Calibration hydrographs at RGS 1EE01 for the period 1976-1980.....	75
Figure 4.6: Calibration cumulative volumes (1976-1980).....	76
Figure 4.7: Validation cumulative volumes (1981-1984).....	76
Figure 4.8: NAM calibration result for period 1976-1980.....	76
Figure 4.9: Validation hydrograph for the period 1981-1984 ($R^2 = 0.840$).....	77
Figure 4.10: Validation results for the period 1981-1984 ($R^2= 73.5\%$).....	77
Figure 4.11: Scatter plot of peak flow discharges at 1EE01 after BC-transformation ($\lambda = 0.25$).....	78
Figure 4.12: Modelled and observed peak flow extreme value distribution.....	79
Figure 4.13: Cumulative water balance volume for observed and simulated discharges	79
Figure 4.14: The Nzoia River basin network (grids are in UTM).....	81
Figure 4.15: Example of a cross-section used to describe the Nzoia main river.....	81
Figure 4.16: Confluence between the main Nzoia River and Kipkaren River.....	82
Figure 4.17: The calibration hydrograph results at RGS 1EF01.....	84
Figure 4.18: MIKE 11 scatter calibration plot for simulated and the observed discharge.....	84
Figure 4.19: The validation hydrograph results at 1EF01.....	85
Figure 4.20: MIKE 11 scatter validation plot for simulated and the observed discharge	86
Figure 4.21: Observed and modelled empirical peak flow extreme value distribution	87

Figure 4.22: Cumulative volume for observed and simulated discharges.....	87
Figure 4.23: Grid point dialogue in MIKE 11 River network.....	88
Figure 4.24: MIKE View Computational grid points.....	89
Figure 4.25: Discharge correlation between dam 42A and dyke section.....	90
Figure 4.26: Discharge correlation between dam 34B and dyke section.....	91
Figure 4.27: Regulated outflow from reservoir 42A.....	92
Figure 4.28: Regulated outflow from reservoir 34B.....	92
Figure 4.29: Regulated outflow from reservoir 35.....	93
Figure 4.30: Flood mitigation through storage reservoir 42A.....	94
Figure 4.31: Flood mitigation through storage reservoir 34B.....	94
Figure 4.32: Flood mitigation through storage reservoir 35.....	94
Figure 4.33: Regulated flow from Dam 42A to Rwambwa (1EF01).....	95
Figure 4.34: Regulated flow from Dam 34B to Rwambwa (1EF01).....	95
Figure 4.35: Nzoia River flow simulation results (no dams).....	96
Figure 4.36: Reservoir 42A regulated flow simulation results.....	97
Figure 4.37: Reservoir 34B regulated flow simulation results.....	97
Figure 4.38: Reservoir 35 regulated flow simulation results.....	98
Figure 4.39: POT flows at Rwambwa before dams' implementation.....	100
Figure 4.40: POT flows at Rwambwa after implementation of dam 42A.....	101
Figure 4.41: POT flows at Rwambwa after implementation of dam 34B.....	101
Figure 4.42: POT flows at Rwambwa after implementation of dam 35.....	102
Figure 4.43: Exponential Q-Q Plot for no dam peak flows.....	104
Figure 4.44: Pareto Q-Q plot for no dam peak flows.....	105
Figure 4.45: Slope U-H Q-Q Plot for no dam peak flows.....	105
Figure 4.46: Slope Exponential Q-Q plot for no dam peak flows.....	106
Figure 4.47: Graphical plot for the four flood mitigation scenarios.....	107
Figure A 1: IDW procedure used in gap filling daily rainfall data.....	119

Figure B 1: Thiessen polygon map for Sub basin C.....	122
Figure B 2: Thiessen polygon map for Sub basin B.....	122
Figure B 3: Thiessen polygon map for Nzoia basin.....	123
Figure C 1: Calibration hydrograph at Webuye (1DA02).....	125
Figure C 2: Calibration cumulative volumes at Webuye (1DA02).....	126
Figure C 3: Calibration result at Webuye ($R^2 = 76.7\%$).....	126
Figure C 4: Calibration hydrograph at Kipkaren (1CE01).....	126
Figure C 5: Calibration cumulative volumes at Kipkaren (1CE01).....	127
Figure C 6: Calibration result at 1CE01 ($R^2 = 77.2\%$).....	127
Figure D 1: Location of Kipkaren reservoir (35).....	128
Figure D 2: Location of Webuye reservoir (34B).....	128
Figure D 3: Location of Anyiko/Rambula reservoir (42A).....	129
Figure F 1: UH-Slope Plot for dam 42A regulated peak flows.....	134
Figure F 2: Exponential Q-Q Plot for dam 42A regulated flow.....	134
Figure F 3: Exponential Slope Q-Q Plot for dam 42A regulated flows.....	135
Figure F 4: Pareto Q-Q Plot for dam 42A regulated flows.....	135
Figure F 5: Slope U-H Quantile-Quantile Plot for dam 34B regulated flows.....	136
Figure F 6: Exponential Q-Q Plot for dam 34B regulated flow.....	136
Figure F 7: Exponential Slope Q-Q Plot for Dam34B regulated flow.....	137
Figure F 8: Pareto Q-Q plot for Dam 34B regulated flow.....	137
Figure F 9: U-H Slope Q-Q plot for dam 35 regulated discharge.....	138
Figure F10: Exponential Q-Q plot for dam 35 regulated discharges.....	138
Figure F 11: Slope-Exponential Q-Q plot for dam 35 regulated discharge.....	139
Figure F 12: Pareto distribution for simulated discharge at dam site 35.....	139

LIST OF NOTATIONS

- A - Cross-sectional area
 C - Chezy's resistance coefficient
 C_r - Courant number
 n - Manning roughness coefficient
 g - Gravitational acceleration
 Q - Discharge
 q - Lateral inflows
 R - Hydraulic radius
 α - Momentum distribution coefficient
 v - Velocity
 h - Water level
 E_a - Actual Evapo-transpiration
 E_p - Potential rate of evaporation
 k - Recession constant
 K_p - independency period
 γ - Extreme value index
 λ - Box-Cox parameter
 C_v - Coefficient of variation
 Q_m - Modelled /simulated flow
 \bar{Q}_o - Average of the observed flow
 R^2 - Coefficient of determination

LIST OF ABBREVIATIONS AND ACRONYMS

CAS- Concise Achievable Solutions

CK1, 2- Time constant for routing overland flow

CKIF – Time constant for routing interflow

CKBF – Time constant for routing baseflow

1-D – One dimensional

DEM- Digital Elevation Model

DHI – Danish Hydraulic Institute

DSS- Decision Support System

ECQ- Hydrological Extreme Value analysis tool

FD- Finite Difference

GIS – Geographical Information System

HD- hydrodynamic

IDW- Inverse Distance Weighting

JICA – Japan International Corporation Agency

KMD- Kenya Meteorological Department

MAR- Mean Areal Rainfall

MWI- Ministry of Water and Irrigation

MUK_VLIR-OUS- Moi University and Flemish Inter University Council- University Development Cooperation: VLIR- Vlaamse interuniversitaire Raad; UOS- Universitaire Ontwikkelingssamenwerking.

NWCPC- National Water Conservation and Pipeline Corporation

UTM- Universal Transverse Mercator

WRMA- Water Resource Management Authority

NBCBN- Nile Basin Capacity Building Network

GOK- Government of Kenya

WETSPRO- Water Engineering Time series Processing tool

WMO- World Meteorological Organisation

MWL- Maximum Water Level

FRL- Full Reservoir Level

DSL- Dead Storage Level

POT- Peak-Over -Threshold

UH- Generalized Quantile excess function

GPD- Generalized Pareto Distribution

RGS- River Gauging Station

MSE- Mean Square Error

TOF- Threshold for overland flow

SWAT- Soil and Water Assessment Tool

TIF- Threshold for interflow

TG- Threshold for groundwater recharge

WKCD&FMP- Western Kenya Community-Driven Development and Flood Mitigation Project

ACKNOWLEDGEMENT

This study could not have been successful without the assistance of several institutions and wonderful people. I would therefore like to express my sincere appreciation and grateful acknowledgement to my supervisors, Dr. J. Kibiiy, Prof. S. Shitote and Prof. P. Willems for their constant guidance, invaluable advices,

suggestions, and help throughout the study period. I was greatly privileged to have worked under them. Specifically, Prof. P. Willems for introducing me into the fascinating and complex world of modelling water-based systems and according me the practical experience required in understanding and running the model. In particular, his guidance was very helpful during the model formulation. Prof. S. Shitote for providing the required link in understanding the MIKE 11 code through his vast knowledge in Numerical methods, I am sincerely grateful. Dr. J. Kibiiy for consistently reviewing, guiding and updating my knowledge in hydrology so that I was able to link theory to the practical area of modelling and also for incorporating me in his research activities and hence providing the funds and logistics during data collection and acquisition. I give my special appreciation.

I am grateful to the Water Resource Management Authority (WRMA) and Kenya Meteorological Department (KMD) for making available the data required for this study. Specifically I acknowledge the support given by Mr. J. Oruta of WRMA and Mr. J. Maina of KMD.

I sincerely thank my colleagues' at the Department of Civil and Structural Engineering, the team work was great and specifically Mr. G. Nyandwaro, for his superb support.

I am deeply indebted to the Department of Civil and Structural Engineering and the MUK-VLIR_UOS project for the opportunity they granted me to undertake the M.Sc. studies.

Last but certainly not the least; I would especially want to thank my wife Mary Rutto, and my children for their patience, encouragement, love and understanding they gave me all this period of the study. To all these wonderful people, I say thank you.

Over and above all, thanks to the Almighty God. Surely His Grace is sufficient (2nd Corinthians 12:9).

DEDICATION

This thesis is dedicated to my wife, sons and daughters.

CHAPTER ONE

INTRODUCTION

1.1 BACKGROUND OF STUDY

Nzoia basin in Western Kenya covers an area of 12,709 km² and is prone to annual floods (Githui, 2007). These floods result in displacement of people and destruction of property. River Nzoia is one of the biggest rivers in western Kenya. The length of the river is 355km, with a mean discharge of 118m³/s. However the flow regime of the Nzoia varies and is occasionally as low as 20m³/s and with extreme floods that surpass 1,100 m³/s, which is the proposed protection level for the dykes for a 25 year return flood. Deposition of silt is heavy especially at the plains, which reduce the height of the river banks, hence the flooding (NBCBN, 2010). The Ministry of Water and Irrigation (MWI) has been implementing flood control work in the Budalangi flood plains through rehabilitation of dykes, river training and river de-silting, but the problem has not been eliminated (CAS Consultants, 2006).

Through a partnership between the Government of Kenya and the World Bank there are advanced plans to construct multipurpose reservoirs in the Nzoia River basin in order to contain the floods and provide water for irrigation and other uses (NWCCPC, 2009).

Several hydrological modelling studies on flood management have been carried out in the Nzoia Basin (NBCBN, 2010). However, none of these studies have addressed the impacts of incorporating reservoirs in the Nzoia River system for flood mitigation in the basin. This study set out to investigate the use of hydrological and hydraulic modelling in order to evaluate the effect of constructing the proposed reservoirs on stream flow, and especially the flooding problem in Budalangi.

In this study the effectiveness of the proposed flood storage reservoirs to control the perennial flooding problem at Budalangi flood plains was evaluated using the integrated hydrologic-hydraulic MIKE 11 model. The model was selected because it contains modules for rainfall-runoff simulations for predicting the reservoir catchment runoff and hydrodynamic (HD) model for river flow simulations. It also has the ability to test different flood mitigation scenarios before and after dam construction.

1.2 SIGNIFICANCE AND JUSTIFICATION OF THE STUDY

The proposed reservoirs not only target flood control but also hydroelectric power, irrigation and water supply. Because these different purposes always cause conflicts and disputes during the sharing of water resource the developed model can be used to set operational strategies. Using the computer based MIKE 11 simulation model, the impacts of different dam sites alternatives is forecasted and evaluated before implementing the construction.

The flood plain with an area of approximately 128,000 hectares has the potential to feed the majority of the district population in Budalangi and is therefore a very significant resource (NWCPC, 2009). In order to balance the release of the flood water downstream from the reservoirs and at the same time not to cause flooding, adequate knowledge of the amount of water required to simulate a flood and the timing of these in relation to upstream and local rainfall in the catchments can be conveniently obtained by use of hydrological modelling.

1.3 STATEMENT OF THE PROBLEM

The flooding problem at Budalangi flood plains is recurrent and managing it is a challenge. The structural flood mitigation measures adopted have been the construction of earthen dykes, which breach often leading to loss of life and property. People in the lower catchment are taken unawares when the floods occur because the upper catchments receive heavy rainfall than the plains. To tame the flooding there

has been concerted effort by the Government of Kenya in partnership with the international community, in particular the World Bank to construct multipurpose reservoirs in mid-catchment of the river Nzoia basin.

Currently there is no management scheme using modelling of reservoir storage and releases of the flood have been formulated in this basin. This research study focused on using MIKE 11 model to carry out rainfall-runoff modelling into the proposed reservoirs, and hydrodynamic simulation in the river system from the dam sites down to the flood plains. The aim was to evaluate the mitigation effects of introducing the reservoirs in the river Nzoia system.

1.4 RESEARCH OBJECTIVES

1.4.1 The Main Objective

The broad objective of this study was to evaluate the effectiveness of the proposed reservoirs as flood mitigation measure in the Nzoia River basin using MIKE 11 model.

1.4.2 The Specific Objectives

- i. To calibrate and validate the NAM rainfall-runoff model for each reservoir sub-basins.
- ii. To calibrate and validate the MIKE 11 hydrodynamic model for use in flood mitigation modelling in the Nzoia river basin.
- iii. To simulate the flood mitigating effect of each of the proposed reservoirs on downstream flooding at Budalangi flood plains.

1.5 STUDY AREA

The Nzoia River basin is located in western Kenya and is part of Lake Victoria basin (Figure 1.1). The basin lies between latitudes 1° 30'N and 0° 05'S and longitudes 34°

and 35° 45'E. The Nzoia River originates largely from Cherangani Hills, at a mean elevation of 2300m above sea level and drains into Lake Victoria at an altitude of 1100m (NBCBN, 2005). The main tributaries of Nzoia River include: Lusumu, Kipkaren, Sergoit, Kuywa, Koitobos, Noigamaget, Moiben, Little Nzoia and Ewaso Rongai. The area under this study is the catchment immediately upstream the flood prone zone at Budalangi and is 12,656 km².

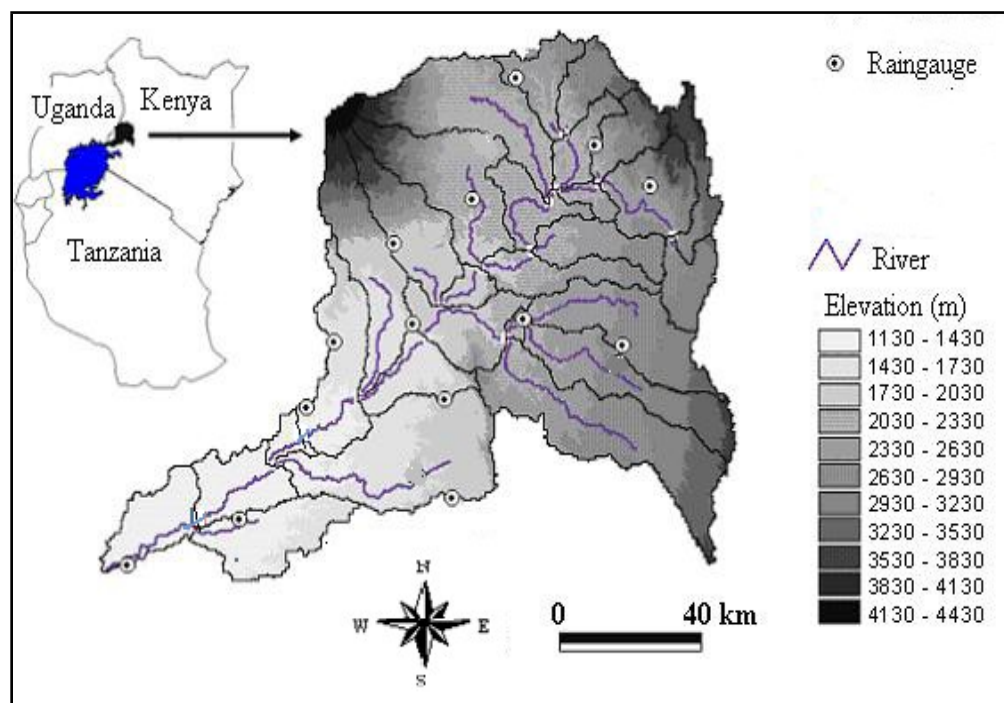


Figure 1.1: Map of Study Area

1.5.1 The Hydrology of River Nzoia Basin

River Nzoia experiences perennial flooding in its lower reaches especially the Budalangi area of Busia district. The flood prone area is generally flat and swampy. There are two rainfall peaks in the catchment. The first peak comes in the month of April to June, while the other occurs in July to November. January through March is dry months in Nzoia. Comparatively to other parts in Kenya, the basin receives high rainfalls whose average annual value varies between 1000 to 1500mm. The rainy

season from October to early December bring devastating floods in the basin (Makhanu, 2005; Sadiq et al., 2011).

The length of the main stream is about 252 km with a fall of about 1200m giving a 0.5% slope in the upper reaches, which reduces to 0.04% in the lower reaches over at least 30km. Over this stretch the river meanders and causes deposition of silt due to the low gradients. The sediment accumulates and reduces the discharge capacity of the river channel so that it over flows its banks' causing flooding in the lower reaches of the basin. (NBCBN, 2010).

The main drainage rivers in the Nzoia River basin are as shown in Figure 1.2.

1.5.2 History of Budalangi Floods and Dykes

The flooding in Budalangi region of western Kenya is as old as River Nzoia owing to its location as a low lying with flat terrain, which finds the river in its senile stage; hence flooding hazard is unavoidable. However, floods became a real hazard in Budalangi since 1940s. Flood disaster occurred in 1945, 1948, 1951, 1961-1962, 1975, 1977, 1978, 1997 –1998 (El Nino rains), 2001, and 2002, 2003 (Mango, 2003). Lately floods have occurred in 2006, 2008 and 2011 (KMD, 2011).

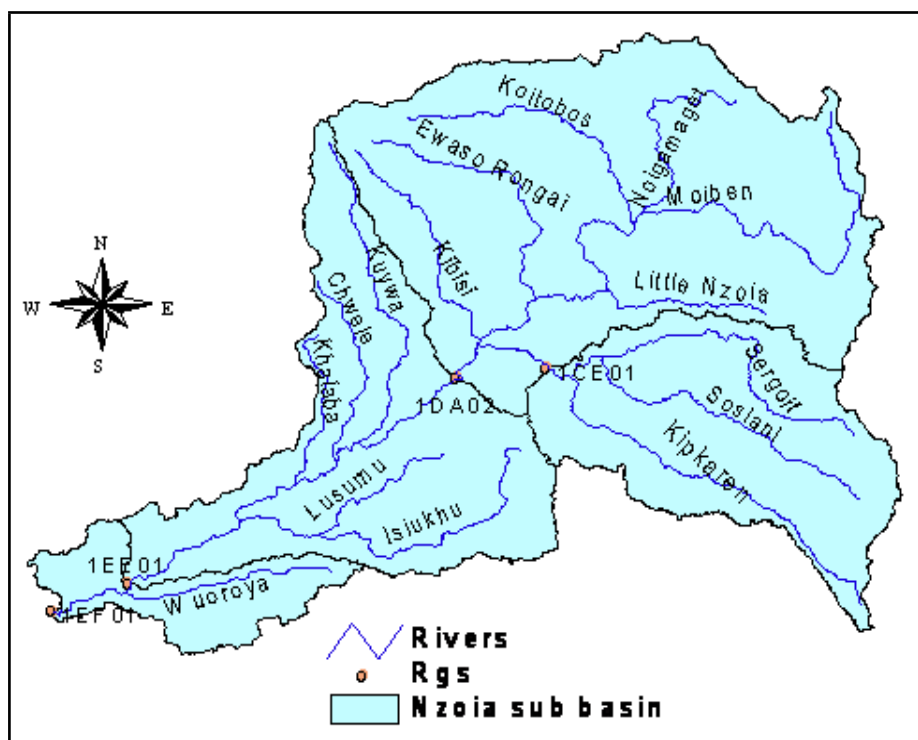


Figure 1.2: The main drainage rivers and the river gauging stations (RGS)

CHAPTER TWO

LITERATURE REVIEW

2.0 INTRODUCTION

This chapter will highlight the role of flood mitigation reservoirs, rainfall-runoff modelling process at the reservoir catchments through a deterministic lumped conceptual model (NAM), Time Series analysis using a Water Engineering Time Processing tool (WETSPRO), and then river flow simulation through hydraulic modelling using MIKE 11 Software and finally the role of Extreme Value Analysis in peak flow prediction to the flood mitigation reservoirs

Previous studies done in the Nzoia River (TAHAL, 2007) on the detailed design of the proposed dams for flood mitigation forms the necessary background to this study. Studies in hydrological modelling in the basin have been undertaken by various researchers in the area of flood forecasting using other models other than the ones that will be used in this study; however their studies did not incorporate the impacts of reservoir systems in the river basin for predicting different flood mitigation scenarios.

In related studies, Ngo et al., (2008) applied the NAM module and the hydrodynamic model MIKE 11 to simulate the flow in the Red River, including the Hoa Binh reservoir to represent the effect of reservoir operation decisions on downstream flooding in Hanoi. The MIKE 11 was used to adjust the operation rules of the reservoir and a rule curve was implemented in MIKE 11 for the simulation for reservoir regulation.

Tawatchai (1996) simulated flood flow along the upper Nan River covering a flow distance of 100km, including its upstream rivers in northern Thailand. The models used were the MIKE 11 for flood routing, the NAM rainfall-runoff watershed model

and HEC-5 reservoir routing model. As a result of the study a flood control scheme consisting of flood control reservoir and construction of dykes was recommended for implementation along the upper Nan River.

Khan (1997) formulated different flood mitigation scenarios based on the volume of the forecasted flood using NAM rainfall-runoff model for the control of severe flooding in Pakistan. It was found necessary to formulate a hypothetical reservoir release scenarios' using the MIKE 11 hydrodynamic flow routing model depending upon the volume of catchment forecasted flood.

This research focused on the application of an integrated hydrologic-hydraulic MIKE 11 model that evaluated the effectiveness of individual proposed reservoir in mitigating the flooding problem at Budalangi.

2.1 FLOOD MITIGATION RESERVOIRS

Flood mitigation reservoirs store all or a portion of the flood waters particularly during peak floods, and then releases the water slowly. Space within a reservoir is generally reserved to store impending floods (Figure 2.1). Small to medium floods generated from the catchment are fully captured by the reservoirs. However extreme floods are only partially attenuated and their transformation downstream is delayed. The extent of attenuation depends on the available storage capacity vis-à-vis the magnitude of the flood event (WMO, 2006).

In order to provide maximum attenuation of the peak flood, it is imperative that maximum possible storage space is available at the time when the floods impinge upon the reservoir. This can be achieved by drawing down the reservoir level to a minimum possible (dead storage) by appropriate operation in accordance with flow discharge into the reservoir.

2.2 RESERVOIR STORAGE ZONES

The storage capacity in a reservoir is divided into three or four levels as shown in Figure 2.1. These specific levels and parts are defined as follows:

i) Maximum Water Level (MWL)

This is the water level that is ever likely to be attained during the passage of the design flood. It depends upon the specified initial reservoir level and the spillway gate operation rule. This level is sometimes called Highest Reservoir Level (HRL) or the Highest Flood Level (HFL).

ii) Full Reservoir Level (FRL)

It is the level corresponding to the storage which includes both inactive and active storages and also the flood storage. This is the highest reservoir level that can be maintained without spillway discharge or without passing water downstream through sluice ways.

iii) Dead storage Level (DSL)

Below the level, there are no outlets to drain water in the reservoir by gravity. It is the total storage below the lowest discharge outlet. It is available to contain sedimentation

iv) Live storage

This is storage between full supply level and dead storage

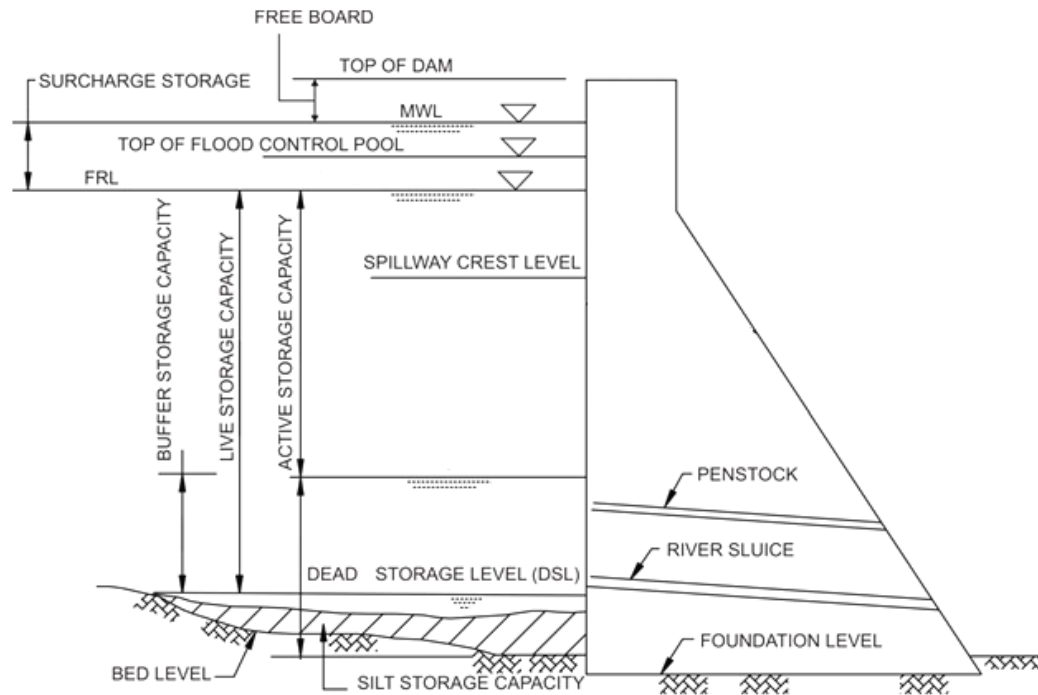


Figure 2.1: Reservoir operation levels in flood mitigation (Bhawan, 1999)

2.2.1 Ideal Reservoir Operation for Flood Control

Among the measures of flood control, a storage reservoir with gates to control the outflow is the most effective means. The moderation of flood through storage is achieved by storing part of the flood volume in the rising phase and releasing gradually the same in receding phase of the flood (Bhawan, 1999).

The regulation consists of storing the peak flows over and above the safe carrying capacity of the channel at the floodplain, in the reservoir as shown in Figure 2.2. The pertinent objective is to minimize downstream flooding. The reservoir is released gradually after the passage of the flood to provide space for control of subsequent floods.

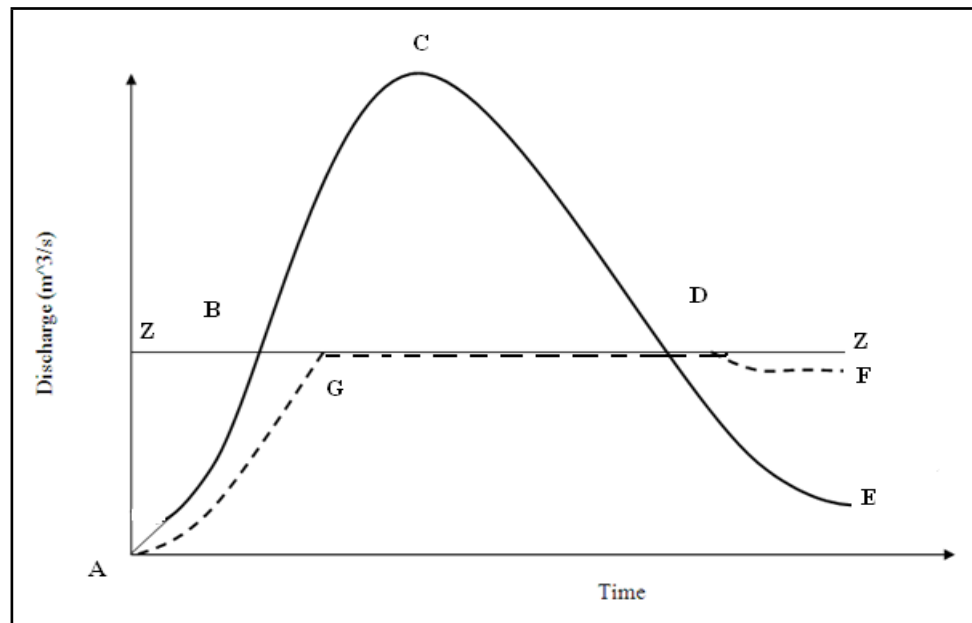


Figure 2.2: Ideal operation of a reservoir for flood control (After Bhawan, 1999)

In Figure 2.2, ABCDE and line ZZ represents the inflow hydrograph and the non damaging carrying capacity of the river channel downstream of the reservoir, respectively.

If there is no reservoir, from the time corresponding to point B upto D, the flood water will spill over the channel banks and cause flooding. The regulation for the reservoir is given by the dotted line AGDF. The release is gradually increased from point A onwards, making sure that at no point the release exceeds the safe carrying capacity of the river channel. This is achieved by storing the volume between the curve BCD in the reservoir, and after point D, the reservoir is emptied gradually.

The normal mode of operation during floods (Figure 2.3) is to make releases less than or equal to the safe carrying capacity of the downstream channel as long as there is empty storage in the reservoir.

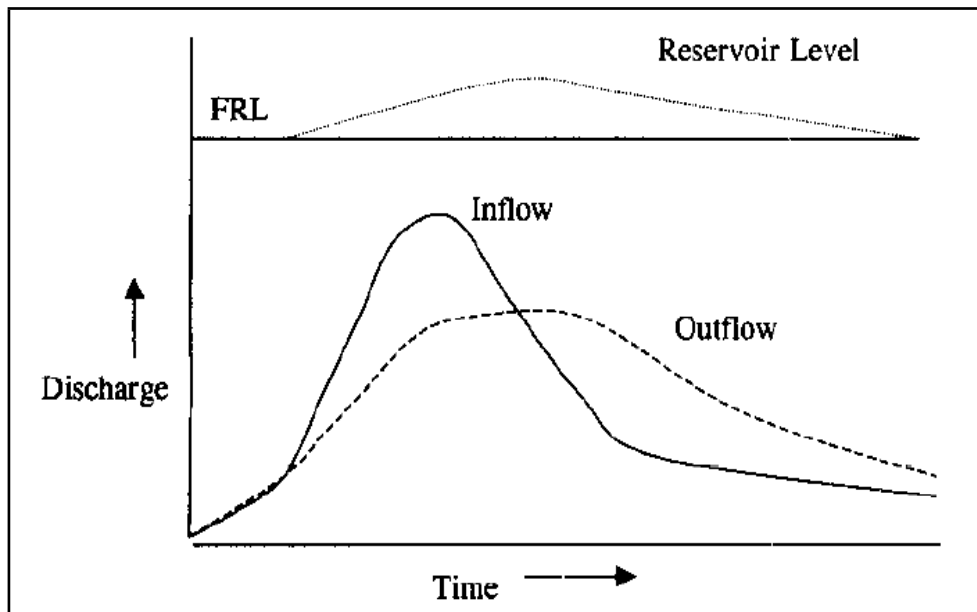


Figure 2.3: Normal mode of flood control reservoir operation (After Bhawan, 1999)

The reservoir level is allowed to rise above the full reservoir level (FRL). The maximum level upto which the reservoir level can rise is known as the maximum water level (MWL). The zone between the FRL and MWL is normally exclusively reserved for flood control. After the flood has peaked, the reservoir is gradually brought back to FRL. This strategy involves use of inflow forecasts and therefore, the confidence of the operator in making pre-releases depends on the reliability and timely availability of reservoir inflow forecasts.

2.2.2 Operation of a Multipurpose Reservoir System

In case of multipurpose reservoirs, permanent allocation of the space exclusively for flood control at the top of conservation pool is necessary. The size of a flood control space may vary with time according to the magnitude of floods likely to occur. The flood storage allocation at different times of the year is so determined that incoming floods would be absorbed or mitigated to a large degree. In non-flooding season, this space is utilized for conservation uses. The reservoir operations also include the periodic assessment of future incoming volumes based on the rainfall information gathered from rain gauge stations in the catchment. Reservoir release decisions are

based on intuition and judgement of the operator in situations where information on inflows is not available. In order for the release decisions to be effective, the information on the likely inflows should be available to the operator. Therefore there is need to develop a strategy for operating a reservoir based on information on current inflow magnitude and its characteristics. Estimation of empty storage requirements during various time periods forms part of flood moderation operations. In this decision, forecasts of inflows into reservoir obviously play a vital role in increasing the flood moderation efficiency without reducing conservation benefits. Forecast of runoff contributions from river channels upstream of the flood plains is mandatory for taking release decisions (Bhawan, 1999).

2.3 FLOOD MODELLING: NEED FOR MODELLING FLOODS

In general a model is understood as a simplified representation of the natural system it attempts to describe. Many of the phenomena that can be identified in water based system are so complex in their generation and prediction that we have to resort to models to help us understand what is going on, and to make predictions or forecasts of what will happen (Price, 2009).

Some of the reasons we use models are:

- i) To understand what is going on in complex water based systems
- ii) To make forecasts of future values
- iii) To predict the consequences of structural changes in the modelled system
- iv) To predict the response of a system to extreme unseen events

A simple conceptual model is sufficient to describe rainfall-runoff accurately and a detailed hydrodynamic model is used for river routing (Willems, 1998).

Currently, there are no flood control reservoirs in the Nzoia River. There is therefore an apparent need to have a computer based Decision Support System (DSS) that will assist stakeholders to evaluate various flood mitigation scenarios thereby analysing

the significance of each scenario against aims and objectives of the dam proponents before implementation.

The modelling study of the Nzoia River basin involved the use of MIKE 11, a hydrodynamic (HD) model for flood routing in the Nzoia River. The HD model is supported by a deterministic, lumped conceptual module (NAM) for rainfall-runoff simulations.

2.4 MIKE 11 MODEL

MIKE 11 is a general mathematical modelling system for the simulation of flows and water levels in rivers, reservoirs and canals. MIKE 11 contains modules for run-off simulations (NAM), hydrodynamics (HD), flood forecasting, transport and dilution of dissolved substances, sediment transport, and river morphology as well as various water quality processes. It allows the flexible operation of flood control and reservoir structures and has an interface to GIS allowing for preparation of model input and presentation of model output in a GIS environment (DHI, 2007).

It provides a one dimensional description of the flood propagation along a river network using governing equations based on the mass and momentum conservation principle. It solves the Saint Venant equations of continuity and momentum (Vu Minch Cat, 2007).

The solutions to the equations are based on the assumptions that:

- i) Water is incompressible with insignificant variation in density
- ii) Flow is one dimensional
- iii) The pressure is assumed to be hydrostatic i.e. the vertical acceleration is neglected

- iv) The effect of boundary friction and turbulence can be accounted for with the introduction of empirical relations such as Chezy's and Manning friction factors

The governing equations of continuity and momentum are as given in equations 2.1 and 2.2 (DHI, 2007).

Continuity Equation

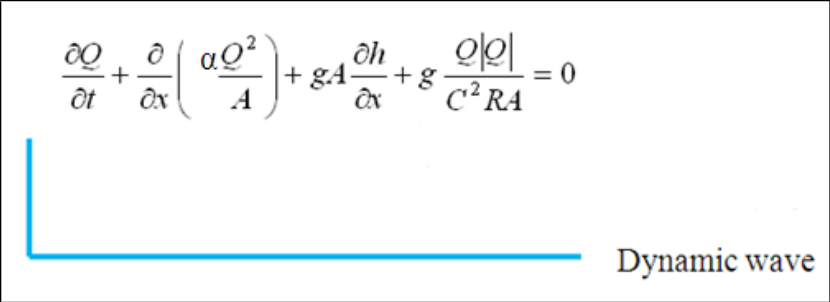
$$\frac{\partial Q}{\partial x} + \frac{\partial A}{\partial t} = q$$

[2.1]

Momentum Equation

$$\frac{\partial Q}{\partial t} + \frac{\partial}{\partial x} \left(\frac{\alpha Q^2}{A} \right) + gA \frac{\partial h}{\partial x} + g \frac{Q|Q|}{C^2 RA} = 0$$

[2.2]



Where

Q = Discharge (m³/s)

A = Area of flow (m²)

q = Lateral inflow (m³/s/m)

g = Acceleration of gravity (m/s²)

C = Chezy's resistance coefficient (m^{1/2}/s)

α = Momentum distribution coefficient

R = Hydraulic radius (m)

h = Stage above horizontal reference (m)

2.4.1 Solution Scheme

The MIKE 11 hydrodynamic model is based on the complete nonlinear St. Venant equations. Equations 2.14 and 2.15 are transformed to a set of implicit finite

difference equations with computational grid consisting of alternating Q- and h-points, i.e. points where the discharge, Q and water level h, are computed at each time step (Figure 2.4). Q-points are always placed midway between neighbouring h-points (DHI, 2007).

The implicit scheme has flexible requirements for selection of the computational time steps and distance intervals which have been proven to be very efficient, and excellent numerical stability and reliability in numerous unsteady flow modelling applications (Chow et al., 1988).

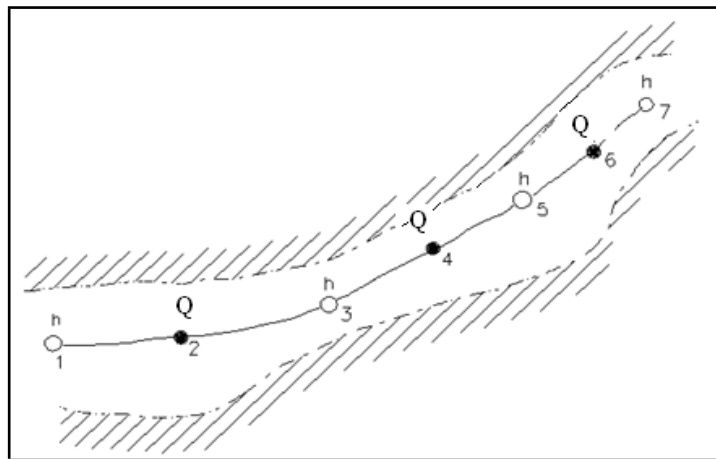


Figure 2.4: Channel section with computational grid

The adopted numerical scheme is a 6-point Abbott scheme as shown in Figure 2.5.

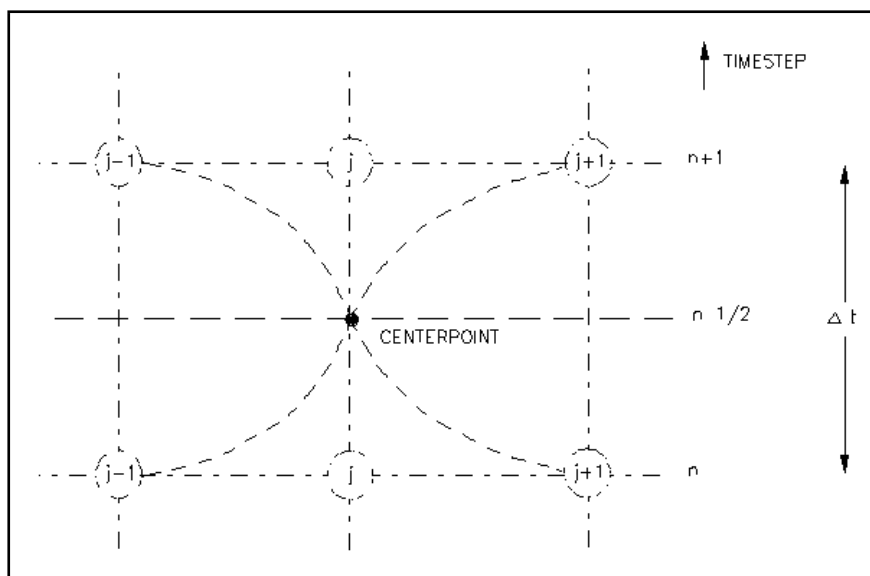


Figure 2.5: Centred 6-point Abbott scheme

The water level and flow are calculated at each time step, by solving the continuity equation and the momentum equation using a 6-point Abbot scheme with the continuity equation centred on h-points and the momentum equation centred on Q-points as shown in Figure 2.6 and 2.7 respectively (DHI, 2007; Price, 2009).

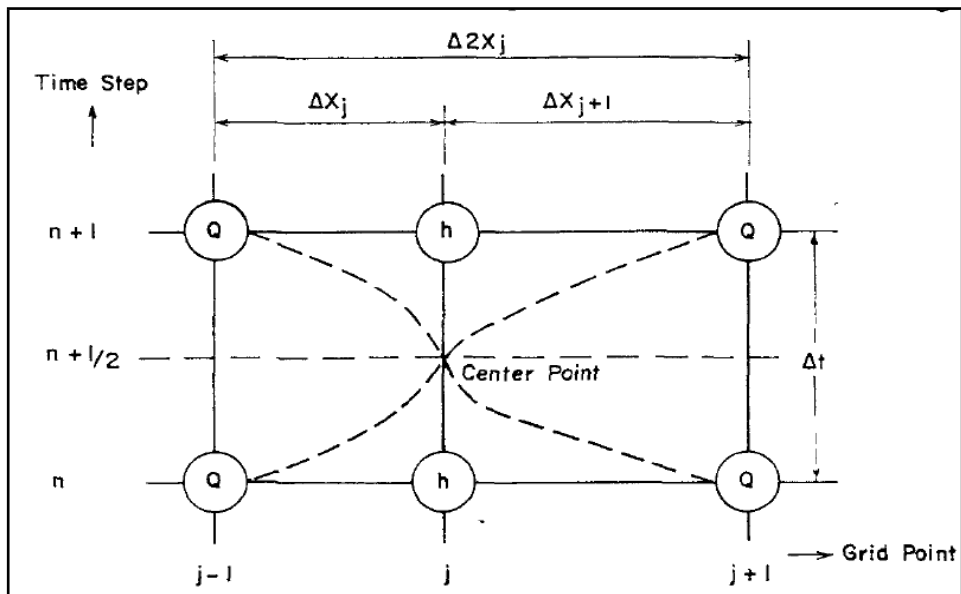


Figure 2.6: Centering of continuity equation in 6-point Abbot Schemes

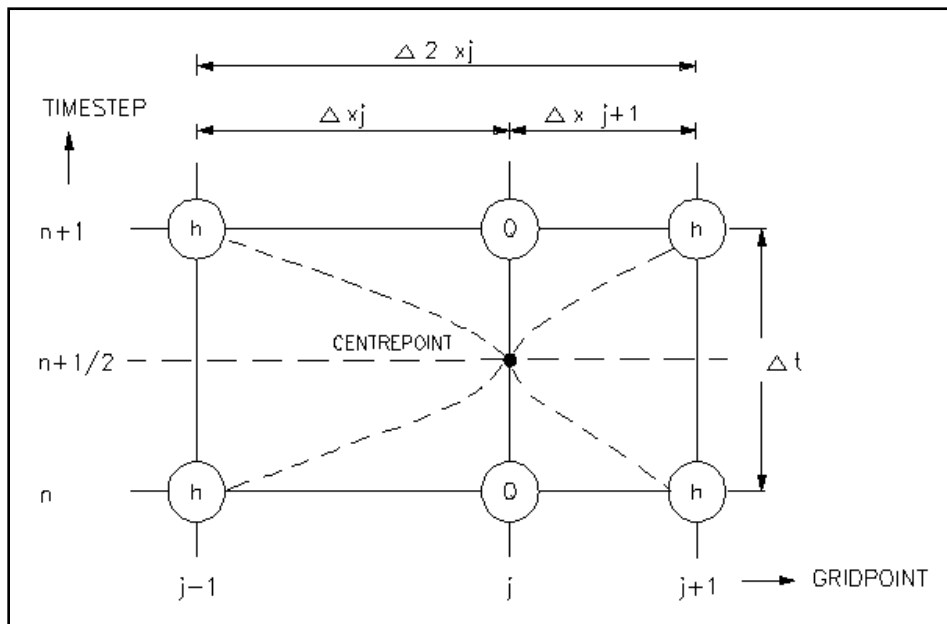


Figure 2.7: Centering of momentum equation in 6-point Abbott scheme

The Courant condition for stability is used to cater for the maximum accuracy of MIKE 11 model (DHI, 2007).

2.4.2 Courant Condition

The Courant condition (Courant and Friedrichs, 1948) is used for selecting the time step in the finite difference scheme used in MIKE 11. Typically a value of the Cr of the order of 10 to 15 is used (DHI, 2007).

The Courant number is given by equation (2.3).

$$C_r = \frac{(v + \sqrt{gy})\Delta t}{\Delta x} \quad [2.3]$$

Where, v = velocity (m/s)

y = flow depth (m)

g = gravitational acceleration

Δt = time step

Δx = distance step

2.5 NAM MODEL

NAM model contains a set of linked mathematical statements describing, in a simplified quantitative form, the behaviour of the land phase of the hydrological cycle (Figure 2.8), and produces a time series of catchment run-off and subsurface contributions to stream flow. The simulated catchment runoff is split conceptually into three components: surface runoff (overland flow), interflow, and base flow components (DHI, 2007).

A conceptual model includes both mathematical equations and description of the flow processes that are required for the particular purpose of modelling (Refsgaard, 2007).

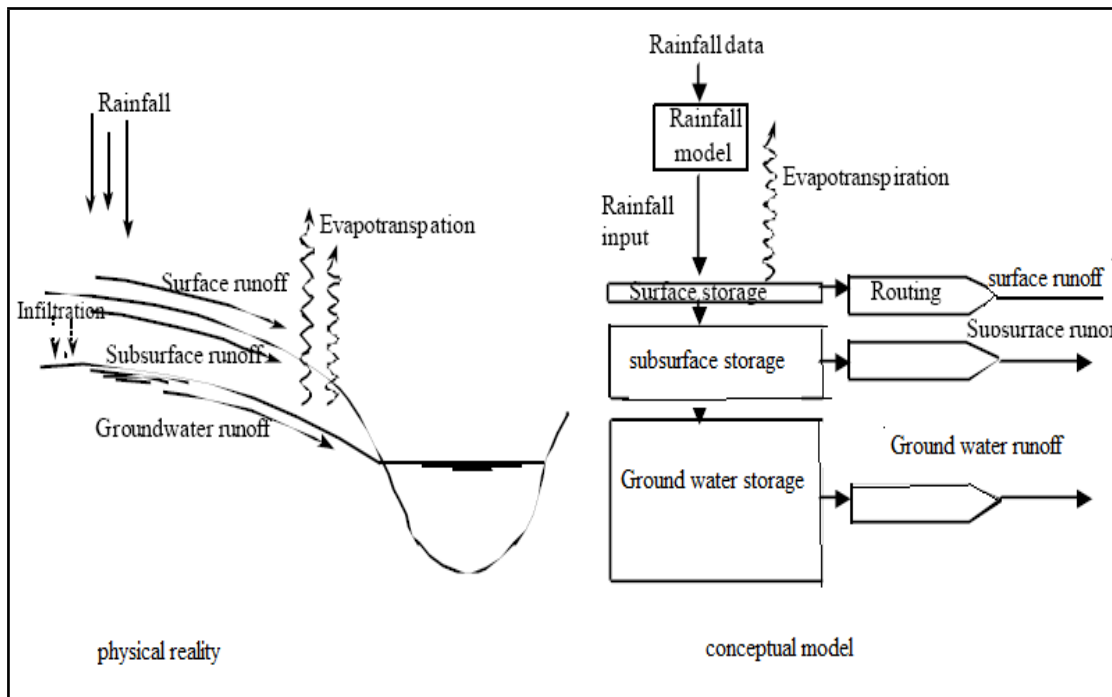


Figure 2.8: Lumped conceptual rainfall-runoff modelling

2.5.1 Model Structure

NAM simulates the rainfall-runoff process by continuously accounting for the water content in three different and mutually interrelated storages that represent different physical elements of the catchment (Figure 2.9). These storages are:

- i. Surface storage
- ii. Lower or root zone storage
- iii. Groundwater storage

In addition NAM allows treatment of man-made interventions in the hydrological cycle such as irrigation and groundwater pumping. Lumped conceptual models are characterized by simple structure, minimum data requirements, fast set up and calibration and by being easy to use. Being a lumped model, NAM treats each catchment as a single unit. The parameters and variables represent, therefore, average values for the entire catchment. As a result some of the model parameters can be evaluated from physical catchment data, but the final parameter estimation must be

performed by calibration against time series of hydrological observations (DHI, 2007).

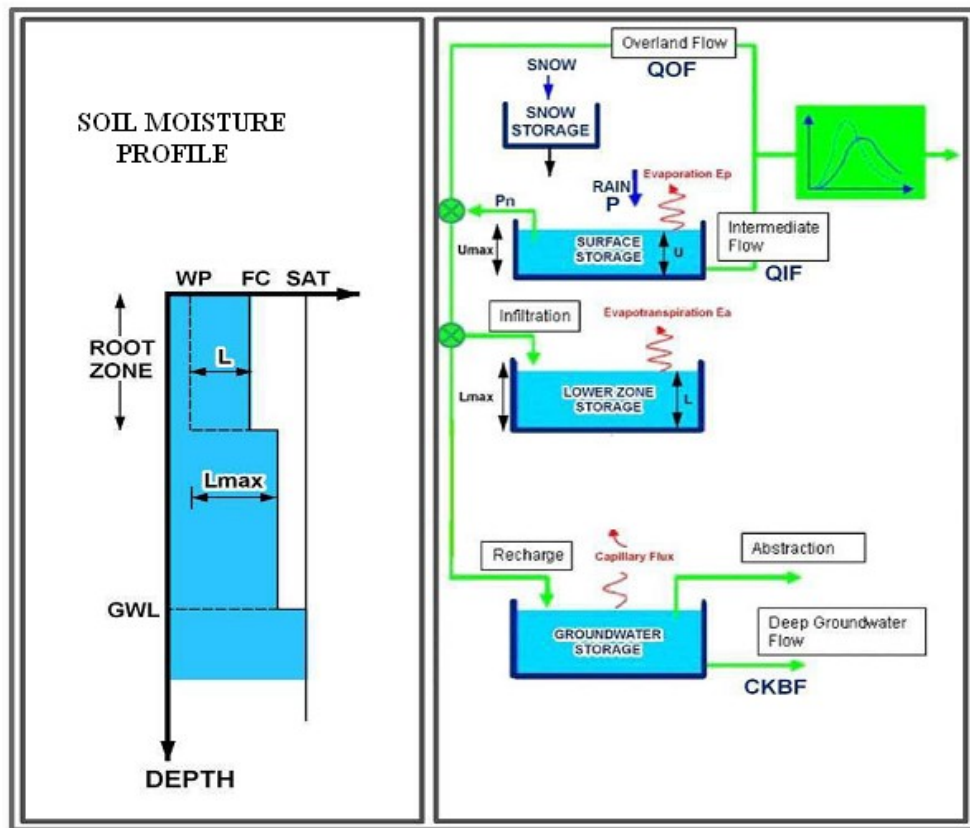


Figure 2.9: Structure of the NAM model (DHI, 2007)

2.5.2 Basic NAM Modelling Components

A short description of each of the NAM model parameters is presented below (DHI, 2007).

i) Surface storage (U_{\max})

U_{\max} [mm] defines the maximum water content in the surface storage. When there is maximum surface storage, some of the excess water, PN , will enter the streams as overland flow, whereas the remainder is diverted as interflow and groundwater storage.

ii) Root zone storage (L_{\max})

L_{\max} (mm) denotes the maximum water content in the root zone storage. L_{\max} is an average value for the various soil types and root depths of the individual vegetation types for the entire sub catchment. Since the actual evapo-transpiration is highly dependent on the water content of the surface and root zone storages, U_{\max} and L_{\max} are the primary parameters to be changed in order to adjust the water balance in the simulations. In the preliminary stages of the model calibration, it is recommended to fix the relation between U_{\max} and L_{\max} , leaving one storage parameter to be estimated. As a rule, $U_{\max} = 0.1 L_{\max}$ can be used.

iii) Evapo-transpiration (E_a)

Evapotranspiration affects the surface and lower zone storage (Figure 2.8). If the amount of water in the surface storage zone (U) is less than the amount of potential evapotranspiration ($U < E_p$), then the remainder of the water is assumed to be taken up by the roots of vegetation in the lower zone storage as actual evapotranspiration (E_a). The rate of actual evapotranspiration is proportional to the potential evapotranspiration and the relative soil moisture content $\left(\frac{L}{L_{\max}} \right)$ and is calculated by the equation 2.4.

$$E_a = (E_p - U) \frac{L}{L_{\max}} \quad [2.4]$$

iv) Root zone threshold value for overland flow (TOF)

The threshold for overland flow (TOF) determines the relative value of the moisture content in the root zone $\left(\frac{L}{L_{\max}}\right)$ above which overland flow is generated. Overland flow is only generated if the relative moisture content in the root zone is larger than TOF. An increase of TOF will delay the start of runoff as overland flow. Threshold value range between 0 and 70% of L_{\max} , and maximum values allowed is 0.99.

v) Root zone threshold value for inter flow (TIF)

The root zone threshold value for inter flow (TIF) determines the relative value of the moisture content in the root zone $\left(\frac{L}{L_{\max}}\right)$ above which interflow is generated. Interflow is generated only if the relative moisture content in the root zone storage is larger than TIF. Typical values are $0 \leq \text{TIF} \leq 1$

vi) Root zone threshold value for ground water recharge (TG)

TG determines the relative value of the moisture content in the root zone $\left(\frac{L}{L_{\max}}\right)$ above which ground water recharge is generated. The main impact of increasing TG is less recharge to the ground water storage. Recharge to the ground storage is only generated if the moisture content in the lower root zone storage is larger than TG.

vii) Overland flow

When $U > U_{\max}$, then there is excess surface zone storage water (P_N) as well as infiltration to the lower zone storage. The amount of water that contributes to overland flow Q_{OF} is assumed to be proportional to P_N and the relative soil moisture content of the lower zone storage. Q_{OF} denotes the part of P_N that contributes to overland flow, and is given by equation 2.5.

$$Q_{OF} = \begin{cases} CQ_{OF} \left(\frac{L - TOF}{L_{max} - TOF} \right) P_N & \text{for } \frac{L}{L_{max}} > TOF \\ 0 & \text{for } \frac{L}{L_{max}} \leq TOF \end{cases} \quad [2.5]$$

where

CQ_{OF} is the overland flow runoff coefficient ($0 \leq CQ_{OF} \leq 1$).

It determines the division of excess rainfall between overland flow runoff and infiltration. Small values of CQ_{OF} would be expected for a relatively flat catchment with a high permeability substrate, whereas high values would be expected for the opposite extreme. The remainder of P_N that does not become overland flow ($P_N - Q_{OF}$) percolates into the lower zone storage (increasing the soil moisture content (L) and deeper into the groundwater storage.

TOF is a threshold for overland flow in the sense that no overland flow is generated if

the relative soil moisture content of the lower zone storage $\left(\frac{L}{L_{max}} \right)$ is less than TOF.

viii) Interflow

The interflow contribution (QIF) is assumed to be proportional to U and vary linearly with the relative moisture content of the lower zone storage. The interflow contribution is assumed to be proportional to the surface storage zone (U) and vary linearly with the relative moisture content of the lower zone storage and is given by equation 2.6.

$$QIF = \begin{cases} (CKIF) \frac{L - TIF}{L_{max} - TIF} U & \text{for } \frac{L}{L_{max}} > TIF \\ 0 & \text{for } \frac{L}{L_{max}} \leq TIF \end{cases} \quad [2.6]$$

ix) Time constant for overland flow (CK1,2)

The time constant for overland flow (CK1, 2) determines the shape of hydrograph peaks. The routing takes place through two linear reservoirs (serial connected). The routing through two linear reservoirs considers CK1 for the first reservoir and CK2 for the second reservoir. High, sharp peaks are simulated with small time constants,

whereas low peaks, at a later time, are simulated with large values of these parameters. Values in the range of 3 - 48 hours are common.

x) Time constant for Interflow (CKIF)

The time constant for interflow (CKIF) determines the amount of interflow, which decreases with larger time constants. Values in the range of 500-1000 hours are common.

xi) Time constant for routing baseflow (CKBF)

The time constant for routing baseflow (CKBF) determines the shape of the simulated hydrograph in the dry periods. Typically values are $0 \leq \text{CKBF} \leq 1$.

xii) Groundwater recharge

The amount of water that contributes to recharging the model's groundwater storage (G) is assumed to be dependent on the relative soil moisture content of the lower zone storage as shown in equation 2.7.

$$G = \left\{ \begin{array}{ll} (PN - QOF) \frac{\frac{L}{L_{\max}} - TG}{1 - TG} & \text{for } \frac{L}{L_{\max}} > TG \\ 0 & \text{for } \frac{L}{L_{\max}} \leq TG \end{array} \right\} \quad [2.7]$$

Where TG is the root zone threshold value for groundwater recharge.

2.6 HYDROLOGICAL TIME SERIES ANALYSIS

To evaluate the performance of the NAM rainfall-runoff model, the discharge time series were processed by means of a number of sequential processing tasks. These include separation of the river flow series in subflows, split of the series in nearly independent quick and slow flows hydrograph periods and extraction of nearly independent peak flows.

Most river flow series show quick flow and slow flow components. The quick flow component might be further split into overland flow/surface runoff and interflow/subsurface flow component. This classification allows separate evaluation

of the rainfall-runoff by Subflow separation techniques using a numerical digital filter (Chapman, 1991; Eckhardt, 2005).

A time series of total rainfall-runoff discharges can be separated into its Subflow by use of a Water Engineering Time Series Processing tool (WETSPRO).

It runs under Microsoft Excel. The tool combines the standard Excel spreadsheets for data input and presenting results and the standard Excel charts for plotting of results.

This is a generalization of the Chapman (1991) filter which is based on the linear reservoir modelling concept (Willems, 2004a).

The tool makes use of specialized techniques for:

- i) Separation of river flow series into the different Subflow components based on Subflow filter technique
- ii) Selection of independent peak flow and low flow values from the flow series based on hydrologic independence criteria
- iii) Separation of flow series in nearly independent quick flow and slow flow periods based on hydrograph separation techniques
- iv) Empirical flood frequency through Extreme Value Analysis

2.6.1 Subflow Separation and Filtering

To achieve the Subflow separation and filtering a numerical digital filter technique is used to split the rainfall-runoff time series in the hydrological Subflow of quick flow (overland flow and interflow) and slow flow components (baseflow/groundwater runoff). The numerical digital filter technique is based on the linear reservoir modelling concept as shown in Figure 2.10.

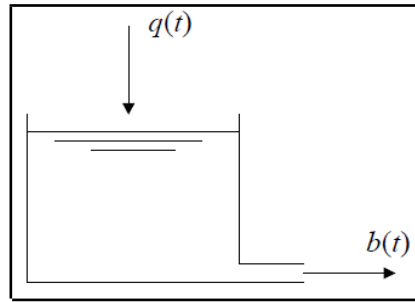


Figure 2.10: Input and output series of a linear reservoir model.

In a linear reservoir model (Figure 2.10) the outflow discharge $b(t)$ is dependent on the inflow discharge $q(t)$ as shown by equation 2.8.

$$b(t) = \exp\left(-\frac{1}{k}\right)b(t-1) + 1 - \exp\left(-\frac{1}{k}\right)\left(\frac{q(t-1) + q(t)}{2}\right) \quad [2.8]$$

Where

k = reservoir constant or recession time. The units of k is equal to duration Δt of the time step $[t-1, t]$

$q(t)$ = total inflow time series

$b(t)$ = the time series of the filtered component (with recession time k).

A generalization of the recursive digital filter (Figure 2.11) proposed by Chapman (1991) is recommended because it is able to link the parameters of the filter and the lumped hydrological characteristics of the catchment (Willems, 2009).

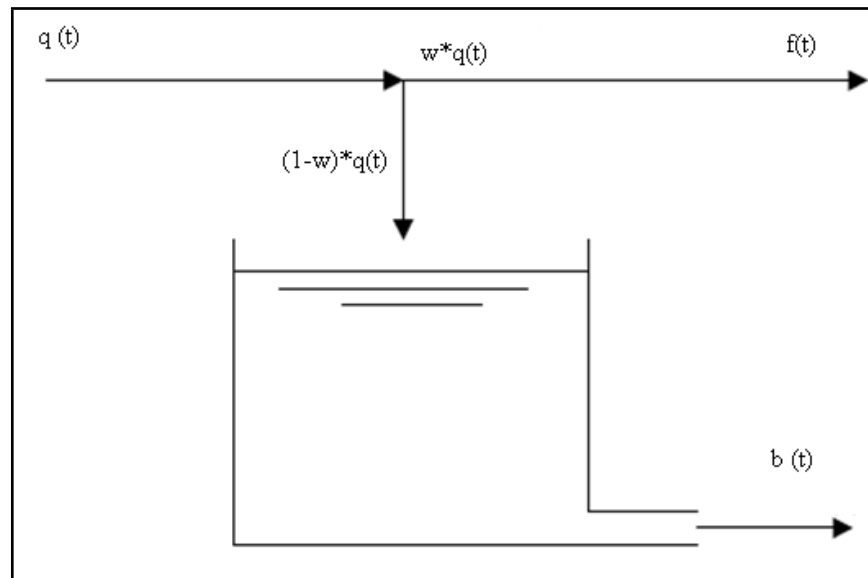


Figure 2.11: Generalization of the Chapman-filter

In Figure 2.11 the total time series $q(t)$ is the sum of the filtered component $b(t)$ i.e. the slow flow (base flow), and the higher frequency component $f(t)$, i.e. the quick flow (overland flow and interflow). The working principle of the filter can be explained as the routing of high frequency components ($f(t)$) through a linear reservoir with a fraction w representing the cumulative values in the series that is related to the filtered component. The parameter w represents the average fraction of the quick flow volumes over the total flow volumes and its' value can be estimated by numerical calibration.

2.6.2 Selection of Peak-Over-Threshold (POT) In the Discharge Series

A partial duration series (PDS), sometimes denoted as peak-over-threshold (POT) is an alternative to the annual maximum series (AMS) method for analysis of extreme hydrological events. It considers exceedance of a pre-selected threshold. Although the method can handle all kinds of extremes it has been primarily applied to flood studies (Rosberg and Madsen, 2004).

Willems (2009) proposed a method for selecting POT values based on a criteria for inter-event-time, the inter-event low flow discharge and the peak height (Figure 2.12). Two subsequent peak events are considered nearly independent when the following three conditions are fulfilled:

- i) The time length τ of the falling limb of the first event exceeds a time k_p

$$\tau > k_p$$

where k_p is the independency period and can be taken equal to the recession constant of the quick flow, or higher (e.g two or three times the recession constant).

- ii) The discharge drops down- in between the two events to a fraction lower than

$$f \text{ of the peak flow: } \frac{q_{\min}}{q_{\max}} < f \text{ or close to the baseflow } q_{base} : \frac{q_{\min} - q_{base}}{q_{\max}} < f$$

The fraction f is taken as the upper limit of the baseflow fraction in the peak flow (5% -15%)

- iii) The discharge increment $q_{\max} - q_{\min}$ has a minimum height q_{lim} (threshold):

$$q_{\max} - q_{\min} > q_{lim}$$

The procedure for peak flow selection has three parameters: K_p , f and q_{lim} . It is based on the concept that a peak flow event can considered largely independent from the next one, when the inter-event discharge drops down to a low flow condition or almost to the baseflow. Under this condition the quickflow component attributed to the peak flow events are indeed nearly independent (Willems, 2009).

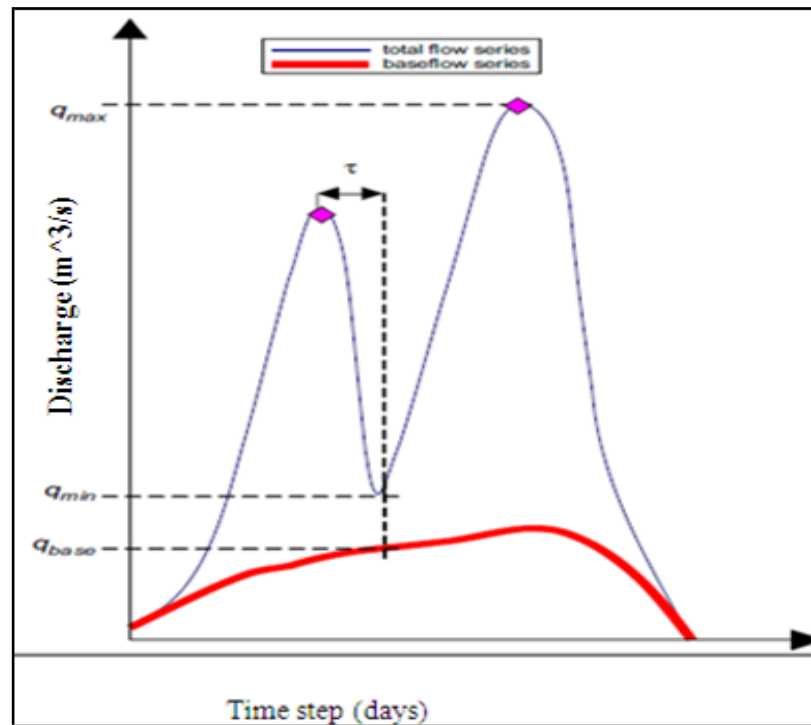


Figure 2.12: Parameters used in the criteria to select independent POT values

(After Willems, 2009)

2.6.3 Extreme Value Analysis

An extreme value analysis is required to accurately describe the recurrence rates of floods. This description can be done either based on long term time series of discharges or long term simulation results from mathematical models (Willems, 1998).

In extreme value analysis, the tail of the distribution describing the probability of occurrence of extreme events is analysed and modelled by making use of quantile plots. Making use of the different types of quantile plots, an analysis can be made of the shape of the distributions' tail, and discrimination can be made between heavy tail (pareto distribution), normal tail (exponential) distribution and light tail (weibull) distribution as summarized (Willems, 2009):

- a. The distribution tail can be considered normal ($\gamma = 0$) when:

- i) In the exponential quantile plot: the upper tail points tend towards a straight line.
 - ii) In the pareto quantile plot : the upper tail points continuously bend down.
 - iii) In the generalized quantile (UH) plot : the slope in the upper tail approaches the zero value.
- b. The distributions' tail is heavy ($\gamma > 0$) when:
- i) In the exponential quantile plot: the upper tail points continuously bend up.
 - ii) In the pareto quantile plot : the upper tail points towards a straight line
 - iii) In the UH-plot :the slope in the upper tail is systemetically positive.
- c. The distributions' tail is light ($\gamma < 0$) when :
- i) In the exponential quantile plot : the upper tail continuously bends down
 - ii) In the pareto quantile plot : the upper tail points also continuously bend down
 - iii) In the UH-plot :the slope in the upper tail is systematically negative.

In hydrological applications, the classes $\gamma = 0$ and $\gamma > 0$ most frequently appear. In many of these applications, the extreme value index γ has a small positive value and the distinction between the two classes is of primary importance (Willems, 2009).

2.6.4 The Return Period for the Extreme Events

Based on the selected peak flows (q_{\max}), the empirical cumulative frequency distribution of the peak flows can be plotted after ranking in descending order ($q_{(1)} \geq q_{(2)} \geq \dots \geq q_{(n)}$) and using a specific plotting position to calculate the empirical exceedence probability (P_i) for each flow value $q_{(i)}$. In order to calculate the return period for the POT extremes equation (2.9) is used (Willems 2009).

If $G(x)$ represents the probability distribution of the extremes above a threshold x_t calibrated to t observations in n periods (e.g. years), the return period, T of the exceedance level x_T then equals:

$$T = \frac{n}{t} \times \frac{1}{1 - G(x_T)} \quad [2.9a]$$

$$\text{But } G(x) = 1 - \left(1 + \gamma \left(\frac{x - x_t}{\beta} \right)^{1/\gamma} \right) \text{ if } \gamma \neq 0 \quad [2.9b]$$

$$G(x) = 1 - \exp\left(- \frac{x - x_t}{\beta} \right) \text{ if } \gamma = 0 \quad [2.9c]$$

Hence for exponential distribution:

$$T = \frac{n}{t} * \frac{1}{\exp\left(- \frac{x - x_t}{\beta} \right)} \quad [2.9d]$$

Where T = return period (years)

n = total number of years

t = number of exceedences of threshold level x_t

β = slope of the distribution quantile-quantile plot

x_t = threshold discharge

x = theoretical discharge

x_T is the T -year event

A Peak-Over-Threshold (POT) extreme value analysis was used to identify the independent maximum flow data points in the given set of daily flow data. The flow maxima data is filtered and then fitted to the Generalized Pareto Distributions (GPDs) to establish its extreme value index γ which is critical in shaping the tail of the distribution, Three categories can be identified for $\gamma < 0$, $\gamma = 0$ and $\gamma > 0$ for a given RGS. Daily independent maxima high flow series was extracted from the flow series using WETSPRO software and subjected to statistical analysis (Willems, 2004b).

2.7 HYDROLOGICAL AND METEOROLOGICAL DATA

Model calibration relies on the quality of data available. Hydrological data must be cleaned from random and systematic errors (Fekadu,1999).

2.7.1 Errors in hydrological/ meteorological data

The types of error encountered in hydrological data are:

- i) Instrument errors and change of measuring sites and techniques. These type of errors can be identified using mass curve and double mass curve analysis. The intercomparison plots of the same variables at adjacent stations can help to verify the consistency of data series.
- ii) Data inputing and computation errors. Errors can be revealed by time series plot and visual inspection of the graphs
- iii) Flow computation errors. Discharge rates are computed from continous stage records using an established rating curve (stage-discharge relationship) at a gauging site on a river. Some of the causes of errors in discharge computation include instability of the cross-section at the river bank and bed.

2.7.2 Data Quality Control

The consistency and continuity of rainfall data are very important in statistical analyses such as time series analysis for hydrological modelling. Both consistency and continuity may be disturbed due to change in observational procedure and missing observations (De Silva et al., 2007).

Inconsistency in a rainfall record can be identified by graphical or statistical methods such as double mass curve analysis, the Von Neumann ratio test, cumulative deviations, likelihood ratio test, and run test (Sergio, 2010).

The filling of the gaps generated by inconsistent data is essential, and different procedures and approaches are available to accomplish this task. The most common methods used to estimate missing rainfall data are Normal Ratio method, Inverse

Distance method, and Arithmetic Mean method/ Local Mean method (Chow et al., 1988), and Aerial Precipitation Ratio method (De Silva et al., 2007).

a) Arithmetic Mean method/ Local Mean method

If the normal annual precipitations at surrounding gauges are within the range of 10% of the normal annual precipitation at station X, then the Arithmetic procedure could be adopted to estimate the missing observation of station X (Chow et al., 1988).

b) Normal Ratio method

This method is used if any surrounding gauges have the normal annual precipitation exceeding 10% of the considered gauge (Chow et al., 1988).

c) Inverse Distance method

In this method, weights for each sample are inversely proportionate to its distance from the point being estimated (Chen, 2012).

d) Aerial Precipitation Ratio (APR) method

This method was developed based on spatial distribution of daily rainfall without accounting for the historical recurrence. The method leads the extension of point rainfall records to Thiessen Polygon areas. The APR method assumes the contribution of rainfall from surrounding stations is proportionate to the Thiessen polygon area claimed by each station without considering the missing gauge, when the station of missing values is excluded (De Silva, 1997).

2.7.3 Determination of Areal Rainfall

Single point precipitation measurement is quite often not representative of the volume of precipitation falling over a given catchment area. Rainfall over an area is usually estimated from a network of rain gauge stations. To calculate the spatially

distributed rainfall for an area, the point rainfall needs to be converted to areal rainfall (Shaw et al., 2011).

Standard and commonly used methods of deriving areal rainfall over a given area from rain gauge measurements at the rainfall stations are: Arithmetic means, Thiessen polygon, Isohyet, and Inverse Distance Weight. These methods yield good estimates in flat terrain, if the gauges are uniformly distributed and individual gauge catches do not vary widely from the mean (Ghanemi, 2011).

The Thiessen method is a widely recognized scheme proven to be reasonably accurate at modelling actual precipitation distributions (Al Hallaq et al., 2008).

The primary assumption is that areas closest to a precipitation station are more likely to experience similar rainfall conditions to those measured at the station location. Thiessen polygons are graphical techniques which calculate station weight based on the relative areas of each measurement station in the Thiessen polygon network. Thiessen polygons are often used to assign real weights of various points in a rainfall station to each polygon in runoff catchment. The weights are often used to calculate an area average rainfall for runoff catchments (Chow et al., 1988; Chen, 2012).

The general formula to calculate area weighted average precipitation is as given in equation 2.10.

$$MAR = \frac{P_1 A_1 + P_2 A_2 + P_3 A_3 + \dots + P_n A_n}{A_1 + A_2 + A_3 + \dots + A_n}$$

$$= \frac{\sum_{i=1}^n P_i A_i}{\sum_{i=1}^n A_i}$$

[2.10]

Where

MAR = mean areal rainfall

P_i = rainfall points of the stations located at the centroid of the polygons

A_i = areas of each polygon

n = no of gauges

The Thiessen weights are the ratio of the gauge's polygon area divided by the area of the catchment.

$$w_i = \frac{A_i}{A_T}$$

Where A_T =total basin areas

A_i = area defined by the Thiessen polygon

2.8 ASSESSMENT OF MODEL PERFORMANCE

Since it is difficult to characterise the performance of rainfall- runoff models with only one statistic, use is made of a set of multiobjective set of correlated statistics and supporting graphical criteria. Statistical measures alone have limitations because the indices are not effective in communicating qualitative information such as trends, types of errors and distribution patterns is achieved by graphical display of simulated and observed flows (Willems,1998).

The ability of the model to simulate the observed stream flow discharges was tested with the following goodness-of-fit statistics:

2.8.1 The Coefficient of Determination (R^2)

The coefficient of determination measures how much of the variance is explained by the model. It is a good measure of how well the model fits the data. It is defined as the square of the correlation coefficient as given in equation 2.11 (Krause et al., 2005).

$$R^2 = \left[\frac{\sum_{i=1}^n (O_i - \bar{O})(P_i - \bar{P})}{\sqrt{\sum_{i=1}^n (O_i - \bar{O})^2} \sqrt{\sum_{i=1}^n (P_i - \bar{P})^2}} \right]^2 \quad [2.11]$$

Where O_i = Observed discharge (m^3/s)

P_i = Predicted or simulated flow (m^3/s)

\bar{O} = Mean of the observed discharge (m^3/s)

\bar{P} = Mean of the predicted or simulated flow (m^3/s)

n = number of data points (sample) used for the calibration or validation

The range of R^2 is from 0 to 1, which describes how much of the observed dispersion is explained by the prediction. A value of zero equates to no correlation, while a value of 1 represents dispersion of the prediction equal to that of the observation. The drawback of using R^2 for model evaluation is that R^2 results can be misleading if the model in general is over- or underpredicting. This problem can be detected by comparing predicted and observed values within the period of study (Krause et al., 2005; Nejadhashemi et al., 2011).

2.8.2 Mean Error (ME)

Based on a number of different observations of the discharge the ME is given by equation (2.12).

$$ME = \bar{E}_Q = \sum_{i=1}^n \frac{Q_m(i) - Q_o(i)}{n}$$

$$\bar{E}_Q = \sum_{i=1}^n \frac{E_Q(i)}{n} \quad [2.12]$$

Where E_Q = model residual i.e the difference between each flow observation (Q_o) and the corresponding model result (Q_m). the ME is commonly used to measure the average systematic difference between the simulated and the observed values (Willems,1998).

2.8.3 Root Mean Square Error (RMSE)

This method is regarded as a measure of absolute error between the computed and observed flows. The RMSE values tend to be zero for perfect agreement between observed and simulated values. RMSE is defined by the relation of equation (2.13).

$$RMSE = \sqrt{\frac{\sum_{i=1}^n (Q_o(i) - Q_m(i))^2}{n}} \quad [2.13]$$

Since the RMSE is a function of the same magnitude of observed flows, only results obtained by different models when applied to the same catchment and for the same period can be compared. The requirement of a good model is to obtain a small root mean square error as much as possible (Shamsudin, 2002).

2.8.4 Squared Standard Deviation of Model Residuals

The total uncertainty in the model results (the model output) can be quantified by calculation of the squared standard deviation (equation 2.14) of the differences between modelled and observed runoff values (Willems,1998).

$$S^2_{EQ} = \sum_{i=1}^n \frac{\left(E_Q(i) - \bar{E}_Q \right)^2}{(n - 1)} \quad [2.14]$$

Where, E_Q (model residual) is the difference between each flow observation Q_o and the corresponding model result Q_m .

\bar{E}_Q (mean error) is the average systematic difference between the simulated and the observed values.

2.8.5 Bias of Residuals

The bias and efficiency indices allow comparison of model performance when applied to various ranges of catchments. Positive values of bias indicate overestimation, whereas negative values indicate underestimation of flows (Willems,1998). Bias of residuals is calculated as shown in equation (2.41).

$$Bias (\%) = \frac{\sum_{i=1}^n [Q_m(i) - Q_o(i)]}{\sum_{i=1}^n (Q_m)} \times 100 \quad [2.15]$$

Where Q_m =Modelled daily flow (m^3 / s)

Q_o =Observed daily flow (m^3 / s)

n = Total number of data points used for calibration or validation.

2.8.6 Graphical Goodness-of-Fit Plots

Goodness-of-fit statistics such as equations:(2.38), (2.39), (2.40) and (2.41) summarises goodness-of-fit information only in a few numbers and values. Willems (1998) proposed that the model performance can be evaluated in a detailed way by complimenting the statistics with graphical goodness-of-fit plots. These plots compare the Q_m and Q_o values. The calculation of these plots were achieved through the use of WETSPRO- Software .The graphical model evaluation were based on the following plots:

- i) Scatter plot for peak flow maxima (after Box-Cox-transformation) in order to evaluate the peak flow maxima.
- ii) Comparison of cumulative volumes for total flow, overland flow, interflow and baseflow in order to evaluate the overall water balance of the model and the distribution between subflows.
- iii) Extreme value distibution peak flow maxima in order to evaluate model performance in extreme high flow conditions.

2.8.7 Model Calibration

Model calibration is a process in which raw hydrological models are refined adequately to represent observed flows throughout the simulation period and the study area. It is a process where in the model parameters are tuned within justifiable limits to match field measurements. The accuracy of a model prediction for different flows and time periods depends on the quality of the calibration process. Reasonable model calibration provides confidence in the application of a model for different time periods and hypothetical scenarios (Rohan, 2009).

2.8.8 Model Verification/Validation

Model validation can be defined as the comparison of model output to observed data for data set that was not included in the calibration process of the model. Often the model performance during calibration is used as a measure of the predictive capability of a model. However, the credibility of a site specific model's capability to make predictions about a reality must be evaluated against independent data (Refsgaard , 2007).

In designing suitable model validation tests a guiding principle should be that a model should be tested to show how well it can perform the kind of task for which it is specifically intended (Klemes, 1986). He proposed the following types of test schemes corresponding to different situations.

- i) The split-sample test is the classical test, being applicable to cases where there is sufficient data for calibration. The available data record is divided into two parts. A calibration is carried out on one part and then a validation on the other part. Both the calibration and validation exercises should give acceptable results.
- ii) The proxy-basin test should be applied when there is not sufficient data for a catchment in question. If for example, streamflow has to be predicted in ungauged catchment Z, two catchments X and Y within the region should be selected. The

model should be calibrated on catchment X and and validated on catchment Y and vice versa. Only if the two validation results are acceptable and simillar can the model command a basic level of credibility with regard to its ability to simulate the streamflow in catchment Z adequately.

CHAPTER THREE

MATERIALS AND METHODS

3.1 INTRODUCTION

This chapter describes the input data, their source, data processing and the approach adopted to determine the impact of reservoir storage on flood mitigation in the Nzoia River basin. The overall methodology involved model set-up and the calibration and validation of the NAM module and MIKE 11 model for use in predicting the rainfall-runoff from the reservoir catchments to the dam sites and hydrodynamic stream flow

routing from the reservoirs to the flood plain. Finally, reservoir flow regulation and the application of the model in scenario modelling are discussed.

3.2 DATA COLLECTION

The required input data for this study were daily rainfall, daily stream flow, daily evapo-transpiration, topographic maps and reservoir characteristics. Collection of the required rainfall data involved visiting various data sources including Kenya Meteorological Department (KMD) for rainfall and evaporation data, Water Resource Management Authority (WRMA) provided the stream flow data, Survey of Kenya provided the topographic maps and the reservoir information was obtained from a study done by TAHAL (2007). Daily data records of rainfall, stream flow and evaporation were required as input to both NAM and MIKE 11. All the input data for this study are discussed briefly in the following subsections.

3.2.1 Weather Data

Rainfall data were available for twenty five (25) rainfall stations in and around the Nzoia basin and evaporation was available for four weather stations. The recommended minimum density of evaporation stations network within a uniform physiographic area is 50,000 km² per station (WMO, 1994). Appendix A, Table A1 and Table A2 gives a summary of the daily rainfall data and the evaporation data collected respectively. Figure 3.1 gives the location of the rainfall stations in and around the catchment.

3.2.2 Stream Flow Data

The stream flow data were available for four river gauging stations (RGS) in the Nzoia basin. These gauging stations were 1EF01, 1EE01, 1CE01, and 1DA02 (Figure 3.2). The stations had data records ranging from 1970-2009. Appendix A, Table A3 gives a summary of the daily stream flow data, whereas Figure 3.2 shows the

locations of the river gauging stations and the proposed dam sites in Nzoia River basin.

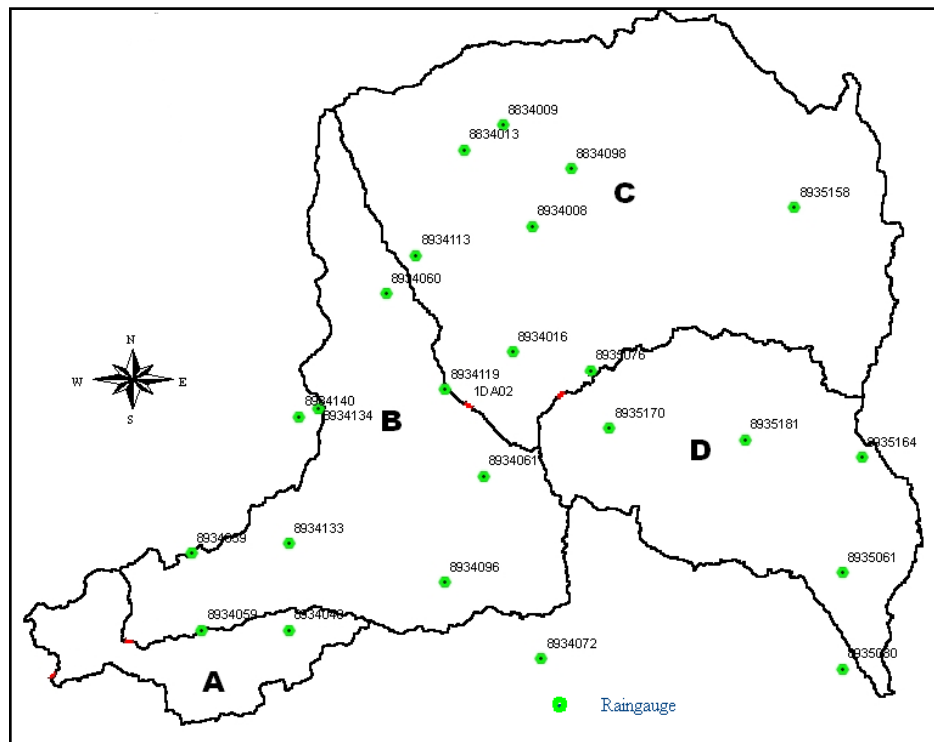


Figure 3.1: Rain gauge network in and around the Nzoia Catchment

3.2.3 Proposed Reservoirs

Three dam sites for construction reservoirs for flood control have been proposed by the Government (WKCDD & FMP, 2006). These are dam sites: 34B, 35 and 42A. The locations of the proposed reservoirs' sites are also shown in Figure 3.2, Appendix A, Table A4 gives the Elevation-Area-Volume relationships characteristics of the proposed reservoirs.

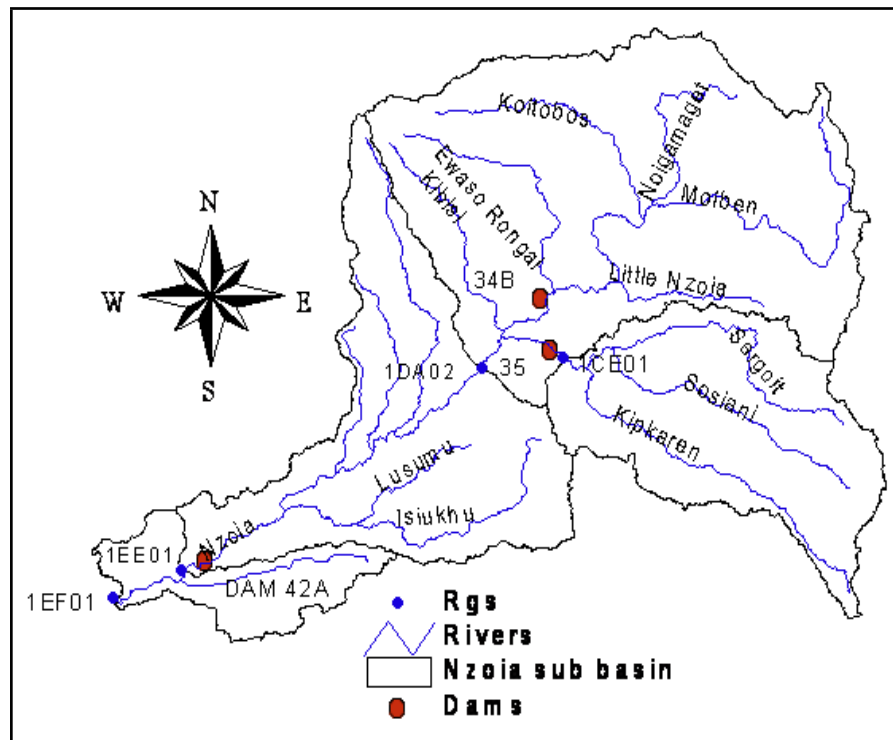


Figure 3.2: The River gauging stations and the proposed reservoirs

3.3 DATA PROCESSING AND QUALITY CONTROL

Rainfall-runoff modelling of a river basin is an important element in the hydrologic analysis to support water resources planning and flood forecasting. Before applying any hydrological model, data analysis should be executed first, to have a complete rather than partial rainfall records (Mauricio and Willems, 2010).

3.3.1 Filling Data Gaps

In this research the Inverse Distance Weighting (IDW) method was used in filling the data gaps. This is the most acceptable method and is widely used for determining the missing rainfall for any scientific analysis (Patra, 2008).

The inverse distance method yields the lowest error when six or seven index gauges are used (Chen, 2012).

$$P_x = \frac{\sum_{i=1}^N \frac{1}{d^2} P_i}{\sum_{i=1}^N \frac{1}{d^2}} \quad [3.1]$$

Where, P_x = estimate of rainfall for the missing values

P_i = rainfall values of rain gauges used for estimation

d_i = distance from each location the point being estimated

N = No. of surrounding stations

From equation 3.0, using six surrounding index gauges the equation 3.1 becomes:

$$P_x = \frac{\sum_{i=1}^6 \frac{1}{d_i^2} P_i}{\sum_{i=1}^6 \frac{1}{d_i^2}} \quad [3.2]$$

$$P_x = \frac{\frac{1}{d_1^2} \times P_1 + \frac{1}{d_2^2} \times P_2 + \frac{1}{d_3^2} \times P_3 + \frac{1}{d_4^2} \times P_4 + \frac{1}{d_5^2} \times P_5 + \frac{1}{d_6^2} \times P_6}{\frac{1}{d_1^2} + \frac{1}{d_2^2} + \frac{1}{d_3^2} + \frac{1}{d_4^2} + \frac{1}{d_5^2} + \frac{1}{d_6^2}} \quad [3.3]$$

P_x = estimate of rainfall for the missing values

P_i = rainfall values of index rain gauges used for estimation for the surrounding stations

d_i = distance from each rain gauge location and the point being estimated.

From equation (3.1), the missing rainfall P_x was interpolated from the nearest six stations by utilizing a Microsoft Excel program (Appendix A, Figure A1).

3.3.2 Density of Rain Gauges

The ratio of total area of the catchment to the total number of gauges in the catchment is defined as rain gauge density. Thus the rain gauge density gives the average area served by each gauge. The optimal number of gauges for estimating the mean areal rainfall over the Nzoia basin was obtained by the statistical analysis as shown in equation 3.3 (Reddy, 1992).

$$N = \left(\frac{C_v}{E_p} \right)^2 \quad [3.4]$$

Where

N = the optimal number of stations

n = number of existing stations

E_p = the allowable percentage of error in estimation of mean areal rainfall

C_v = is the coefficient of variation of the rainfall from the existing stations (n) in percentage

The coefficient of variation (C_v) was calculated by applying the following steps on the data of the existing n (25) stations.

i) Calculate the mean of rainfall from equation: $P_{av} = \left(\frac{1}{n} \right) \sum P_i$ [3.5]

ii) Calculate the standard deviation as: $\sigma_{n-1} = \left[\frac{1}{(n-1)} \sum (P_i - P_{av})^2 \right]^{1/2}$ [3.6]

iii) Compute the coefficient of variation as $C_v = \frac{\sigma_{n-1}}{P_{av}} \times 100$ [3.7]

The allowable percentage of error E_p is normally taken as 5% -10%. If the allowable percent of error in estimating the mean rainfall is taken higher, the catchment will require fewer number of rain gauges and vice versa. If $N < n$ the existing network estimates the average depth of rainfall with an error less than the allowable value of E_p and no more gauges are required to be installed. If $N > n$, the additional gauges required is given by (N-n). Annual rainfall values are normally used in the above

analysis. Additional stations can be established at the appropriate locations giving an even distribution over the catchment (Reddy, 1992; Patra, 2008).

Based on the annual rainfall information from the 25 stations in Nzoia basin the statistical parameters were calculated as:

$$P_{av} = 1405.4 \text{ mm}$$

$$\sigma_{n-1} = 341.7$$

$$C_v = 24.3$$

$$N = 24$$

Based on a 5% permissible error the minimum required number of stations is 24. Hence the 25 rain gauge stations utilized for computing the mean areal rainfall (MAR) are adequate for the Nzoia basin.

3.3.3 Consistency of Rainfall Data

The consistency and continuity of rainfall data are very important in statistical analyses such as time series analysis. Both consistency and continuity may be disturbed due to change in observational procedure and missing observations. When analysing rainfall data, it is essential to check the consistency of the records of the rainfall stations (De Silva et al., 2007).

For Nzoia catchment, the missing data were first estimated using the inverse distance weighting method, and then consistency analysis applied.

Double mass curve method (Gupta, 1989), was used to check the consistency of the stations. This technique is based on the principle that when each recorded data comes from the same parent population, they are consistent. A straight line graph indicates data consistency, whereas non-straight line would indicate data that have been subjected to various changes such as changes in recording stations or shift in

observation practices. A change in slope is normally taken as significant only if it persists for more than five years (Reddy, 1992).

3.3.4 Catchment Delineation

Catchment delineation is the process of identifying the drainage area of a point or a set of catchment discharge points or catchment outlet, and can be based on digital elevation models rather than contour lines (Topographic sheets). Arc GIS 9.2 was used to delineate the catchment and sub catchments boundaries. The stream paths, possible flow directions and catchment divides were determined by using the 30m by 30m resolution digital elevation model (DEM) for Nzoia River basin in the Arc GIS environment.

In the delineation process, the DEM of the Nzoia River basin was loaded to Arc GIS 9.2. This map was projected to the WGS1984 projection system, and then the DEM was pre-processed to remove and fill all the non-draining zones (sinks and spires). The sub basins were delineated by specifying the location of the river gauging stations (RGS). These RGS (1EF01, 1EE01, 1DA02, and 1CE01) formed the basin target discharge outlets points for sub basins A, B, C and D respectively as shown in Figure 3.3. The DEM elevations were used to determine the flow direction. The output cells with a high flow accumulation are areas of concentrated flow and were used to identify stream channels, whereas output cells of zero accumulation are local topographic highs and were used to identify catchment divides.

The proposed reservoirs: 34B, 35 and 42A are found in sub basins C, D and B respectively. Whereas dam sites 35 and 42A are at the catchment outlets, dam site 34B is slightly upstream the river gauging station 1DA02, therefore an un-gauged catchment E was created for dam site 34B (Figure 3.6). The NAM parameters obtained in catchment C were applied to the un-gauged sub basin E during the rainfall-runoff modelling of inflows into the reservoir. The delineated dam sub basins

were used in the rainfall-runoff modelling for the computation of discharge inflows into the proposed dams.

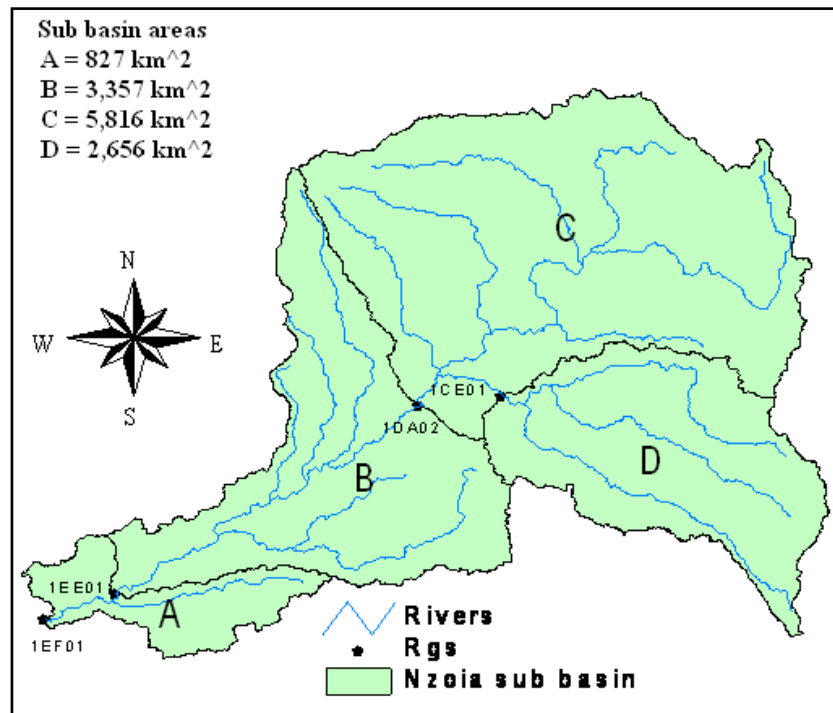


Figure 3.3: The River Nzoia sub basins

3.3.5 Computation of Mean Areal Rainfall (MAR)

Areal rainfall extension that works under Arc View GIS environment was used to delineate the Thiessen polygons and to calculate the areal rainfall. The area of each polygon within the sub-catchment is then divided by the sub-catchment total area and expressed as a percentage to obtain the Thiessen weights which are then multiplied by the daily rainfall amount for each gauging station formed by the polygon in the sub-catchment to give the areal contribution of the point rainfall. The sum of these areal contributions of the point rainfall gives an estimation of the MAR over the sub basin. The constructed Thiessen polygons enclosing the corresponding rainfall stations in the Nzoia catchment is presented in Figure 3.4.

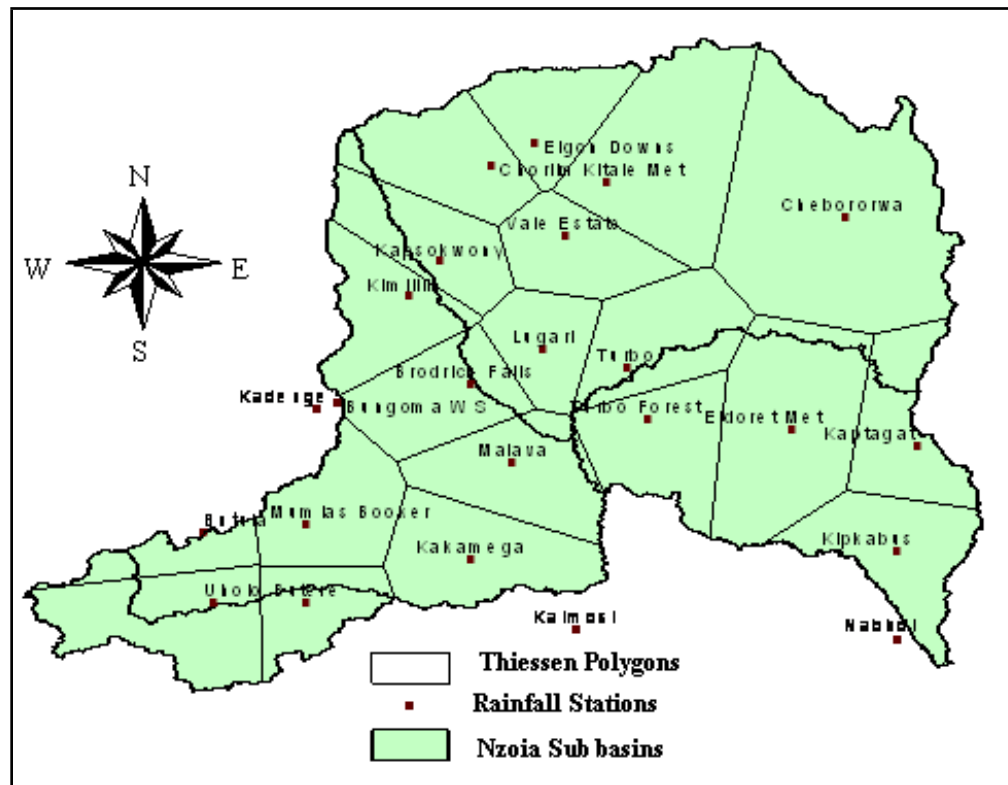


Figure 3.4: Thiessen Polygons constructed for Nzoia sub basins

3.4 SET-UP OF THE NAM MODULE

The study catchment was split into four (4) sub basins as shown in Figure 3.3. The NAM model was set up with observed series of daily rainfall and ETo averaged over the dam catchments. The model structure was fixed with three storage elements, surface, root zone and groundwater storages, and linear reservoir models describing the three storages (DHI, 2008).

3.4.1 NAM Models for the Sub-Basins

Input data for the NAM sub catchments consisted of time series of daily rainfall and potential evapo-transpiration. The NAM parameters were found by model calibration by comparing the model simulated runoff against the time series of observed daily stream flow records of the RGS at the outlet of each sub basin. Each sub basin model requires the following input:

- i) Area of each sub- basins as shown in Figure 3.3.

- ii) Daily time series of Mean Areal Rainfall (MAR). The MAR over the sub basin was determined by the Thiessen polygon method to find the weighting factors of each rainfall station (Figure 3.4) located inside and around each sub basin.
- iii) Potential daily evaporation time series (ETo). Evaporation data was obtained from A evaporation and a pan coefficient of 0.7 (WMO, 1994) was applied to transform pan evaporation to potential evaporation. The resulting average evapo-transpiration for the period 1976-1984 from two meteorological stations (Appendix A, Table A2) in the Nzoia basin was used together with the MAR as input to the NAM module.
- iv) Daily river flow series. The daily stream flow data for the period 1976-1984 from the RGS: 1DA02, 1CE01, 1EE01 and 1EF01 were used for calibration and validation purposes of the model for each sub basin. The discharge was divided into two parts. The period 1976-1980 was used for model calibration whereas the period 1981-1984 was used for model verification/validation.

3.4.2 NAM Calibration

Calibration is an iterative exercise wherein model parameters are tuned within justifiable limits (Appendix C, Table 1) to match observed measurements. In the NAM model the parameters and variables represent average values for the catchment. In general, it is not possible to determine the values of the NAM parameters on the basis of the physiographic, climatic and soil physical characteristics of the catchment because most of the parameters are of empirical and conceptual nature. Thus, the final parameter estimation is performed by calibration against time series of hydrological observations (DHI, 2007; Beven, 2008).

The process of model calibration was done manually by trial and error parameter adjustment and automatic calibration to obtain a good fit between the simulated and observed hydrographs. In manual calibration parameter assessment was achieved through a number of simulation runs along the flow process shown in Figure 3.5.

Observed discharge data at the catchment outlet for the four river gauging stations: 1EF01, 1EE01, 1DA02 and 1CE01 were required for comparison with the simulated runoff for model calibration and validation.

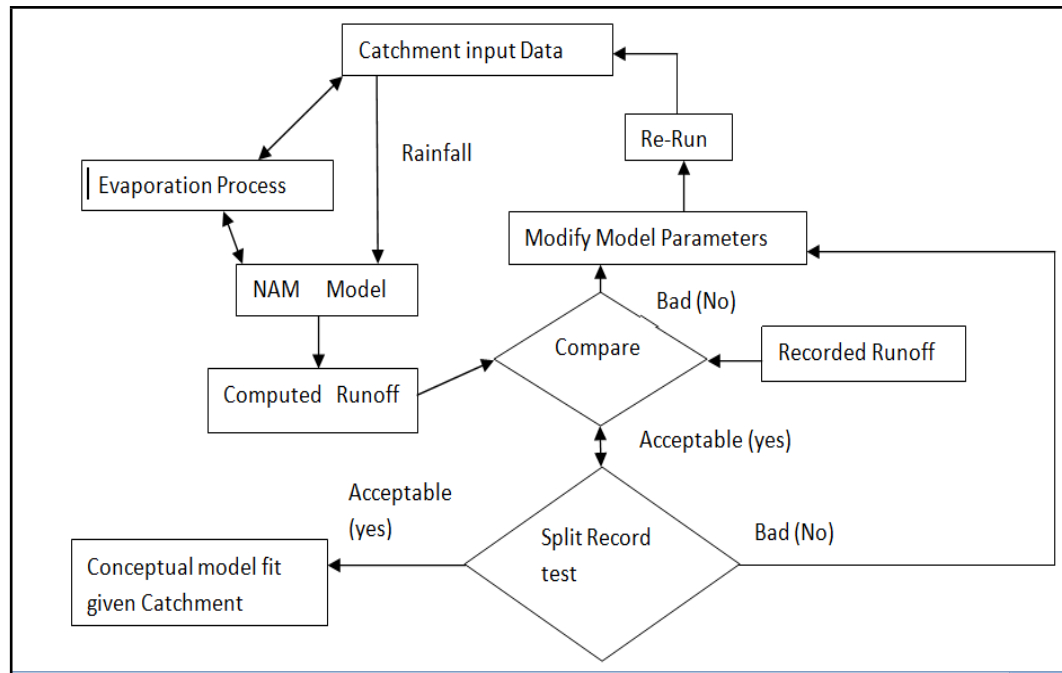


Figure 3.5: NAM calibration process flow diagram

The automatic calibration was to speed up the calibration process and to limit and constrain the most important parameters to a certain range of acceptable values (Appendix C, Table 1). The automatic calibration routine is based on a multi-objective optimization strategy in which four different objectives can be optimized simultaneously. The routine uses the overall volume error (agreement between the average simulated and observed runoff), the overall root mean square error (RMSE) that depicts the agreement of the shape of the hydrograph, and average RMSE of peak flow events and the RMSE of low flow events.

Madsen (2000) presented four different performance measures that emphasized on different aspects of the hydrograph and investigated all possible combinations of each pair of performance measures as objective functions for calibration. In NAM model,

auto calibration is available for nine (9) important parameters representing the surface zone, root zone and ground water storages. The objective functions are:

- i) Agreement between the average of simulated and observed sub basin runoff in order to give a good water balance. This is the overall volume error ($F_1(\Phi)$).

$$F_1(\Phi) = \left| \frac{1}{N} \sum_{i=1}^N [Q_{obs,i} - Q_{sim,i}(\Phi)] \right| \quad [3.8]$$

Where

$Q_{obs,i}$ = the observed discharge at time i.

$Q_{sim,i}$ = The simulated discharge at time i.

Φ = The set of model parameters to be calibrated.

N = The number of time steps in the calibration period.

- ii) Overall Root Mean Square Error (RMSE)

The coefficient of determination (R^2) is a transformed and normalised measure of the overall RMSE (normalised with respect to the variance of the observed hydrograph). Thus minimization of RMSE corresponds to maximization of R^2 .

$$F_2(\Phi) = \left[\frac{1}{N} \sum_{i=1}^N [Q_{obs,i} - Q_{sim,i}(\Phi)]^2 \right]^{1/2}$$

[3.9]

- iii) Average RMSE of peak flow events.

Peak flow events are defined as periods where the observed discharge is above a specified threshold level. The average RMSE of the peak flow events is given by equation (3.9).

$$F_3(\Phi) = \frac{1}{M_p} \sum_{j=1}^{M_p} \left[\frac{1}{n_j} \sum_{i=1}^{n_j} [Q_{obs,i} - Q_{sim,i}(\Phi)]^2 \right]^{1/2} \quad [3.10]$$

Where

M_p =The number of peak flow events in the calibration period

n_j =The number of time steps in each individual peak flow.

Visual and numerical methods were used in the assessment of the goodness-of-fit between the simulated and observed stream flow.

3.4.3 NAM Validation/Verification

A model validity test was performed for the purpose of demonstrating that the calibrated model was capable of making sufficiently accurate predictions. Daily stream flow data for the period 1976 -1980 were used for calibration and 1981-1984 for model verification/validation. The NAM model parameter values obtained during calibration exercise were used in the validation. The resulting streamflow was compared to the observed discharge at the gauging stations.

3.5 SET-UP OF MIKE 11 HYDRODYNAMIC MODEL

The data requirements of the hydrodynamic model are:

- i) Observed daily discharges and water levels.
- ii) Cross-sections of the river. In this study four cross sections were available for four river gauging stations: Webuye (1DA02), Kipkaren (1CE01), Nzoia Market (1EE01) and Rwambwa (1EF01).
- iii) Initial conditions. MIKE 11 has three options of incorporating the initial conditions. In the first option, auto start: it computes the initial values of stage and discharges from the steady state conditions of the given hydrographs. In the second

option the known initial value of stage and discharge can be given to the model while in the third option a hot start computation is possible whereby it automatically abstracts the initial values of stage and discharges from the existing result file, previously computed. The first option of auto start was used in carrying out the HD computations for the Nzoia River reach.

iv) Boundary conditions. The upstream boundary conditions are NAM rainfall-runoff discharge from sub basins E and D. The downstream boundary conditions are the water levels at Rwambwa river gauging station (1EF01).

The rainfall-runoff simulations from the NAM modelled sub basins E and D were introduced into MIKE 11 hydrodynamic model of the river network as upstream boundary input data. Between the two upstream dams (34B and 35) and the downstream boundary at Rwambwa river gauging station (1EF01), the simulated NAM rainfall-runoff time series was uniformly distributed along the Nzoia River branch as shown in Figure 3.6. The results of the Hydrodynamic (HD) model are discharges and water levels.

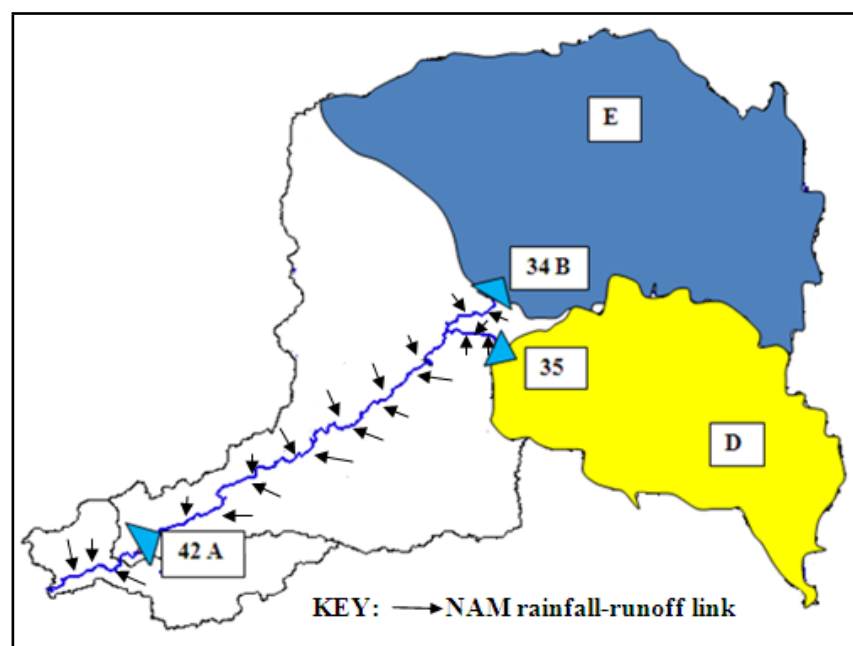


Figure 3.6: Dam catchments and NAM rainfall- runoff link to MIKE 11

To setup the modelling system for this basin the parameters such as river network, upstream and downstream boundary data of the time series of discharge and water levels, hydrodynamic and rainfall-runoff parameters were inputted to the model. Each of the parameters was created separately as explained hereunder.

3.5.1 Network Setup

The network setup was done by digitizing the river networks and branch connections in the modelled river network (Figure 3.7) from the shape files obtained during catchment delineation of the Nzoia River basin. The river network shape file in UTM Zone 36 projection was imported to Arc View 3.3 for on-screen digitization for use in MIKE 11 hydrodynamic modelling. All the river alignments were joined up according to the shape files created from a 30m by 30m resolution DEM.

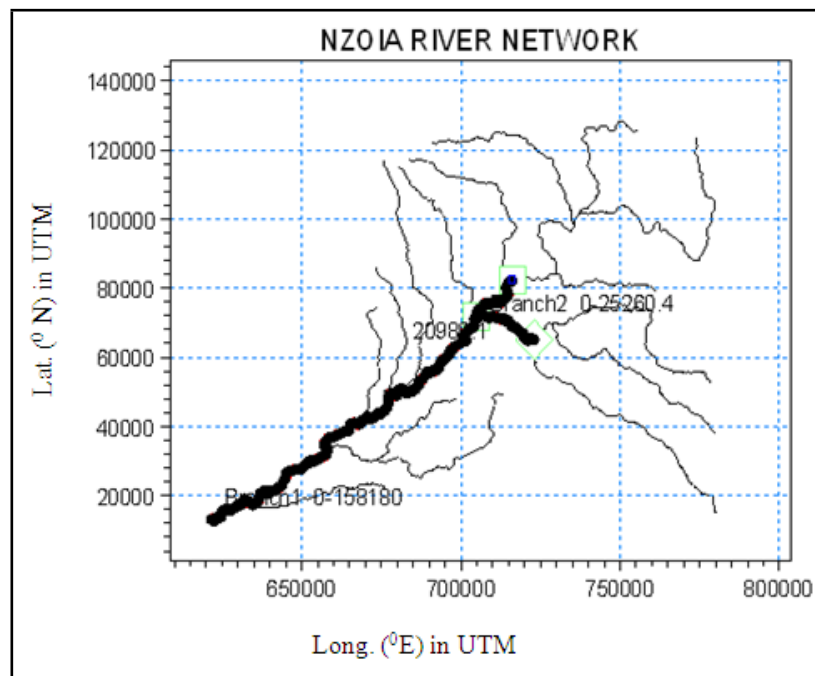


Figure 3.7: Nzoia River Basin Network Setup

3.5.2 Boundary Conditions

For one dimensional model, boundary conditions are required at the upstream and downstream ends, and at locations of any additional fixed constraints in river flow.

The model used the NAM simulated stream flows as upstream boundary conditions from basin C and basin D, and the river stages (water level) from RGS 1EF01 as downstream boundary conditions.

This setup is the most important part of the modelling system. It contains the Hydrodynamic data that need the daily time series data of all the river discharge and water level values. A daily time series of the discharges of Nzoia basin from sub basin C (Webuye) and sub basin D (Kipkaren) were used in the setup of the upstream boundary conditions whereas the water levels at Rwambwa gauging station (1EF01) were used as the downstream boundary data respectively. The setup is shown in Figure 3.8 (a) to (c).

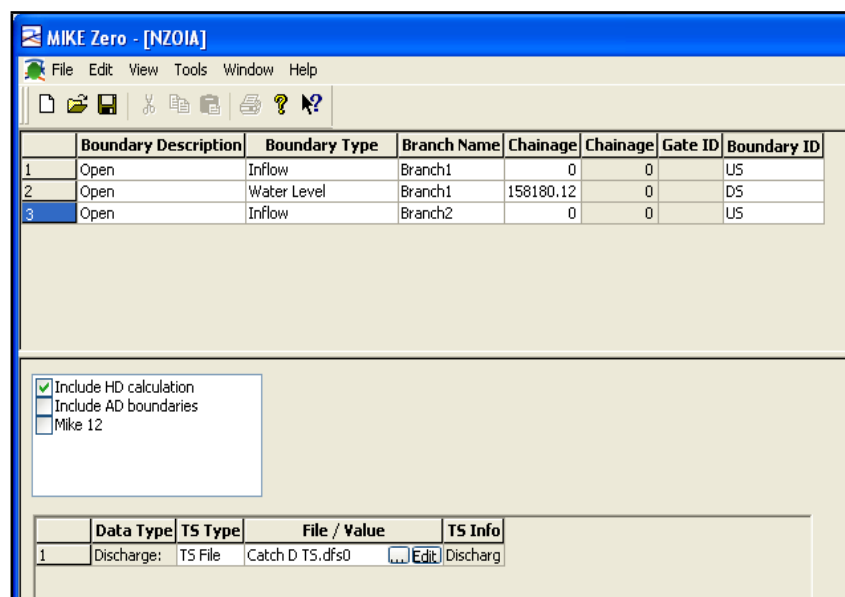


Figure 3.8 a: Hydrodynamic boundary data Setup window

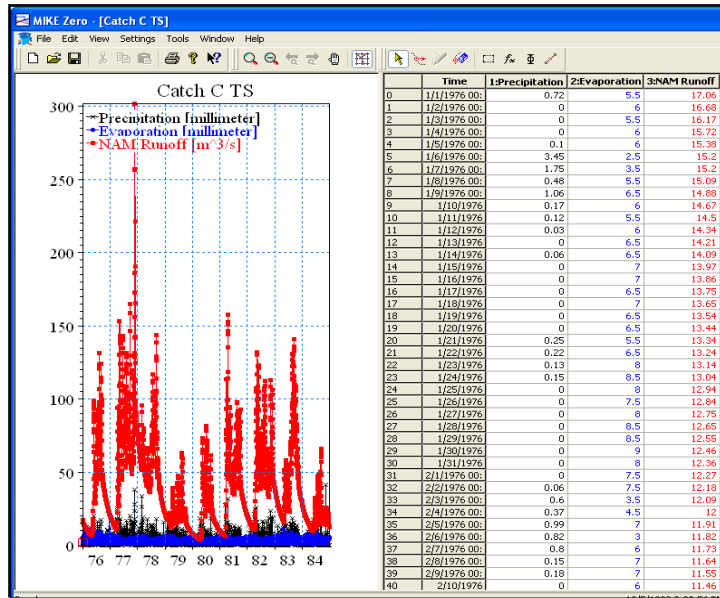


Figure 3.8 b: NAM runoff time Series upstream boundary window

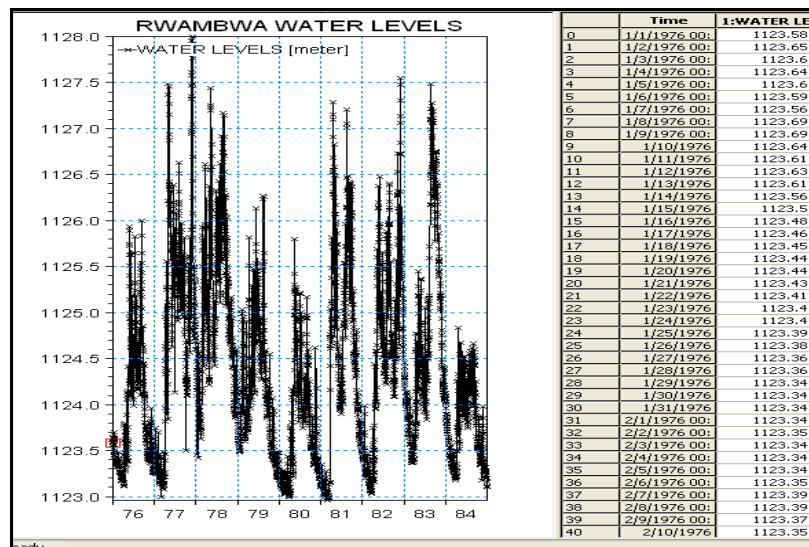


Figure 3.8 c: Water level time series at downstream boundary window

3.5.3 Hydrodynamic Modelling

This setup was done to input all the initial bed resistance (Manning’s n) and discharge data for every modelled reach of the river. It also needs many other parameters as shown in Figure 3.10, but the water level and discharge were the only parameters considered in the HD modelling.

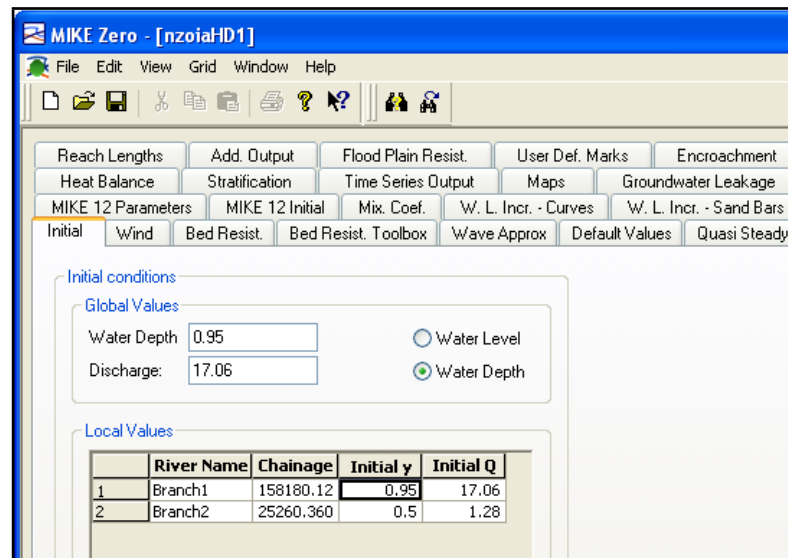


Figure 3.9: Hydrodynamic initial parameters window

3.5.4 Simulation

Simulation is the final stage of the modelling setup where it simulates all the parameter data that were setup in the model. MIKE 11 Hydrodynamic model needs to call in all the following parameter files (Figure 3.7 – Figure 3.9) to run the simulation:

- i) Network of river data (.nwk 11)
- ii) Cross section data (.xns 11)
- iii) Boundary data (.bnd 11)
- iv) Hydrodynamic parameters (.hd 11)
- v) Results file (.res 11)

The simulation will provide the result of discharge and water level for the whole modelled system of the Nzoia River Basin. The input setup is as shown in Figure 3.10.

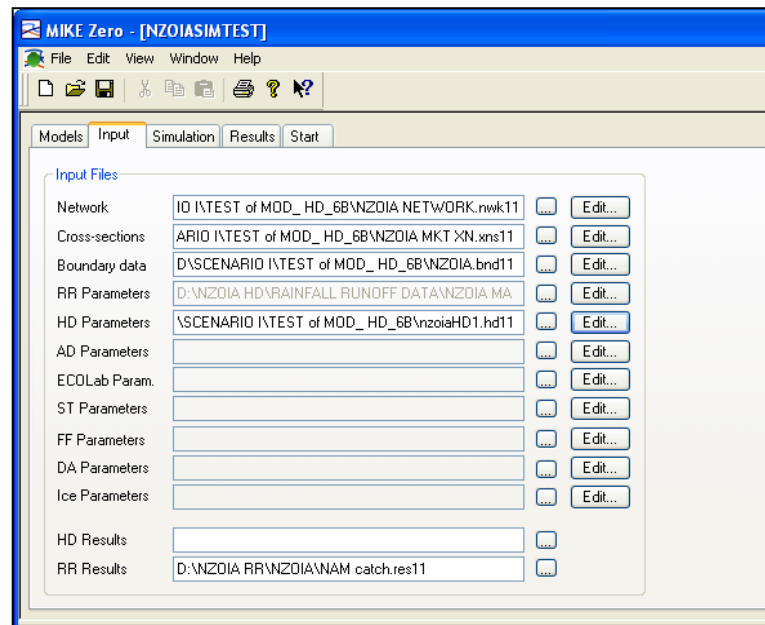


Figure 3.10: Simulation input setup window

3.5.5 MIKE 11 Model Calibrations and Validation

The calibration was done by comparing the simulated hydrograph and discharge measurements at the gauging stations. These comparisons can indicate how to adjust the Manning's n along the river reach.

From these comparisons the Manning's n of the routing river elements along the river were adjusted until the best fitted hydrographs of the simulated and observed discharges were obtained. Model validation was checked for hydrograph shape, hydrograph maxima, and water balance by cumulative volume.

3.6 MODEL PERFORMANCE EVALUATION

Model performance was evaluated using coefficient of determination (R^2), Root-Mean-Square Error (RMSE), and graphical methods. The graphical methods were optimized by means of a multi-criteria model evaluation protocol included in the WETSPRO tool as described by Willems (2009). The WETSPRO tool was used to conduct the Subflow filtering, Peak-Over-Threshold selection and related hydrograph separation and construct the model evaluation plots for the simulated and observed

flows in calibration and model verification. This model performance evaluation method includes a multi-objective set of goodness-of-fit statistics and complimentary graphs.

3.6.1 Extreme Value Analysis

The one dimensional simulation of the river network without reservoir was first undertaken using MIKE 11 hydrodynamic model. After calibration and validation of the model, the Peak-Over-Threshold events from the simulated flows were selected, the values ranked in descending order, extreme value distribution fitted and the calibration of the theoretical extreme value distribution parameters obtained for the condition of the river system with and without the dams.

In classical approach, annual maximum flow is commonly used for estimating the return period. The length of the data period is the major concern in this approach. If the length of the data is short, the number of annual maxima is less thus introducing large uncertainty while performing extreme value analysis (Boukhris et al., 2008).

To reduce this uncertainty, independent Peak-Over-Threshold (POT) values for daily stream flow data were used in this research. Selecting independent events for extreme value analysis was vital in order to ensure that the resulting distribution was comprised of unrelated events, thus enabling unbiased analysis to be done.

The identification of extreme events by POT approach was performed using a Water Engineering Time Processing tool (WETSPRO). The selection was based on the method independent of base flow. The parameters calibrated were the recession constant, parameter f , and the minimum peak height (q_{lim}). The next step was to analyze these data separately for distribution plots. This was done by using hydrological extreme value analysis tool, ECQ (Willems, 2004b).

The type of the distribution (heavy tail, normal tail, or light tail) was judged based on behaviour of the tails and its slope in different distribution plots. In the ECQ software, the extreme value index Gamma (γ) shapes the tail of the distribution.

In order to find the optimal estimation of Gamma, a threshold value x_t was determined. This threshold value is the point of maxima deviation of the extreme tail of the distribution from the main distribution. It is the threshold that minimizes the mean square error (MSE) of the regression and was determined based on the least MSE of the extreme value Quantile-Quantile (Q-Q) plot.

3.7 SCENARIO ANALYSIS

At any station along a river downstream of a dam, the degree of improvement in flood control is determined by the percentage of the total catchment area which is controlled by the reservoir and the distance from the dam to the flood plain (Pircher, 1990).

To control flooding in the Nzoia Basin reservoirs could be used to contain the peak stream flows. After the set up of the MIKE 11 hydrodynamic model, simulation was carried out in the period 1976-1984 for the two scenarios, namely:

- i) Scenario I: River system without reservoirs
- ii) Scenario II: River system with reservoirs

The two scenarios were considered with an aim of seeking to investigate the flood mitigation ability of implementing the dams in the Nzoia River system. The main output of this simulation included water levels and river discharge. The MIKE 11 simulation results were extracted and visualised using MIKE View post-processing tool.

3.7.1 Simulation of Model with Reservoirs

The inflow to each of the proposed reservoirs consisted of the upstream local inflow from the NAM model. The regulated release downstream from the proposed flood

control reservoirs (Appendix D) was computed by the MIKE 11 hydrodynamic model.

Currently flood warning in the catchment relies on issuing alerts when the water level at the monitoring station (1EF01) just upstream of the flood plain, reaches a predetermined level (Table 3.1). In order to balance the release of the flood water downstream from the reservoirs and at the same time not to cause flooding, flow regulation for each proposed reservoir was implemented based on the flood warning thresholds at Rwambwa River gauging (1EF01) as shown in Table 3.1.

Table 3.1: Flood Threshold water levels and discharges at Rwambwa

Flood Description	Water Level (m)	Flow (m ³ /s)
Flood Alert	2.8	224.77
Flood Warning	3.5	298.18
Dyke Crest Level	5.8	568.15

(Source: WRMA 2011)

From Table 3.1 it is shown that:

- i) There is no risk of flooding if the water level at Rwambwa Bridge is 2.8m and below.
- ii) An alert is given of possible flooding downstream when the water level at Rwambwa Bridge is in the range 2.8 to 3.5m. This the threshold floods that will overtop the river bank at Rwambwa.
- iii) If the water level is above 3.5m, this is the flood warning level and the risk of flooding is high. At 5.8m flooding can occur depending on strength of the dykes.

3.7.2 Reservoir Flood Mitigation Analysis

The procedure for flood mitigation scenario investigation was as follows:

- i) The sub basin outlet at Rwambwa (1EF01) was taken as the downstream boundary in the modelling process and was therefore used to estimate the peak discharge flood before and after dam construction.
- ii) The inflows to the reservoirs were determined using the NAM rainfall-runoff and MIKE 11 flood routing in the river system.
- iii) The regulated outflow hydrographs from the reservoirs were routed downstream to the dyke section at Rwambwa. The flow release from the reservoir was regulated in such way that it should not exceed the safe carrying capacity of the river channel at Budalangi.
- iv) Currently, there are no flood control reservoirs in the Nzoia River. In this study therefore, only one dam at a time was implemented in the Nzoia River system and simulation of the regulated flows undertaken. A comparison of the simulated peak flows between the current conditions (without dam) and after dam construction was performed to evaluate the flood mitigation impact of each reservoir.
- v) Using extreme value analysis, a theoretical extreme value distribution was fitted to the peak flows for both the scenario before and after dam implementation to determine the recurrence interval of the flooding incidence at Budalangi and hence determine which dam implementation will have a better impact in flood mitigation.

CHAPTER FOUR

RESULTS AND DISCUSSION

4.1 INTRODUCTION

This chapter presents the results of the construction and setup of the NAM conceptual model for use in predicting the rainfall-runoff from the reservoir catchments, and the MIKE 11 hydrodynamic model for flood routing in the river system. To evaluate the effectiveness of the proposed reservoirs for flood mitigation, the results of the flow simulation of the river system with and without the proposed reservoirs are presented and compared.

4.2 RAINFALL-RUNOFF MODELLING

The deterministic, lumped conceptual rainfall-runoff model method was used to simulate the river flows; this was constrained by the type of data available. The following types of data are required to perform rainfall-runoff simulations using this method;

- i) Mean Areal Precipitation (mm)
- ii) Evapo-transpiration (ET_o) (mm)
- iii) Area of catchment (Km²)
- iv) Observed discharge at the catchment outlet for calibration and validation

The Nzoia basin was divided into four sub basins (Figure 3.3) based on the available stream flows at river gauging stations: Rwambwa (1EF01), Nzoia market (1EE01), Webuye (1DA02) and Kipkaren (1CE01). These flows were used for reservoir catchment rainfall-runoff analysis, model calibration and validation. The NAM model was successfully calibrated and validated for each dam catchment. The calibration period was from 1976-1980 and validation from 1981-1984.

4.2.1 Mean Areal Rainfall (MAR) Estimation

Rainfall data for the period 1970-2009 were obtained from Kenya Meteorological Department (KMD). The data were converted to GIS platform and then using GIS software (Arc View) Thiessen polygons were developed and the Thiessen weights obtained for each of the sub basin. Station weights are scalar factors (0 – 0.9) used to transform point rainfall observed at a rainfall gauging station into an associated mean rainfall over an area (MAR) that the station represent. The Average catchment's rainfall for each dam site was determined by the application of the Thiessen weights on the daily rainfall at each rainfall station. Figure 4.1 shows the Thiessen polygon map for the Kipkaren sub basin and Table 4.1 shows the Thiessen weights that were used for computing the daily areal rainfall for each station. The computed areal daily rainfall for each sub basin was used as input to the NAM rainfall-runoff model. The same procedure was repeated for the other remaining dam site catchments and the results are shown in Appendix B.

Table 4.1: Thiessen polygon weights for Kipkaren sub basin

Rain gauge Station	KIPKAREN (SUB BASIN D)		
No.	Rain gauge station	Station ID	Thiessen weights
1	Turbo Forest	8935170	0.276
2	Eldoret Met.	8935181	0.364
3	Kaptagat met.	8935164	0.138
4	Kipkabus met.	8935061	0.222

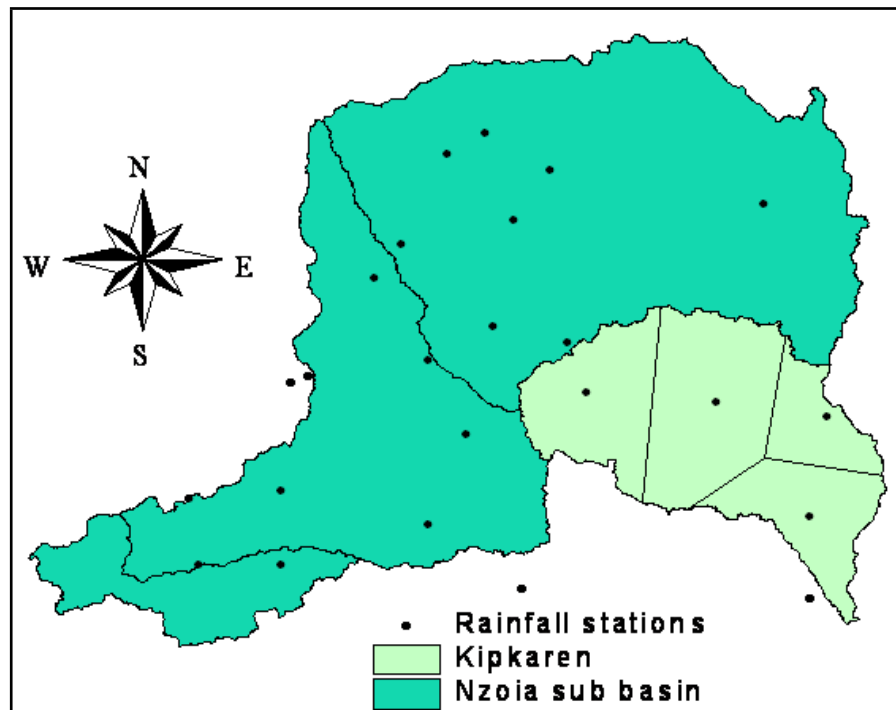


Figure 4.1: Thiessen polygon map for Kipkaren sub basin D

4.2.2 Subflow Separation of Observed River Flow

The rainfall-runoff model requires time series pre-processing of the observed daily river flows prior to its calibration. The required time series pre-processing are:

- i) Hydrological Subflow separation (quick flow, interflow and slow flow)
- ii) Split of the time series in nearly independent quick and slow flow events, and
- iii) Extraction of nearly independent high and slow flow extremes from historical flow records in the catchments

The stream flow data were partitioned into baseflow, interflow and overland flow by use of a Water Engineering Time Series processing tool (WETSPRO). This classification allows separate evaluation of the rainfall-runoff Subflow based on the nearly constant baseflow, interflow and overland flow recession constants (Willems, 2009).

Table 4.2 gives a summary of the Subflow filter results for each sub basin; whereas Subflow filter results are given in Figure 4.2. The overland flow recession constant is the quickest component and has the smallest recession constant whereas baseflow is the slowest component and has the highest recession constant. In Subflow filtering the recession constants are the main parameters affecting the shape of the hydrographs. The recession constant or recession time (CK) of each Subflow can be quantified as the average value of the inverse of the slope of the linear path in the Subflow recession periods of $\ln(\text{discharge})$ -time graph (Figure 4.3 and Figure 4.4). The daily stream flow data used are from RGS 1CE01 for the year 1976 -1984.

Based on the filtering parameter (w) of 0.5 and 0.4 for baseflow and interflow respectively the recession constants obtained were as shown in Table 4.2 for RGS 1CE01. These recession constants were used as estimates of the CKBF, CKIF and CK1, 2 as initial parameter inputs to NAM model setup during calibration for sub basin D.

Table 4.2: Summary of Subflow separation results

Gauging Station	Baseflow (days) (CKBF)	Interflow (days) (CKIF)	Overland flow (days) (CK1,2)
1DA02	64-76	3-6	1
1CE01	55-65	2-5	1
1EE01	75-95	3-7	1
1EF01	110-125	5-8	1

The time series of total runoff discharges are split up into a series of its subcomponents: overland flow, interflow and baseflow. The splitting procedure is based on the clear differences in the order of magnitude of the recession constants of the runoff subflows. The baseflow is first separated from the total rainfall-runoff discharge (Figure 4.3). Interflow is then separated from the combined discharge of

surface runoff and interflow (Figure 4.4). The filter results showing the decomposition of the total input series into base flow and interflow is shown in Figure 4.2.

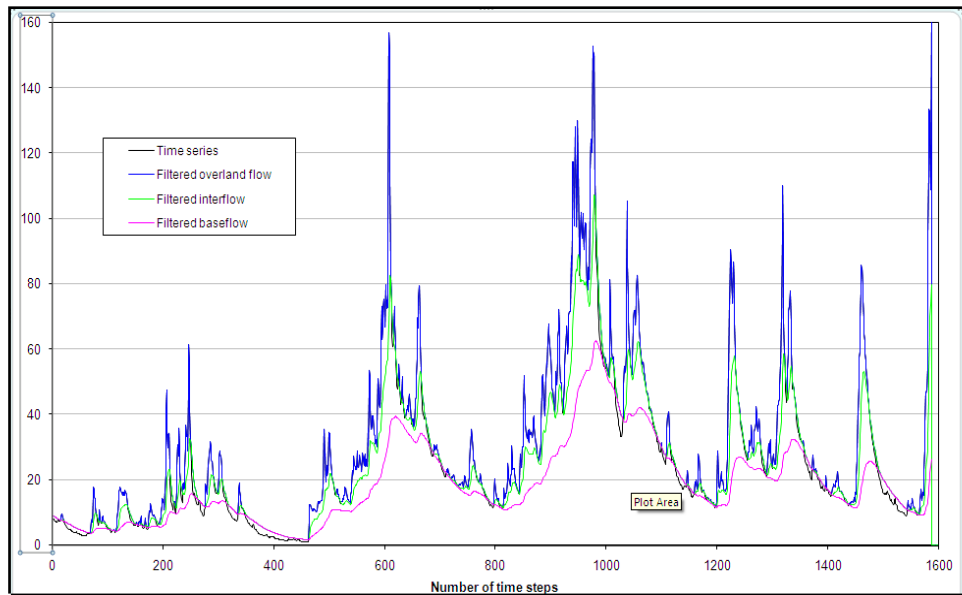


Figure 4. 2: Subflow filter results for daily river flow series of RGS 1CE01.

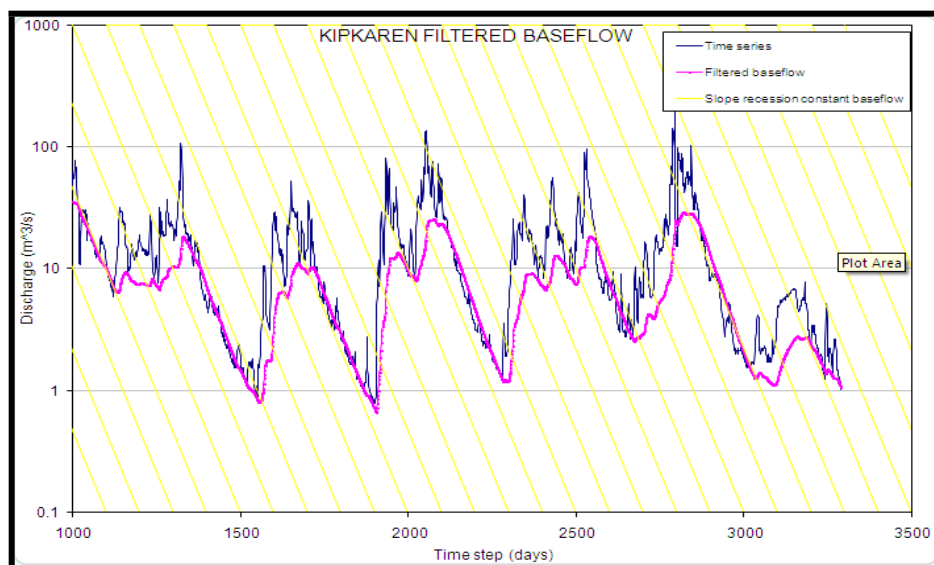


Figure 4. 3: Assessment of the baseflow recession constant for RGS 1CE01

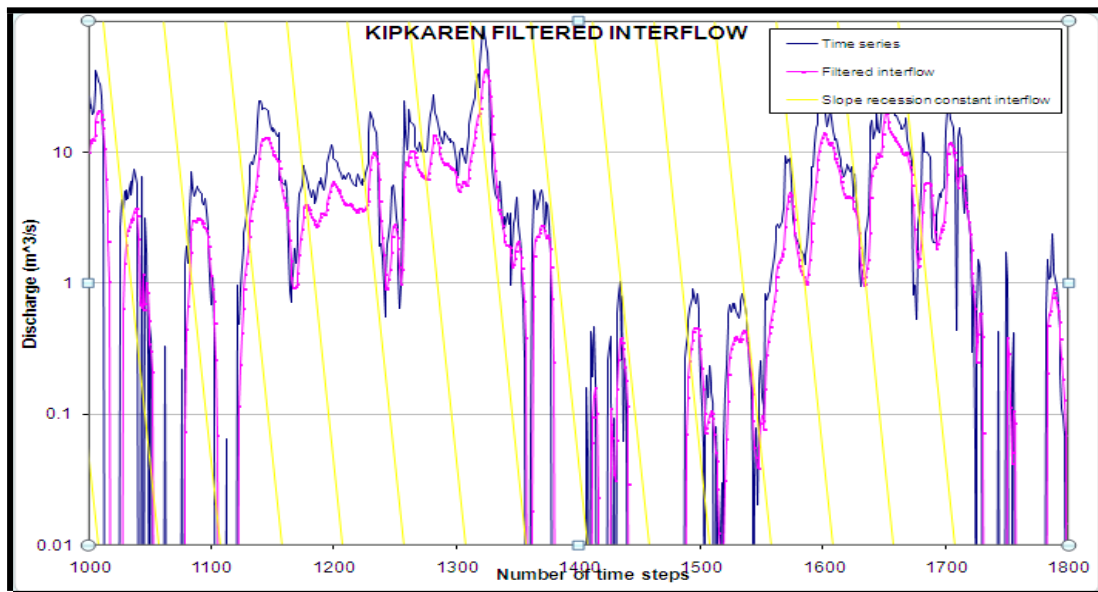


Figure 4. 4: Assessment of the interflow recession constant for RGS 1CE01

4.2.3 Calibration and Validation of NAM Model

The calibration of the NAM rainfall-runoff model was done for each sub basin A, B, C, and D to estimate the optimal values of the nine (9) parameters for the NAM model using rainfall-runoff data between 1976 and 1980 for calibration and between 1981 and 1984 for validation.

Model parameters were determined by manual, trial and error calibration against observations until satisfactory water balance close to zero was obtained, and then automatic calibration was applied to optimize the parameters. The results of the calibrated parameters for the dam site catchments are shown in Table 4.3.

The primary parameters that were changed in order to adjust the water balance in the simulation during the calibration process were the surface storage (U_{max}), root zone storage (L_{max}) and overland flow runoff coefficient (CQ_{OF}). Since the actual evapo-transpiration is highly dependent on the water on the surface and root-zone, U_{max} and L_{max} were the primary parameters adjusted. Since these parameters represent the average value for the entire basin modelled, they cannot in practice be estimated from field data, but an expected interval can be defined as given in

Appendix C, Table 1. The other important parameter was the overland flow runoff coefficient ($C_{Q_{OF}}$). Small values of $C_{Q_{OF}}$ are expected for flat catchments, having coarse sandy soils e.g. in sub basins A and B of the Nzoia River, also large values are expected for catchments having low permeable soils such as clay, bare rocks or steep catchments e.g. in the upper sub basins C and D of Nzoia River as shown in Table 4.3. The other six NAM parameters were adjusted during the calibration in order to fine tune the model.

Figure 4.5 and Figure 4.9 shows the hydrograph plot of the observed and simulation daily stream flow for the calibration period 1976-1980 and validation period of 1981-1984. The coefficient of determination (R^2) of 0.77 and 0.84 suggests that there was a good agreement between the observed and simulated streamflow during this period. The R^2 expresses the proportion of variance of the recorded runoff that can be accounted for by the model and provides a direct measure of the ability of the model to reproduce the recorded flows. R^2 equal to 1.0 indicates that all estimated flows are the same as the recorded flows. In general, R^2 values greater than 0.6 suggest a reasonable modelling of runoff and R^2 values greater than 0.8 suggest a good modelling of runoff for catchment yield studies.

Table 4.3: Calibrated NAM parameters

No.	Parameter	NAM SUB BASINS			
		A	B	C	D
1	U_{\max} (mm)	17.6	17.4	10.2	10.1
2	L_{\max} (mm)	268	272	120	140
3	$C_{Q_{OF}}$ (-)	0.159	0.158	0.542	0.688
4	$CK_{1,2}$ (hr)	44	42	34	28.6

5	<i>CKIF</i> (hr)	496	480	368	226.4
6	<i>CKBF</i> (hr)	3140	2880	2020	1771
7	<i>TOF</i> (-)	0.02	0.0111	0.64	0.536
8	<i>TIF</i> (-)	0.13	0.0303	0.03	0.446
9	<i>TG</i> (-)	0.01	0.0126	0.01	0.0246

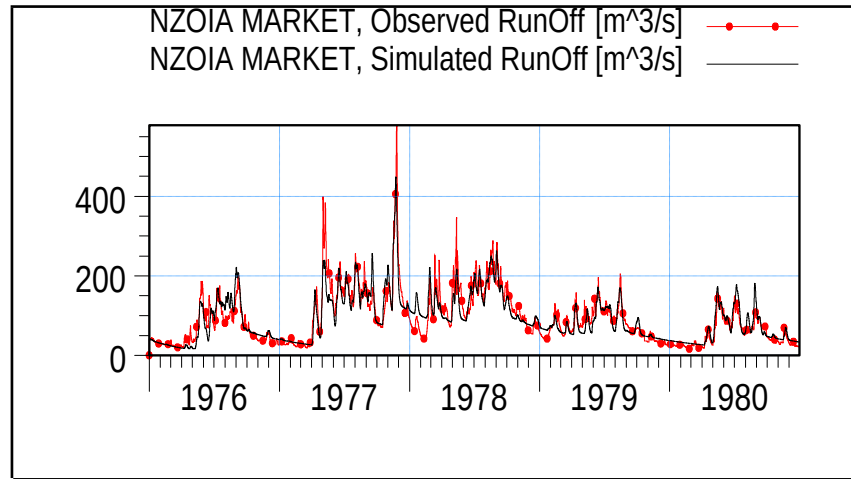


Figure 4.5: Calibration hydrographs at RGS 1EE01 for the period 1976-1980

The volume of flow being simulated past the Nzoia market discharge station was cumulated for the simulation period for both the calibrated and validated volumes, and the results were presented in Figures 4.6 and 4.7. During calibration and validation a R^2 of 0.77 and 0.74 was obtained as shown in Figure 4.8 and Figure 4.10, respectively.

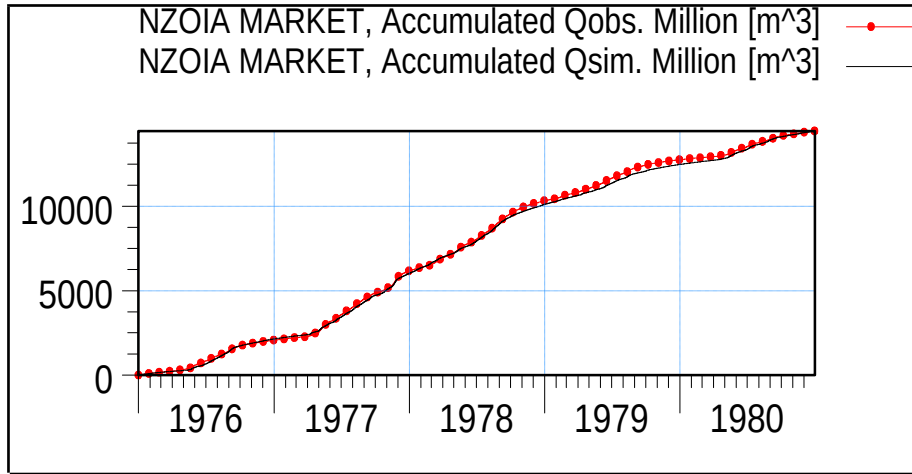


Figure 4.6: Calibration cumulative volumes (1976-1980)

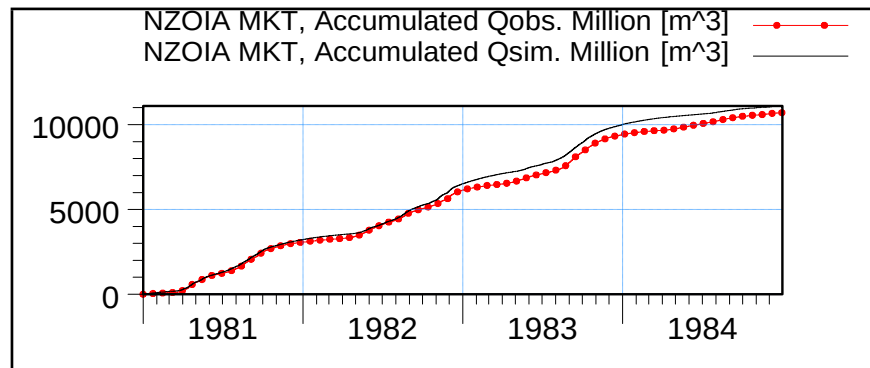


Figure 4.7: Validation cumulative volumes (1981-1984)

		Client: NAM autocalibration		MIKZERO
		Project: Results		
Parameterfile	Date:	R2=0.840, WBL= -0.0% (obs= 244mm/y, sim= 244mm/y)		Revision: 00
NZOIA MARKETRRPar1.rrr	Init:			

Figure 4.8: NAM calibration result for period 1976-1980

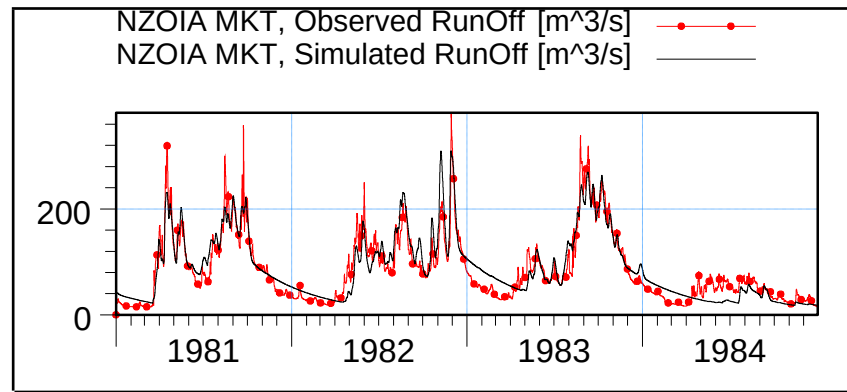


Figure 4.9: Validation hydrograph for the period 1981-1984 ($R^2 = 0.840$)

		Client: NAM calibration		MINEzero
		Project: Results		
Parameterfile NZOIA MKT	Date: RR.rr11/2011	R2=0.853, WBL= -3.7% (obs= 226mm/y, sim= 235mm/y)		
	Init:			

Figure 4.10: Validation results for the period 1981-1984 ($R^2 = 73.5\%$)

The results of the rainfall simulations from the NAM model and the observed discharges at RGS 1EE01 were analyzed using the WETSPRO tool. In rainfall-runoff model residuals typically increase with higher flow values. To avoid this problem Box-Cox (BC) transformation was applied to the river flows to transform the model residuals into a normal distribution.

In the scatter plot of Figure 4.11, the model results (vertical axis) are compared against the flow observations (horizontal axis) at river gauging station 1EE01. The model residuals are shown in this plot as the horizontal or the vertical differences between each point and the bisector. The model residual mean and standard deviation are represented by the solid and the dotted lines.

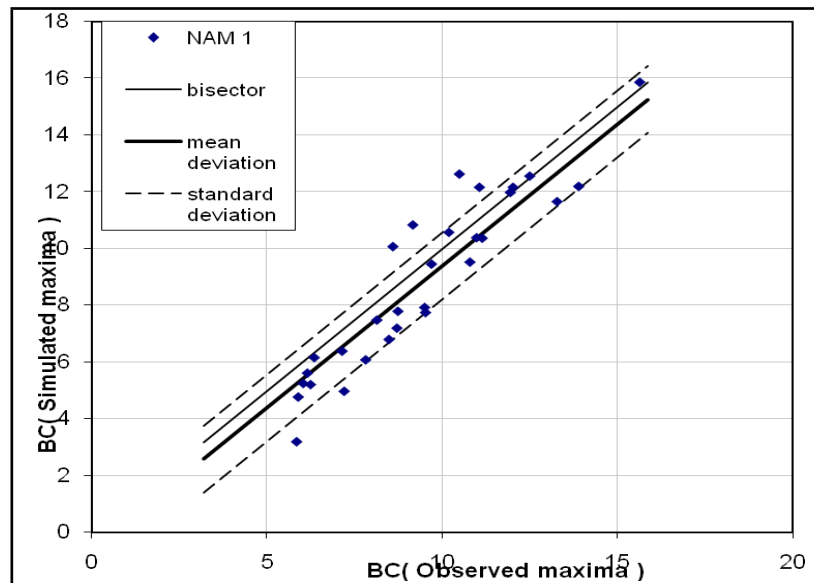


Figure 4.11: Scatter plot of peak flow discharges at 1EE01 after BC-transformation ($\lambda = 0.25$)

From the peak flow comparison in Figure 4.11, it is clearly shown that the NAM model for this sub basin shows lower standard deviations of peak flow deviations from the bisector, but systematically lower mean peak flow, the peak flows are slightly underestimated. It is also evident that there is a good agreement between measured and simulated values. It was observed that the scatter plot of points about the bisector was good for both model calibration and validation.

Figure 4.12 shows an analysis of the performance of NAM model in representing extreme high values. The extreme high flow values were obtained from a Peak-Over-Threshold analysis carried out on the runoff values. The analysis of the performance of the model was done to assess how well the model is simulating high extremes. The peak flows are slightly underestimated by the NAM model, but tend to compare well towards the upper tail of the extreme value distribution.

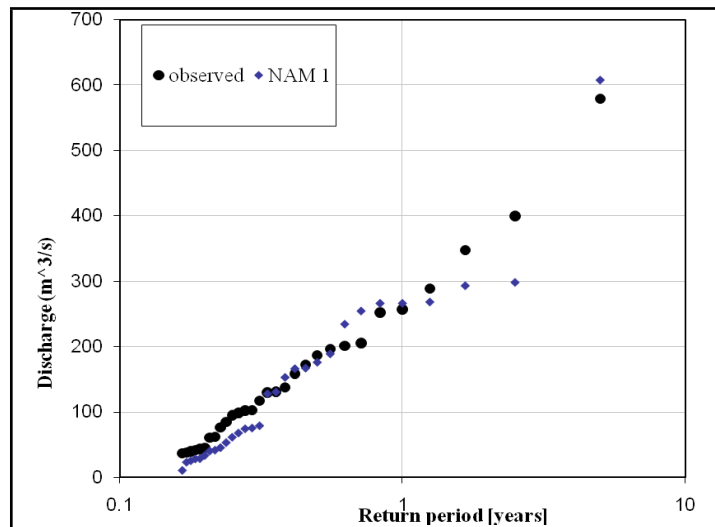


Figure 4.12: Modelled and observed peak flow extreme value distribution

During calibration, water balance which accounts for water in the basin is a major consideration. In Figure 4.13 the simulated water balance volume is compared with the observed water balance volume. A good correlation between the simulated and measured cumulative runoff can be observed though in the case of the higher values of the cumulative volumes are not well correlated.

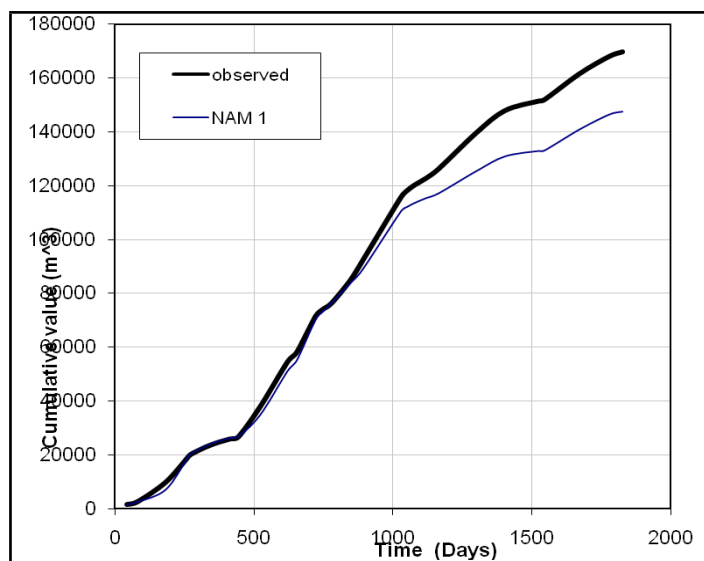


Figure 4.13: Cumulative water balance volume for observed and simulated discharges

4.3. MIKE 11 MODEL RESULTS: HYDRAULIC MODELLING

After implementation of the MIKE 11 hydrodynamic model, simulation was carried out in the period 1976 to 1984. During model set up, the first simulation of the model proved to be unstable. The independent variables Δt and Δx were adjusted severally until model simulation stability was achieved. A space step (Δx) of 280m and a computational time step (Δt) of one (1) minute were selected by trial and error during the manual calibration. The main output of this simulation included water levels and river discharge. The results of the simulation were presented using MIKE View. The subsequent sections present the results of the hydraulic modelling.

4.3.1 Definition of the River Network

The modelling of the Nzoia River network was defined from dam site 34B and 35 as upstream boundary to Rwambwa river gauging station (1EF01) as the downstream boundary. The river network was digitized and defined graphically in MIKE 11. These digitized points were manually created in MIKE 11 river network editor and connected with a reasonable degree of precision to create two branches: Nzoia and Kipkaren. The river network as defined in MIKE 11 is shown in Figure 4.14. Figure 4.15 shows the cross section implemented in the modelled river system at RGS 1EE01. An important aspect in MIKE 11 is the definition of the connection describing the confluence of the two river branches. In order to prevent problem of discontinuities in MIKE 11 setup, the connect branch tool in the tool bar is used and the connection implemented as shown in Figure 4.16.

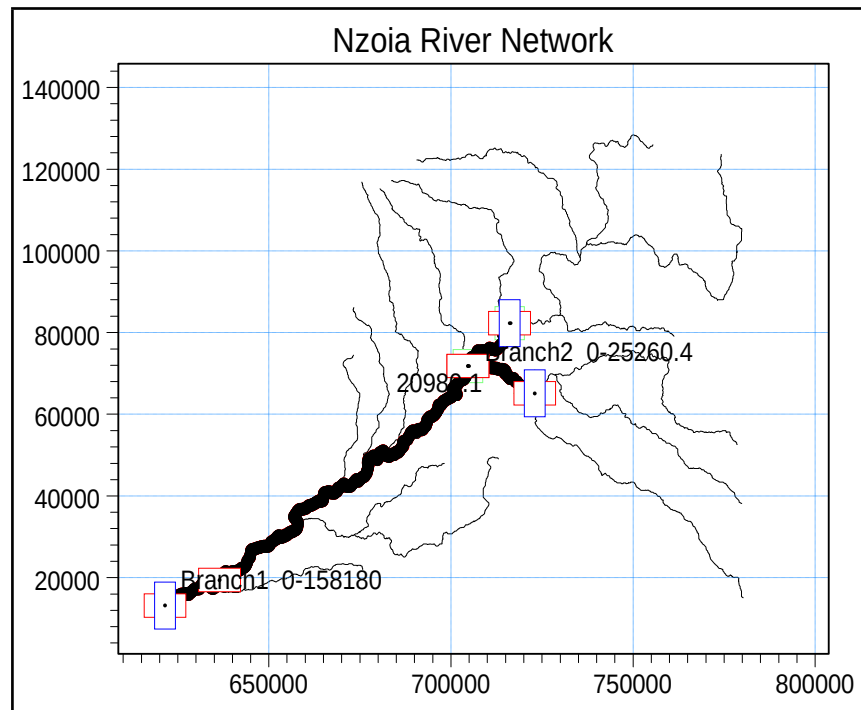


Figure 4.14: The Nzoia River basin network (grids are in UTM)

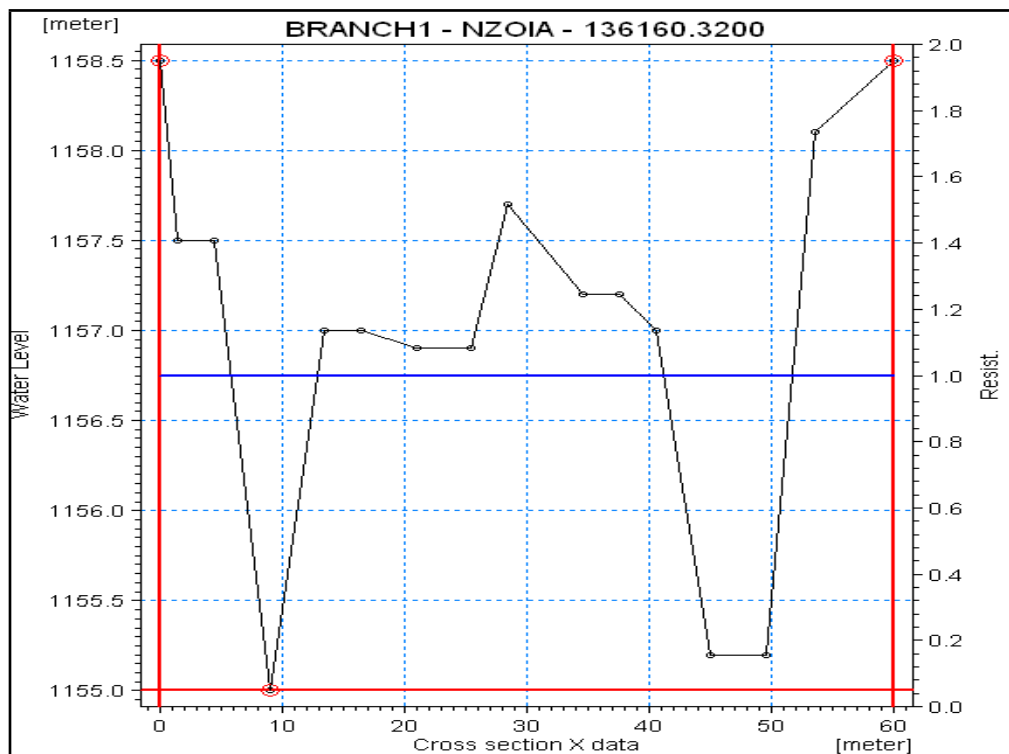


Figure 4.15: Example of a cross-section used to describe the Nzoia main river

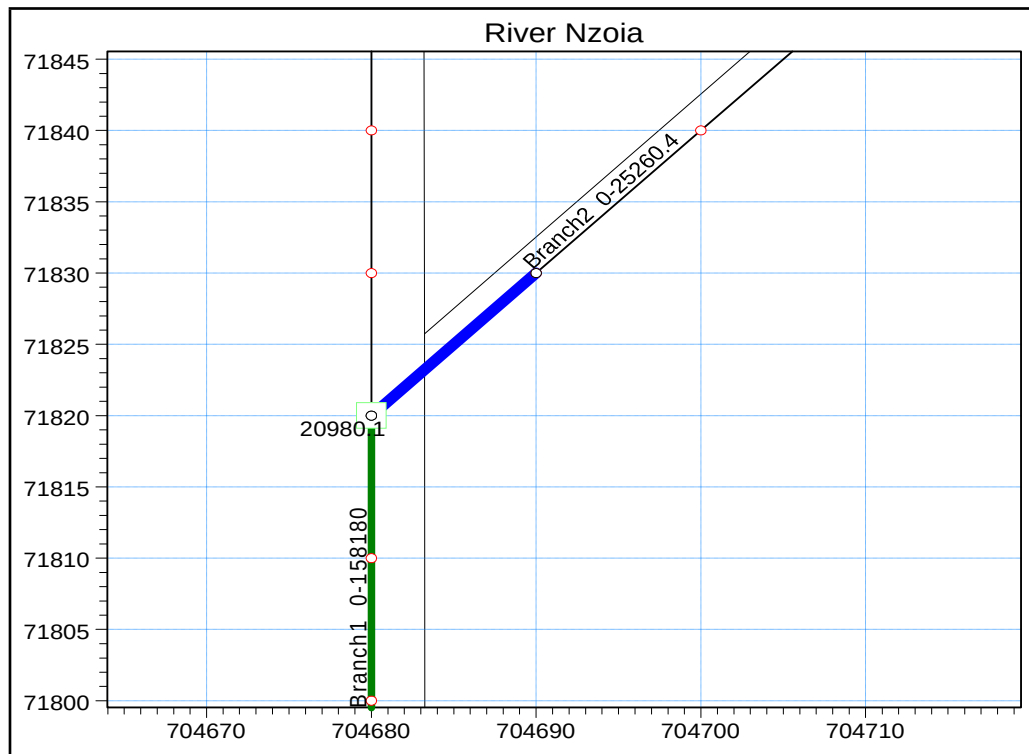


Figure 4.16: Confluence between the main Nzoia River and Kipkaren River

4.3.2 Model Calibration

The model was set up in order to carry out the first simulation run and to adjust it for subsequent calibration phases. The hydrodynamic parameters and variables involved in the modelling that were used in the computations to get convergence of the numerical scheme were as shown in Table 4.4. The model calibration was carried out by comparing the computed (modelled) and observed discharge at Rwambwa river gauging station (1EF01) located at a distance (reach) of 158,180.12m from the upstream boundary condition of the modelled river system. The calibration period considered was the flow of 1976-1980. Figure 4.17 shows the simulation results for the calibration.

Table 4.4: The hydrodynamic variables involved in the model setup

Parameter	Description
Δt	Time step (one minute)
Δx	Maximum distance between computational grid points (280m)
Initial conditions	Initial Water level and discharge

Manning's M	30 (n = 0.033)
-------------	----------------

The calibration of the hydrodynamic module (MIKE 11) can be achieved either by adjusting the bed resistance (Manning's n) until the simulated flows are fitted to the observed flow or by adjusting the independent variables Δt and Δx until no error is available in the model simulation. In this study the latter approach was a major consideration in the calibration process in order to achieve model stability. The accuracy criterion chosen was mainly based on a good simulation of the peak flow that is widely the most critical variables in a flood assessment study.

The model result had an R^2 value of 0.88 or 88% (Figure 4.18) , indicating that the model performance is not perfect but provides a good estimate of the peaks flows as shown in Figure 4.17.

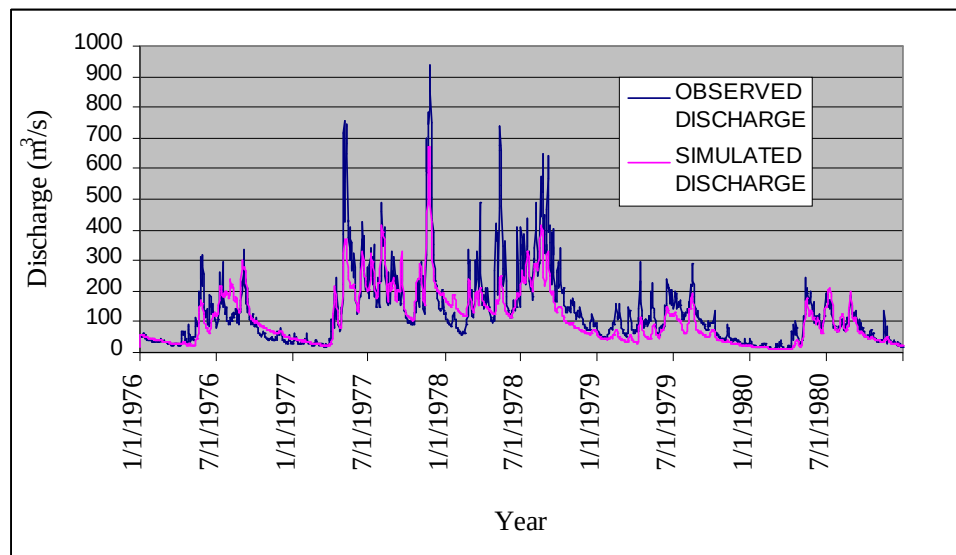


Figure 4.17: The calibration hydrograph results at RGS 1EF01.

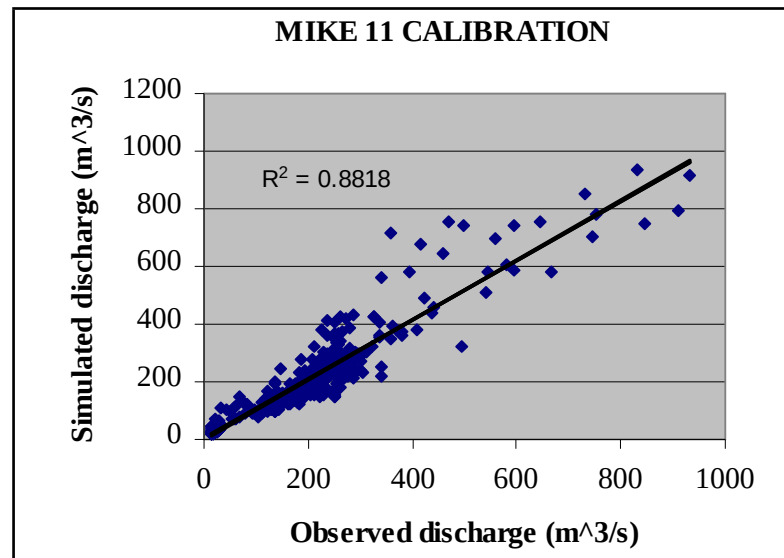


Figure 4.18: MIKE 11 scatter calibration plot for simulated and the observed discharge

4.3.3 MIKE 11 Model Validation

Model validation is implemented by fitting model with data other than that used in the calibration process in order to test the applicability of the model to other time step period. In this study the observed flows for the period 1981-1984 were used to validate the model. During the model validation, the optimized hydraulic parameters (Table 4.4), obtained during calibration are not adjusted any more as validation is meant to verify the calibrated model. Figure 4.19 shows the validation results of the hydrodynamic model.

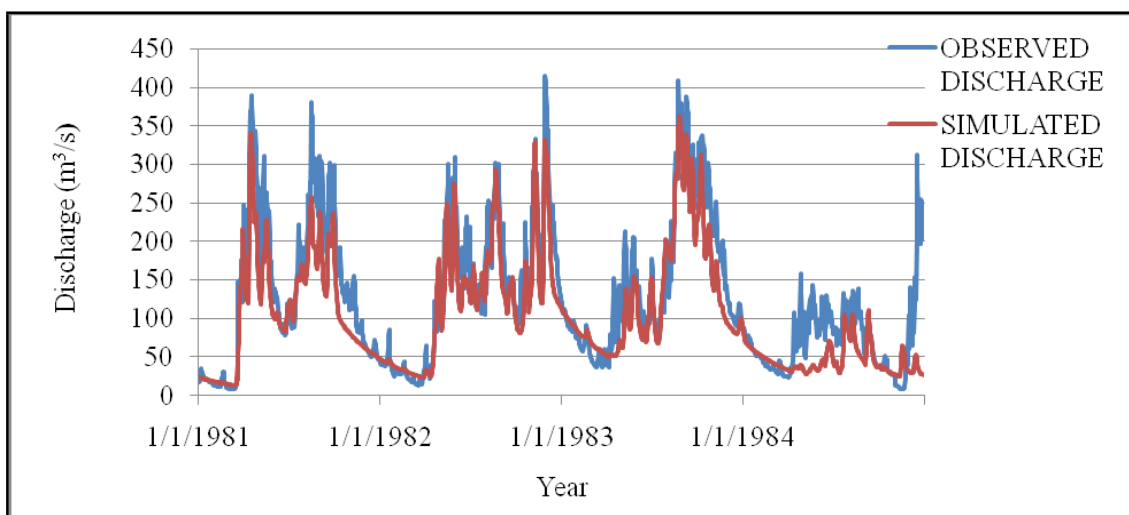


Figure 4.19: The validation hydrograph results at 1EF01.

Figure 4.20 gives the graphical comparison between the predicted and observed discharge during model validation. The predicted discharge do not differ considerably from the observed. The model result had an R^2 of 0.89 during verification which show reasonably good agreement between the observed and simulated flows during the period 1981-1984. After model calibration and validation, the MIKE 11 model captured the hydrologic characteristics in the study area reasonably well and reproduced acceptable daily streamflow simulations. It can be concluded that the model fits fairly well with the observed data, hence the model can be used to predict the design flow into the proposed reservoirs.

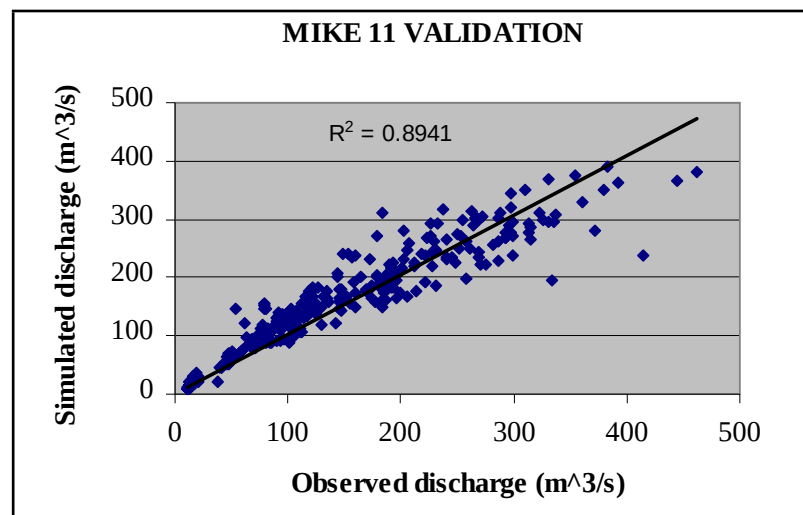


Figure 4.20: MIKE 11 scatter validation plot for simulated and the observed discharge

The MIKE 11 model was evaluated for its ability to predict extreme peak flows. The performance of the model in simulating extremes is shown in Figure 4.21. Though it is evident the model underestimates the peak flows, the model however, has a good simulation capacity in terms of predicting extreme flows. The predictive ability of the

model can be improved by carrying out additional river cross sections at close intervals, a factor which was a limitation in this study.

The performance of the MIKE 11 model was also evaluated based on the cumulative water volumes for both observed and simulated flows at RGS 1EF01 as shown in Figure 4.22. On analysis, the flow hydrographs for the observed and simulated flows follow a similar trend but with lower simulated cumulative volume. The lumped nature of NAM and the limited number of model input parameters may result in more averaged simulated time series compared to observed series. A less automatic /numerical and more physically based step-wise calibration of model parameters can solve this problem. Implementing the hydraulic model of MIKE 11 includes the effect of river routing and hence flatten the NAM results and may increase the underestimation of the peak values.

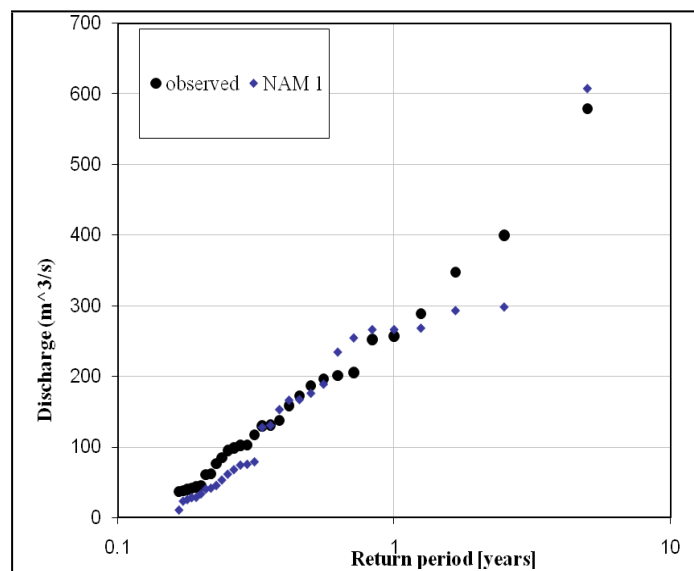
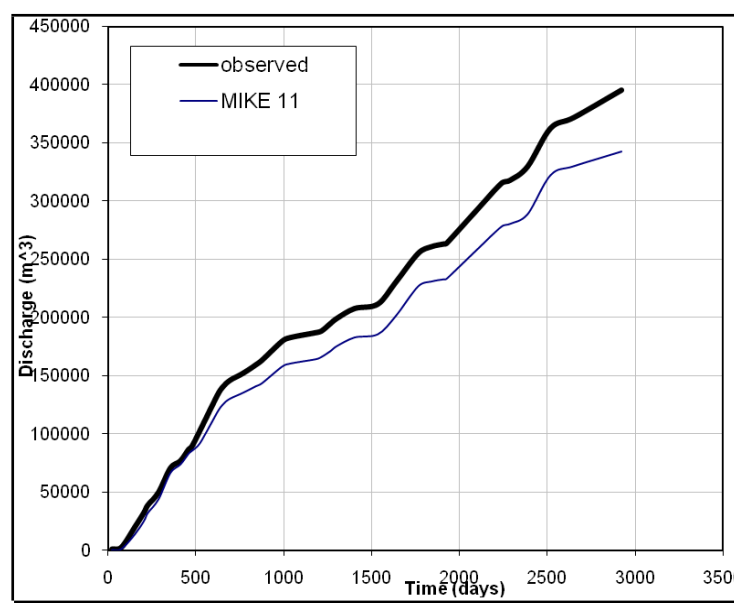


Figure 4.21:
and modelled
peak flow
value
distribution



Observed
empirical
extreme

Figure 4.22: Cumulative volume for observed and simulated discharges

4.3.4 MIKE 11 Simulation Results

The time series output for the simulated discharge was generated from the Q (discharge) points as shown in the dialogue grid point property page in Figure 4.23.

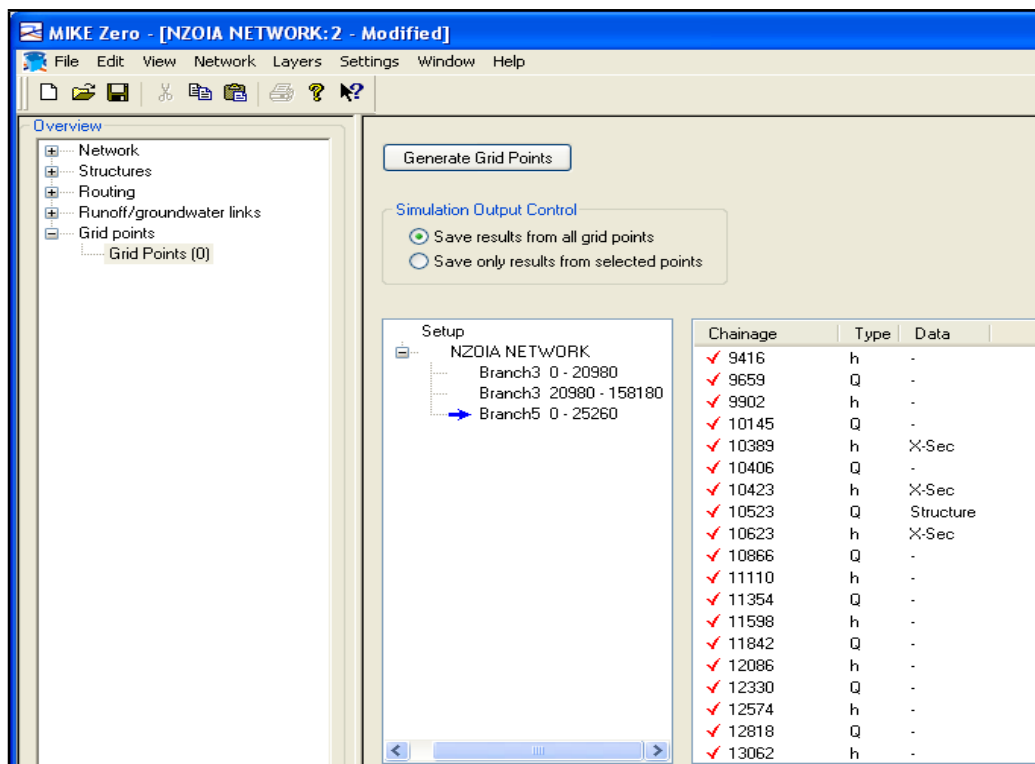


Figure 4.23: Grid point dialogue in MIKE 11 River network

The modelled output was provided at all computational grid points i.e. the h-point (water levels) and Q-point (discharge) as shown in Figure 4.23. The computational points are defined along the river network. The simulated discharge results file was opened in MIKE View (Figure 4.24) and hence the simulated discharge extracted from selected grid points. The selection of the grid points was done by specifying the river name and the coordinates of the point of interest. MIKE 11 uses a staggered grid, which is a grid where water level and discharge are computed at different locations. The extracted simulated discharge was hence taken for flood frequency analysis/ extreme value analysis and simulation during reservoir flood outflow regulation.

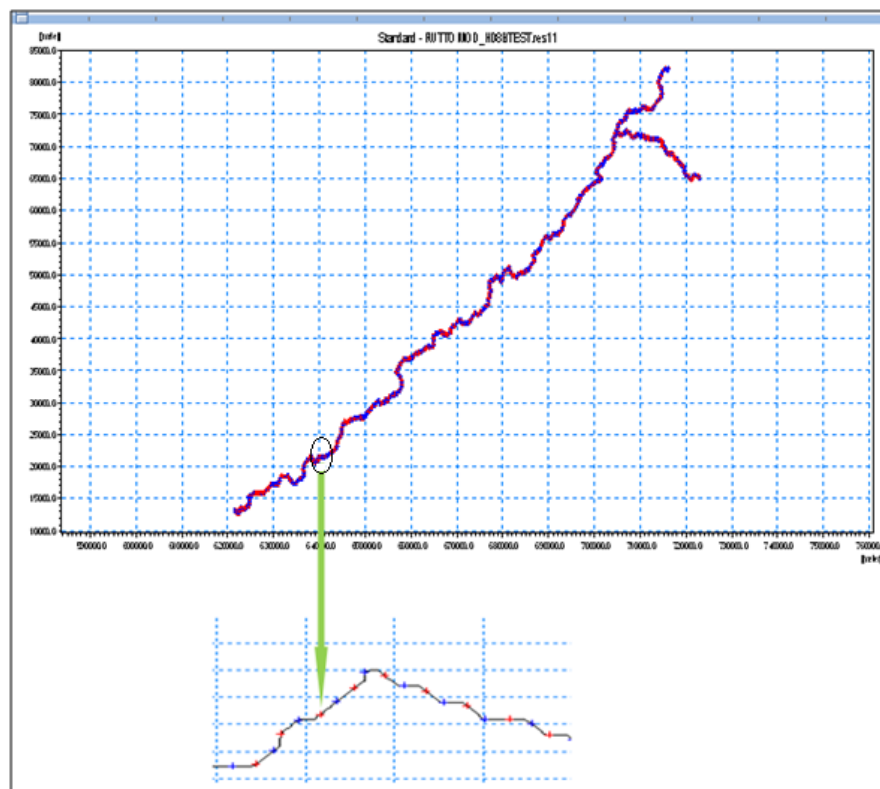


Figure 4.24: MIKE View Computational grid points

4.4 FLOOD MITIGATION THROUGH THE RESERVOIRS

The water level at Rwambwa (1EF01) was used as a key parameter for measuring the safety level of the flow regulation in the Nzoia River. A threshold discharge of

298.18m³/s at a water level of 3.5m (Table 3.1) was used in selecting the desired discharge in order not to overtop the river banks at the dyke section in Budalangi. This is discharge level that can be contained by the dykes already in place.

In this study, three dams: 42A, 34B and 35 were considered for the flood mitigation in the Nzoia River basin.

4.4.1 Flow Regulation at the Reservoirs for Flood Control

Reservoir release decisions are often based on conditions of reservoir inflow, pool elevation and downstream flow rates. Historically these rules have been developed through trial- and- error model simulations of the river reservoir systems, where a set of proposed rules are incrementally adjusted until desired results of release, storage and flow are observed (Ngo et al., 2008).

Because no data on the design of the release structures in the dams exists, a release schedule that reduce flooding downstream of the proposed reservoirs at the dyke section were developed. The reservoir outflow criterion based on a discharge correlation (Figure 4.25 and Figure 4.26) was developed using the discharge time series at the reservoir site and at the dyke section (1EF01) in conjunction with logical statements as shown in Table 4.5. Using the correlation a flood equivalent to the flood threshold level at the dyke section was obtained at reservoirs 42A, 34B and 35.

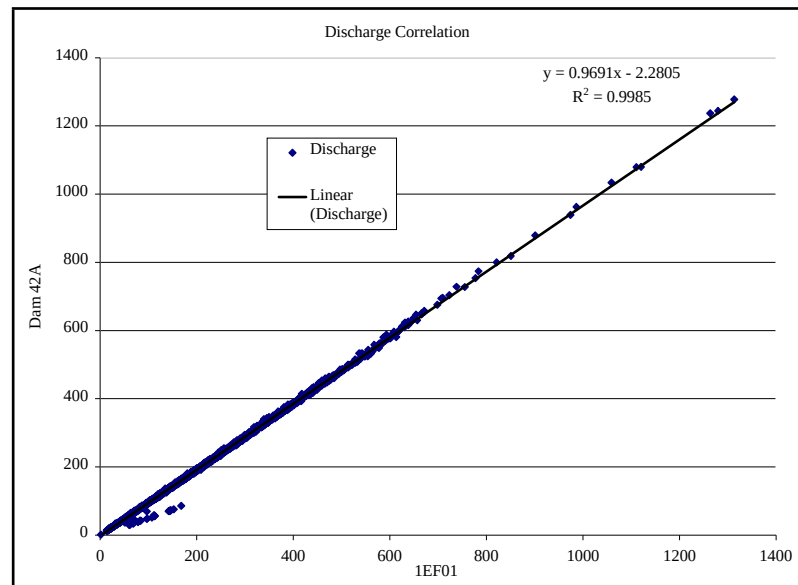


Figure 4.25: Discharge correlation between dam 42A and dyke section

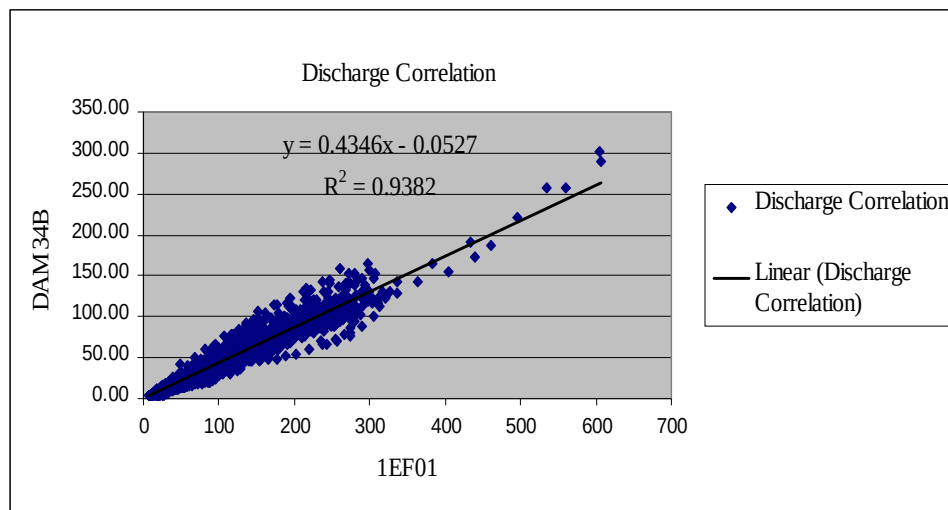


Figure 4.26: Discharge correlation between dam 34B and dyke section

Based on the discharge correlation between the dam sites and 1EF01 (Figure 4.25 and Figure 4.26) a maximum regulated outflow of 287m³/s and 110m³/s and 96 m³/s was implemented at dam 42A, 34B and 35 respectively. Also a flow regulation of 96m³/s was used for dam 35 based on the same discharge correlation.

Table 4.5: Excel Logical statement **for flow regulation at dam 42A, 34B and 35**

Flood Volume Stored in the Reservoir
= IF (Initial Volume in Reservoir < Dead storage),
THEN Storage = (Inflow-Environmental flows)*24*3600, ELSE
IF (Inflow- Threshold flood at Rwambwa) < 0
THEN Reservoir Storage = 0, ELSE
IF (Inflow-Threshold flood at Rwambwa) > 0
THEN Reservoir Storage = (Inflow- Threshold flood at Rwambwa)*24*3600
ELSE
ENDIF.

The flow regulation at the reservoirs was such that at no point does the release exceeds the safe carrying capacity of the river channel. This was achieved by storing in the reservoir the volume above the flood threshold. The simulated inflows and regulated outflows from the reservoirs are given in Figure 4.27, Figure 4.28 and Figure 4.29.

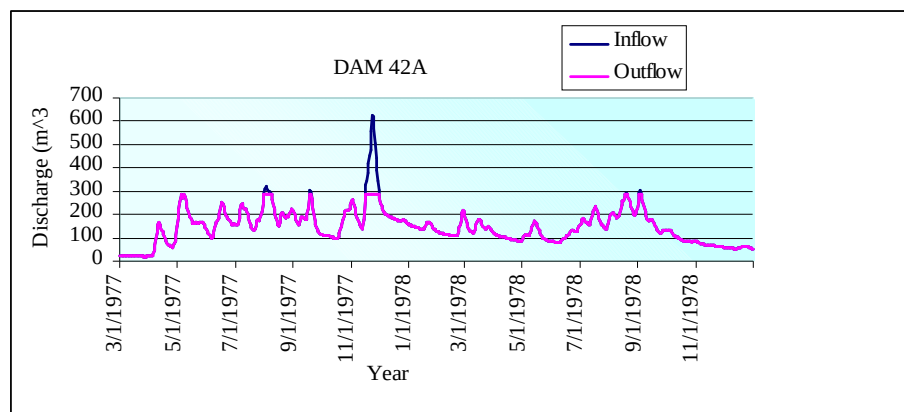


Figure 4.27: Regulated outflow from reservoir 42A

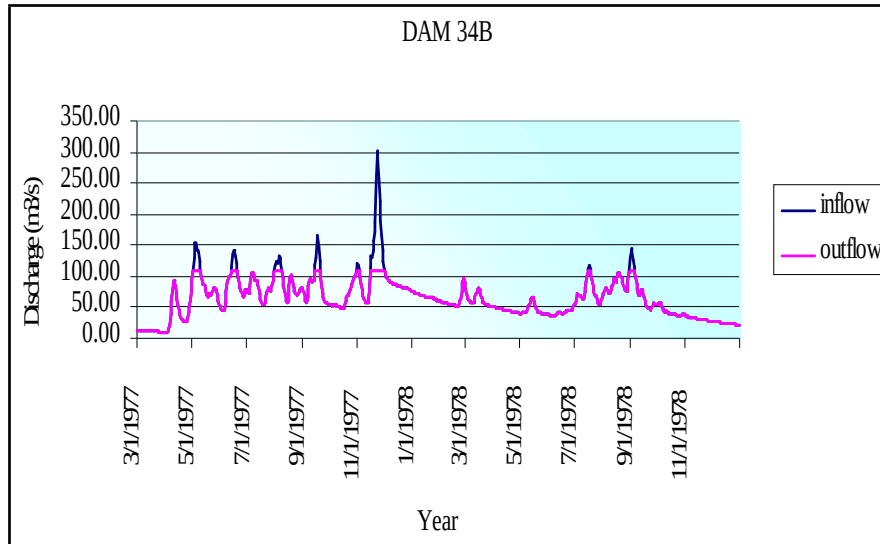


Figure 4.28: Regulated outflow from reservoir 34B

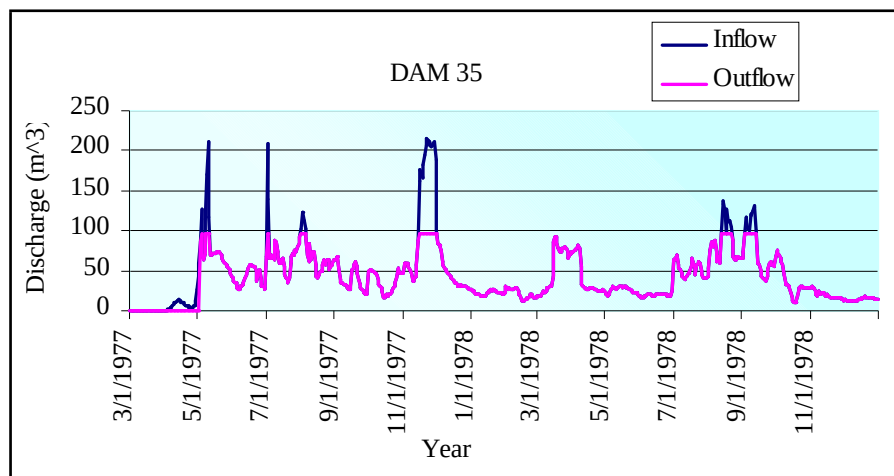


Figure 4.29: Regulated outflow from reservoir 35

The cumulative reservoir storage of the flood peaks in excess of the stipulated flood threshold is given in Figure 4.30, Figure 4.31 and Figure 4.32. The result of reservoir storage scenarios at dam site 42A, 34B and 35 demonstrated the possible effect of the proposed reservoirs in containing the peak stream flows that contribute to flooding in Budalangi.

It was observed that the proposed reservoirs have sufficient capacity to store the flood water in excess of the channel capacity. Dam site 34B is located in the upper

catchment and has a small reservoir catchment area of 4862km² compared to dam site 42A which has a larger reservoir catchment area of 11,829km². The results of the cumulative reservoir storages over the simulation period are shown in Figure 4.30, Figure 4.31 and Figure 4.32.

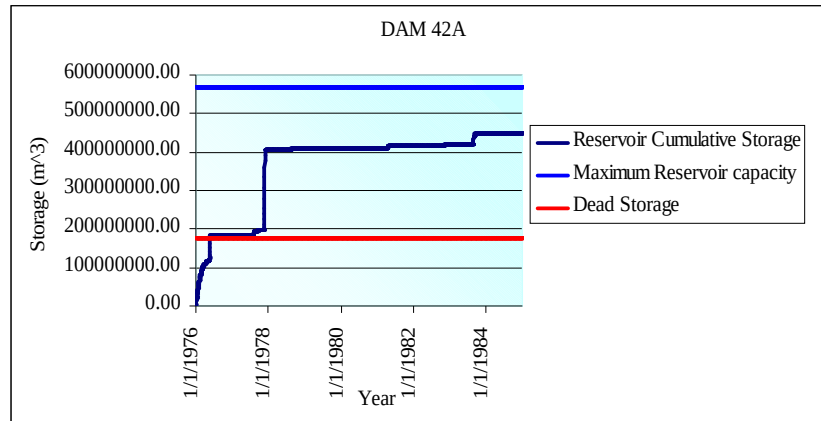


Figure 4.30: Flood mitigation through storage reservoir 42A

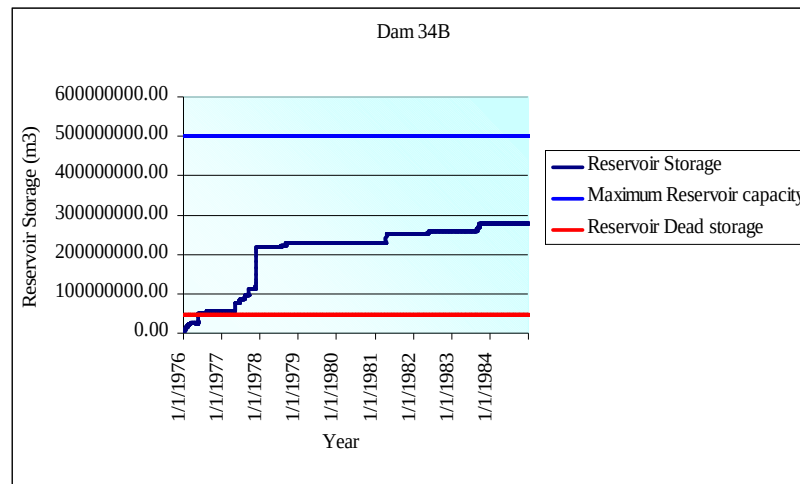


Figure 4.31: Flood mitigation through storage reservoir 34B

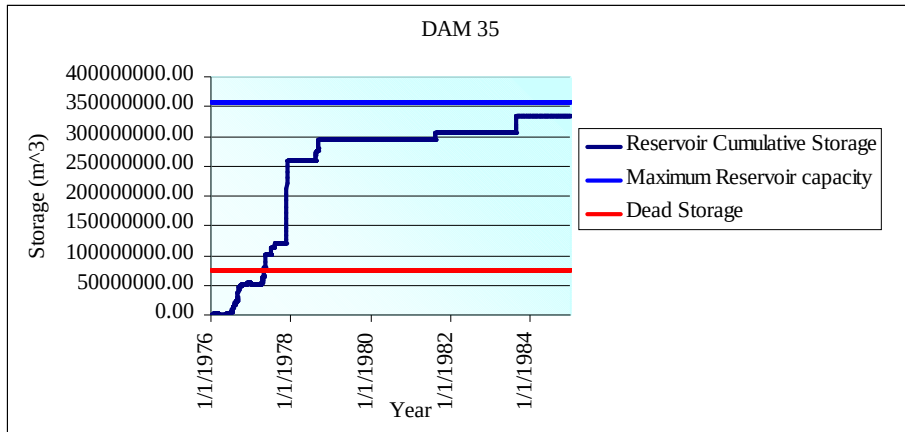


Figure 4.32: Flood mitigation through storage reservoir 35

The inflow to the reservoir site 42A consisted of the upstream local inflow from the NAM model for dam catchments 34B and 35 and MIKE 11 hydraulic routing in the river network, whereas for reservoir 34B and 35, the inflow was based on NAM rainfall-runoff from the dam catchments. The regulated flood release downstream from the reservoirs to RGS 1EF01 was computed by the MIKE 11 hydrodynamic model as shown in Figure 4.33 and Figure 4.34.

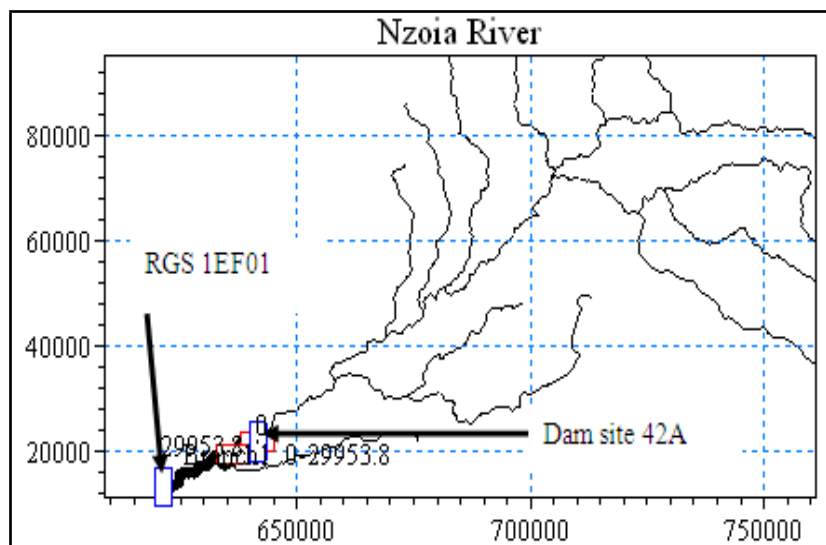


Figure 4.33: Regulated flow from Dam 42A to Rwambwa (1EF01)

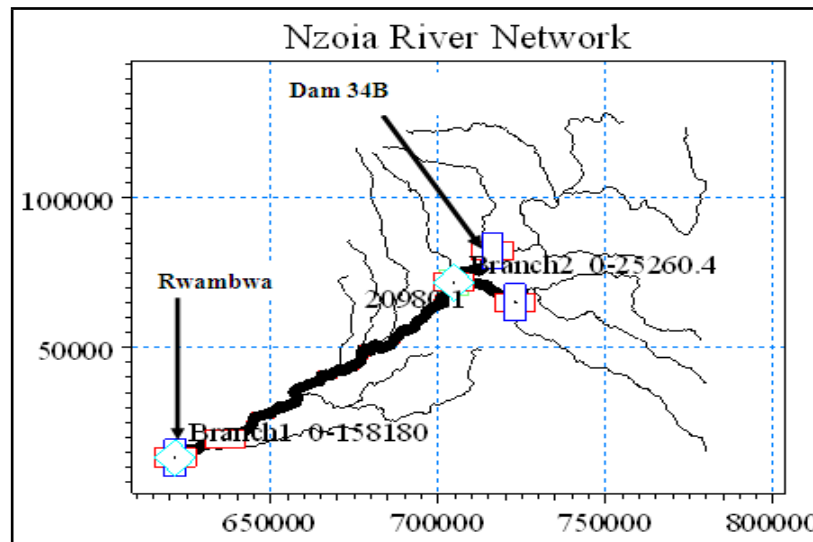


Figure 4.34: Regulated flow from Dam 34B to Rwambwa (1EF01)

4.4.2 Comparison of the Two Scenarios (With and Without Reservoirs)

In the scenario investigation, only one dam at a time was implemented in the river system and the hydrodynamic simulation of the regulated flows from the dam site to Rwambwa river gauging station undertaken. Rwambwa river gauging station was considered as the downstream boundary for these simulations.

Before implementing the reservoirs, flow simulation in MIKE 11 was undertaken. Figure 4.35 gives the resulting hydrograph at 1EF01. The flood peak from the simulated flows was $708\text{m}^3/\text{s}$.

With the implementation of dam 42A the simulated peak flow reduced from $708\text{m}^3/\text{s}$ to $320\text{m}^3/\text{s}$, a reduction of 55 % in the peak flows. However this reduction in the flood peak is slightly higher than the flood warning threshold level of $298.18\text{m}^3/\text{s}$ at Rwambwa river gauging station but not sufficient to cause flooding in Budalangi. Figure 4.36 shows the model results at Rwambwa from the simulation of regulated flows from dam site 42A.

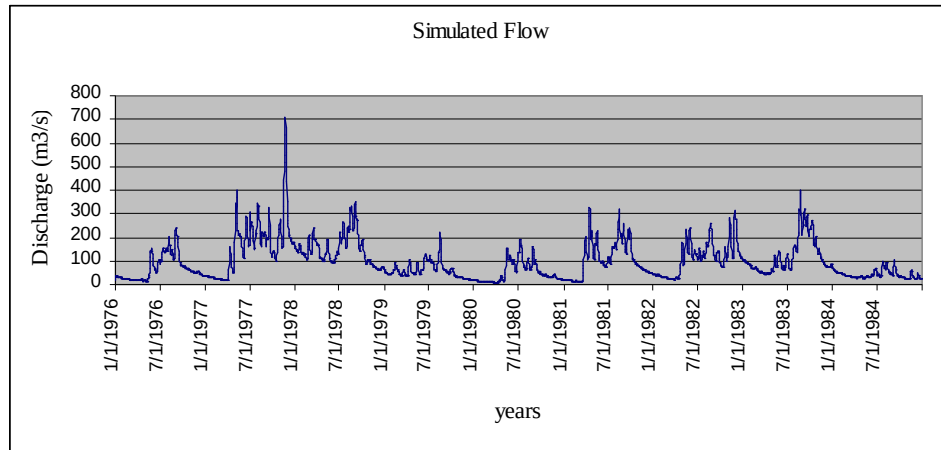


Figure 4.35: Nzoia River flow simulation results (no dams)

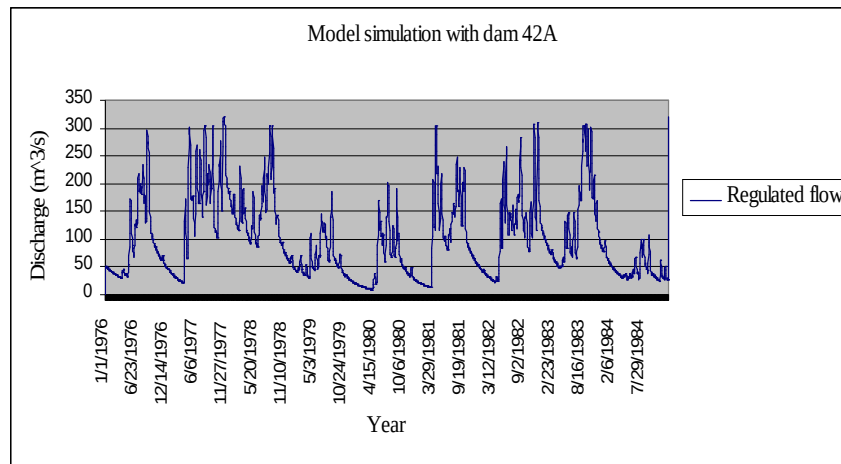


Figure 4.36: Reservoir 42A regulated flow simulation results

The peak flow for reservoir 34B from the simulated regulated flow was $491\text{m}^3/\text{s}$, whereas the peak flow for reservoir 35 from the simulated regulated flow was $601\text{m}^3/\text{s}$. In the implementation of the dam 34B and 35 in the upper catchment of the basin the simulated peak flow reduced by 31 % and 15% respectively. However, it is evident that the flood peak, even after flood regulation could still overtop the Nzoia River banks and hence the implementation of dam 34B and 35 is less effective in controlling the floods. Figure 4.37 and Figure 4.38 shows the model results at

Rwambwa from the simulation of regulated flows from dam site 34B and 35 respectively.

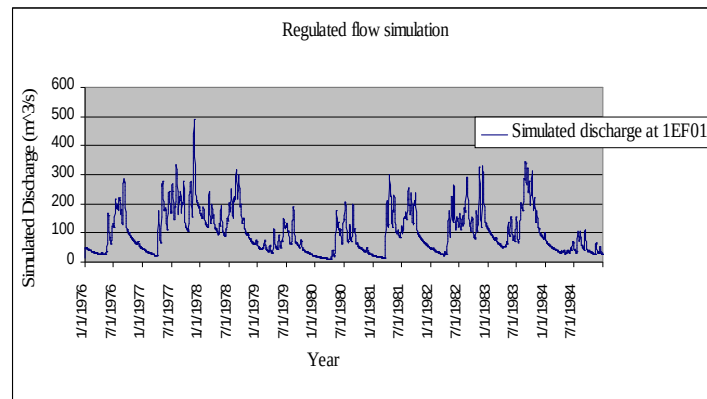


Figure 4.37: Reservoir 34B regulated flow simulation results

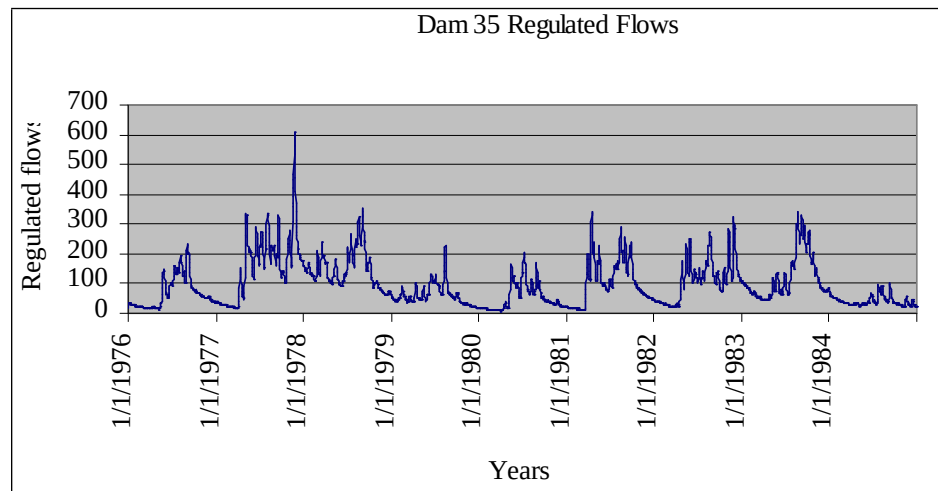


Figure 4.38: Reservoir 35 regulated flow simulation results

In real situation the effectiveness of reservoirs depend on how the reservoirs are managed and operated. They should be emptied to the dead storage volume during the dry season, whereas the outflow should be controlled during the rainy season to avoid downstream flooding.

4.5 HIGH FLOW FREQUENCY ANALYSIS

Hydrologic systems are sometimes impacted by extreme events, such as severe floods. The objective of frequency analysis of hydrologic data is to relate the

magnitude of extreme events to their frequency of occurrence through the use of probability distributions (Chow et al., 1988).

Flood frequency analysis was done so as to identify the flood magnitude for various return periods for the regulated and unregulated flows. The analysis was carried out for each reservoir regulation scenario for the three reservoirs and compared with the condition when no reservoir in the river system. The point of reservoir inflow were determined from the dam site map (Appendix D).

4.5.1. Peak-Over-Threshold Selection

The Peak-Over-Threshold (POT) selection method proposed by Willems (2004a) was used to select the extreme discharge peak events. In this method two successive discharge peaks can be considered largely independent when the smallest discharge in between the two peaks reaches a low value (lower than a fraction of the peak flows).

Peak-Over-Threshold selection was performed using Water Engineering Times Series Processing (WETSPRO) software (Willems, 2004a). The discharges time series from the dam was filtered from the flow series using independence criteria. After decomposition of the input series into its various components using the appropriate sub-filtering parameters, the next step was to isolate the independent high flow series. This was done by using the Peak-Over- Threshold (POT) method. Table 4.6 shows the results of the assessment of the Subflow filter results for the discharge time series at the dam sites 42A, 34B and 35. Figures 4.39, 4.40 and 4.41 shows a graphical plot of the POT results before dam implementation and after implementation of dams: 42A, 34B and 35 respectively.

Table 4.6: Peak flow selection Parameters for the independency criterion

Dam site	K_{BF} (days)	K_{IF} (days)	K_{OF} (days)	Q_{lim} (m^3/s) (Threshold)	Max. ratio difference (f)	Independency period (k_p) (days)
35	95	5	1	24	0.2	10

34B	95	6	1	18	0.2	12
42A	95	4	1	40	0.2	8
No Dam	105	5	1	50	0.15	10

According to Willems (2009) the independency period (K_p) was taken as equal to two times the recession constant of interflow (K_{IF}) in order to attain independence between subsequent quick flow events. The fraction (f) was taken as the upper limit of the baseflow fraction in the peak flow, usually values from 5% to 15% are considered adequate. Parameter Q_{lim} (threshold discharge) was visually judged from the total flow filter results and values assigned as shown in Table 4.6. The selected ranked POT values are given in Appendix E for the three dam sites.

For these reservoir sites, using the parameters in Table 4.6 in the WETSPRO software, thirty-three (33), forty (40) and thirty-eight (38) independent quick flow events were isolated for reservoir sites 42A, 34B and 35 respectively. In each station, these filtered independent high flow values, were ranked for the purpose of fitting them into a Quantile-Quantile (Q-Q) plots in the ECQ tool.

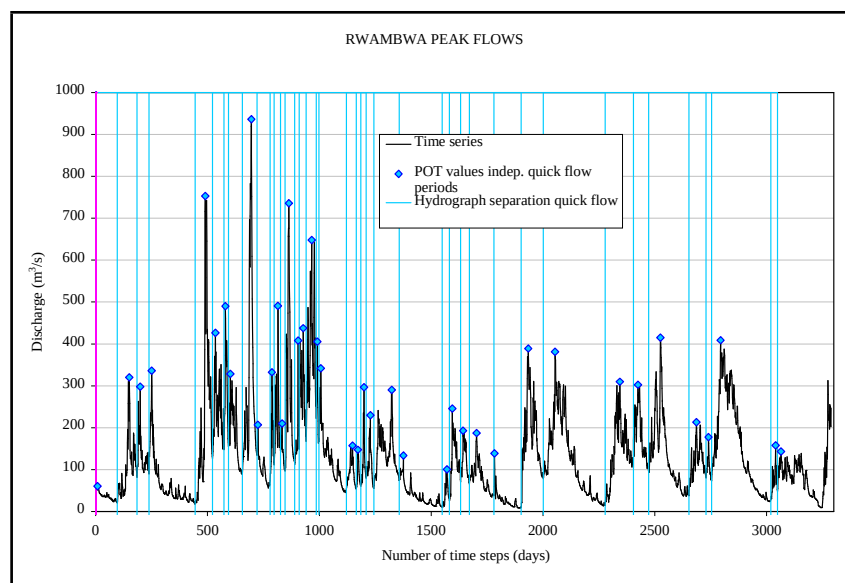


Figure 4.39: POT flows at Rwambwa before dams' implementation

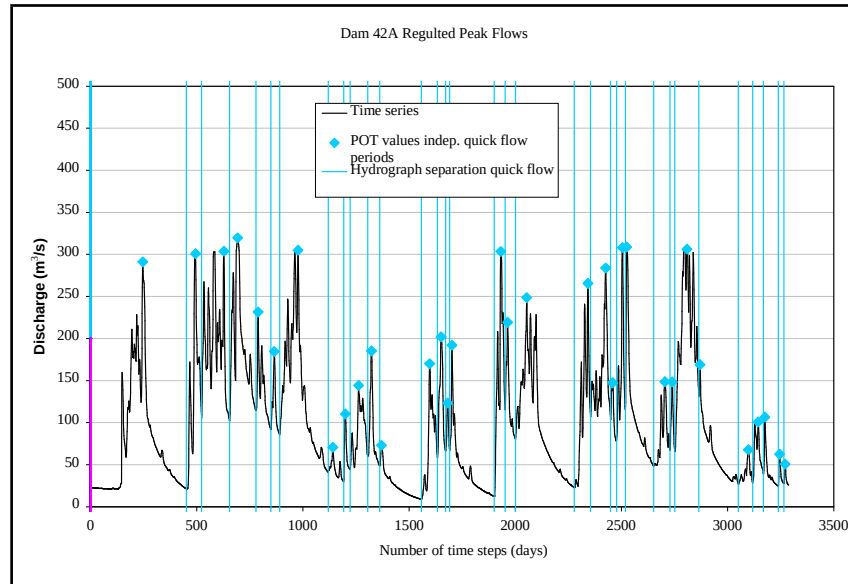


Figure 4.40: POT flows at Rwambwa after implementation of dam 42A

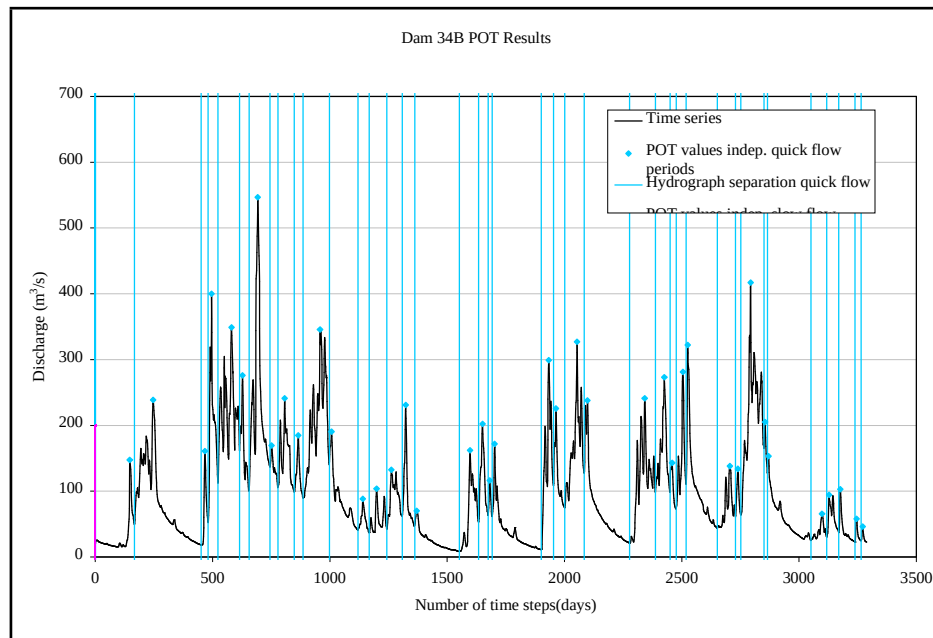


Figure 4.41: POT flows at Rwambwa after implementation of dam 34B

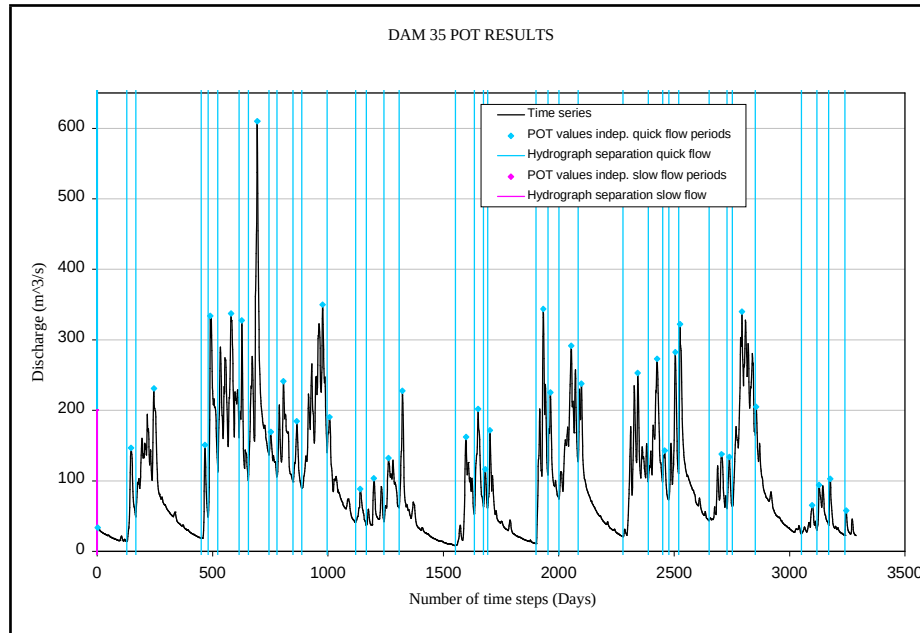


Figure 4.42: POT flows at Rwambwa after implementation of dam 35

4.5.2 Extreme Value Analysis

Extreme value analysis involved the selection of a sequence of extreme events from the dam discharge series. These extreme events are located in the extreme tail of the probability distribution. There are three asymptotic forms of the distributions of extreme values named: Type I (Weibull), type II (Pareto) and type III (Weibull). The discharge data were analysed separately for each dam by using hydrological extreme value analysis tool, ECQ (Willems, 2004b). The type of distribution (heavy tail, normal tail, light tail) was judged based on the behaviour of the tails and its slope in different distribution plots (Exponential quantile plot, Pareto quantile plot and UH-plot). In the ECQ software, the extreme value index (Gamma) shapes the tail of the distribution. The selected independent extremes that were analysed using the ECQ software are given in Appendix E.

Making use of the Quantile-Quantile plots, an analysis was made of the shape of the distributions tail, and discrimination made between heavy tail ($\gamma > 0$), light tail ($\gamma <$

0) and normal tail ($\gamma = 0$). According to Willems (1998), Q-Q plots help to avoid error in the extreme value index that is caused by the selection of a wrong distribution model. Also the Q-Q plot (Quantile-Quantile plot) technique is used to select the suitable statistical distributions for the extreme events in the discharge series. First, Generalized Quantile excess function (UH-estimation) of the extreme value index gamma (γ) was performed to determine the distribution class and the sign of γ .

As an example, for the observed peak discharge inflow for the condition of no dam in the river system, as shown in Figure 4.43, 4.44, 4.45 and 4.46, it was observed from the Quantile-Quantile (Q-Q) plots that:

- i) In the exponential Quantile plot: the upper tail points tends towards a straight line as shown in Figure 4.43.
- ii) In the Pareto Quantile plot, the upper tail points continuously bend down. This is shown in Figure 4.44.
- iii) In the UH-plot: the slope in the upper tail approaches the zero value. This is shown in Figure 4.45.

The tail of the extreme value distribution was therefore considered as “normal” and thus corresponds to an exponential distribution given by equation 4.1.

$$G(x) = 1 - \exp\left(-\frac{x - x_t}{\beta}\right) \quad [4.1]$$

If $G(x)$ represents the exponential probability distribution of the extremes for $x = Q$ above a threshold value x_t calibrated to t observations in n periods (years), considering t observations in n periods, the return period “T” corresponding to the exceedance level x is given by equation 4.2.

$$T = \frac{n}{t} \times \frac{1}{1 - G(x)}$$

[4.2]

Where

β = Slope of the exponential distribution Q-Q plot

n = number of years of data series

T = Return period

t = number of exceedance of threshold level (Threshold rank in Slope exponential Q-Q plot)

x_t = Threshold discharge

x = Generated discharge

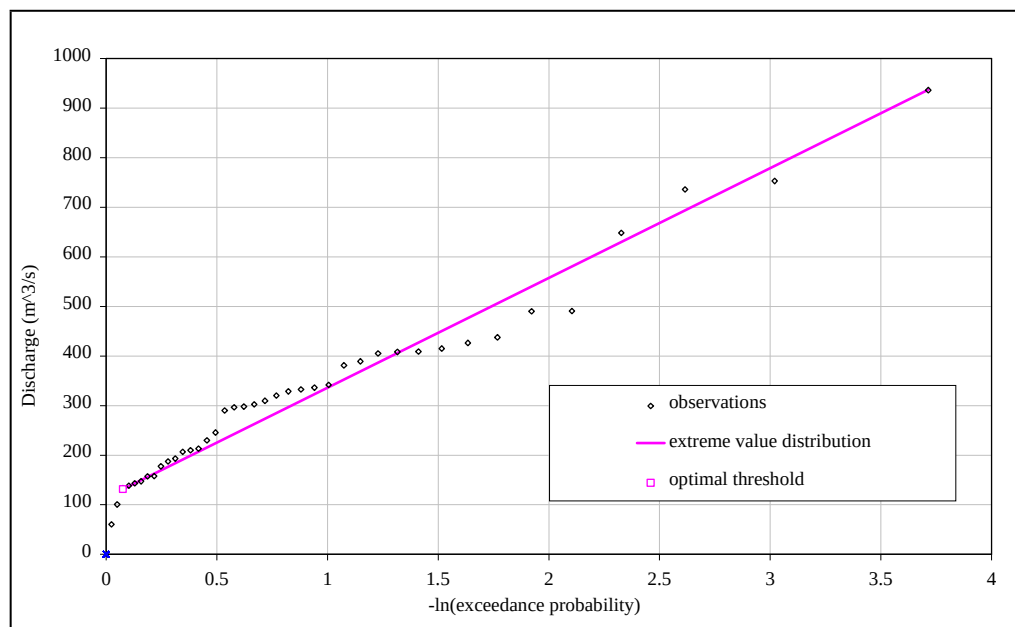


Figure 4.43: Exponential Q-Q Plot for no dam peak flows

These calibration procedures were repeated for the other reservoirs and the extreme value distribution parameters after optimal calibration obtained.

Appendix F shows the extreme value distribution graphs for the other reservoirs sites.

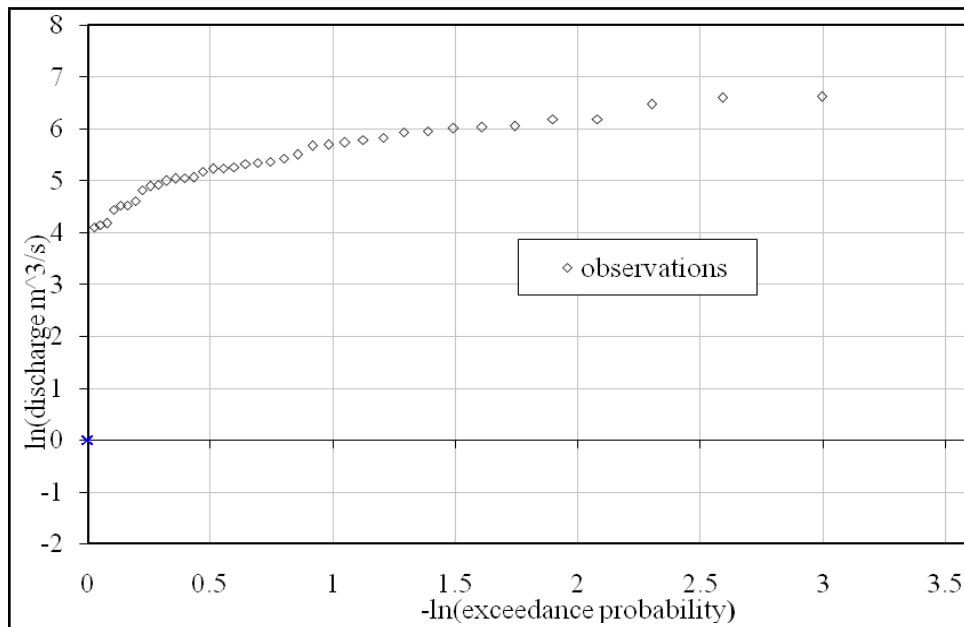


Figure 4.44: Pareto Q-Q plot for no dam peak flows

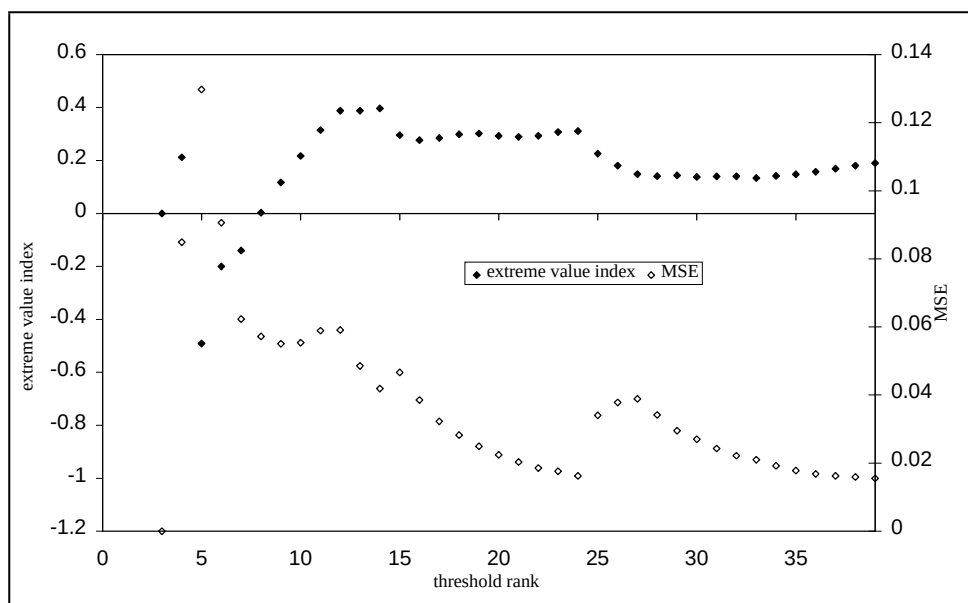


Figure 4.45: Slope U-H Q-Q Plot for no dam peak flows

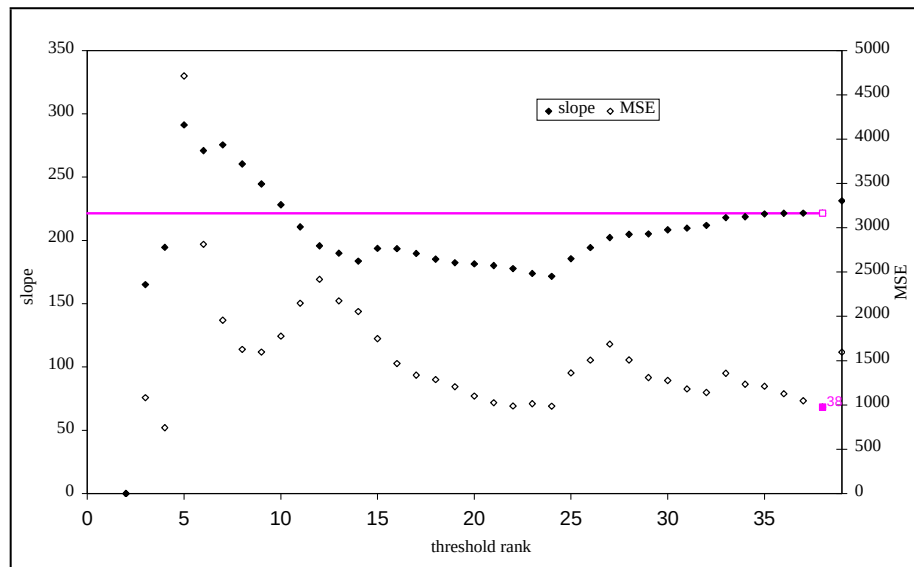


Figure 4.46: Slope Exponential Q-Q plot for no dam peak flows

The plots for this analysis fitted to the exponential distribution with normal tail. The high flow extreme value distribution was calibrated based on regression in the Q-Q plot, according to the method presented by Willems (1998, 2004b). The optimal threshold value x_t of 133.7 m^3/s above which the distribution was calibrated and selected at the flow value with threshold rank $t = 38$ (Figure 4.46). This threshold was chosen at the point above which the mean squared error of the linear regression is minimal. At this threshold the slope of the exponential Q-Q plot gave the value of 221.5 for β . The parameters of the extreme value distributions as shown in Table 4.7 were used to compute the recurrence interval. The theoretical return periods (Appendix G) were obtained by using equation 4.2, and a graphical plot presented in Figure 4.47 for the four scenarios: No dam, dam 42A, dam 34B, and dam 35.

The plots from the regulated flows from the reservoir sites: 42A, 34B and 35 also fitted to the exponential distribution with normal tail. The exponential distribution was calibrated by linear regression in the exponential Q-Q plot above a selected threshold as shown in Appendix F.

Table 4. 7: Theoretical Extreme value distribution parameters

Extreme Value Parameters	No Dam	Dam 42A	Dam 34B	Dam 35
Selection Threshold (t)	38	24	31	30
Gamma (γ)	0	0	0	0
Beta (β)	221.5	96.7	114.7	116.9
Threshold Rank (x_t) (m^3/s)	133.7	144.4	132.4	132.4
Distribution Type	Normal	Normal	Normal	Normal

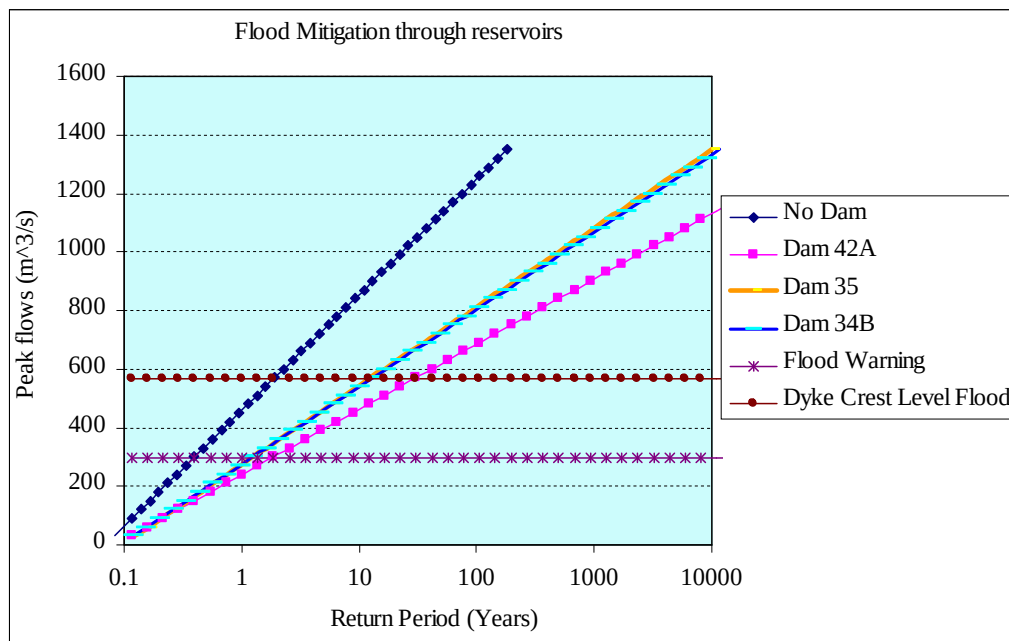


Figure 4.47: Graphical plot for the four flood mitigation scenarios

The return period for flood warning level of 298.15 m^3/s and the dyke crest level flood of 568.18 m^3/s as computed from the parameters of the fitted extreme value distribution for each of the flood mitigation dam implementation scenarios are shown in Table 4.8. Implementation of each of the dams individually reduced the incidence of overtopping of the dykes significantly. The return period of the dyke crest level

flood improved from about 1.7 years to a recurrence interval of over 13 years when dams 35 and 34B are implemented, but the recurrence interval of the same flood increased to 31 years when dam 42A is implemented.

Table 4.8: Summary of recurrence interval for the flood threshold levels

Flood Mitigation	Flood Warning level (298.2m³/s)	Dyke crest level flood (568.2 m³/s)
No Dam	0.5 years	1.7 years
Dam 35	1.3 years	12.7 years
Dam 34B	1.3 years	13.2 years
Dam 42A	1.9 years	30.6 years

CHAPTER FIVE

CONCLUSIONS AND RECOMMENDATIONS

5.1. CONCLUSIONS

The main objective of this study was to evaluate the effectiveness of the proposed reservoirs as flood mitigation measure in the Nzoia River basin using MIKE 11

model. The study approached the problem based on the integration of a rainfall-runoff model (NAM) and a one dimensional hydraulic model (MIKE 11). These models aided in the analysis of flood generation from the River Nzoia catchment and propagation through the river. Only hydrological analysis was done but the dams' implementation will depend on this, and many other factors. MIKE 11 was used to simulate stream flow under two scenarios: With and without reservoirs in the Nzoia River system. The scenarios reflected the effect of the proposed reservoirs on the flooding in the flood plains of Budalangi. From the analysis, the following conclusions can be drawn.

1. The NAM model successfully simulated the rainfall-runoff in the four sub basins of Nzoia River. The coefficient of determination (R^2) of the simulated runoff varied from 0.7 to 0.85 during both model calibration and verification.
2. The hydrodynamic/hydraulic model of River Nzoia system covering the proposed three dam sites was successfully set-up. In particular during calibration the coefficient of determination (R^2) was 0.88 and during validation the R^2 was 0.89. The model can therefore be reliably used to forecast the flood flows for both the design and management of the proposed reservoirs.
3. Based on flood thresholds at Rwambwa dyke section of $298\text{m}^3/\text{s}$ and $568\text{m}^3/\text{s}$ for overtopping the river banks and dykes respectively, it was observed that dam 42A was more effective in flood regulation than dams 34B or 35 in controlling the floods at Budalangi.
4. The incidence of flooding at Budalangi reduced significantly with the implementation of each of the dams. The flood recurrence interval improved from 1.7 years (no dam) to 13 years when dams 35 or 34B was implemented, but the recurrence interval of the same flood increased to 31 years when dam 42A was implemented.

5.2. RECOMMENDATIONS

The objectives set out before this study was to evaluate the effectiveness of the proposed reservoirs as flood mitigation measure in the Nzoia River basin using MIKE 11 model. The following are recommendations made after this study:

1. This study relied on data of a period of nine years; the model results can be improved by using data of a longer duration.
2. The more cross-sections data used in the model, the better the accuracy of the hydraulic simulations. It is therefore recommended that more work is needed in carrying out additional cross section measurements at least every 5km along the river system of Nzoia basin.
3. A number of add-on modules such as the structure operation module (SO) exist for the MIKE 11 model. Using the interface of the SO module reservoirs may be used to set up several control strategies for management of multi-reservoir systems. A further research in this line is therefore recommended.
4. To increase the accuracy of the rainfall-runoff forecasting a more physically based rainfall-runoff models like SWAT, with a possibility of catchment scenario analysis can be used for future accurate predictions in the management of the reservoirs.
5. The operation of a single reservoir for a single purpose does not present many analytical problems, unlike when a reservoir fulfils a number of potentially conflicting objectives or where several reservoirs are operated conjunctively. The multipurpose use and simultaneous operation of reservoirs in the Nzoia basin is therefore recommended for further research.

6. Among the proposed dams, dam 42A was found to be more effective in flood mitigation and it should be constructed with gates to control the outflow from the reservoir

REFERENCES

- Al-Hallaq, A., Sofyan, B., Elaish, A. (2008). Determination of Mean Areal Rainfall in the Gaza Strip Using Geographic Information System (GIS) Technique. *University of Sharjah, Journal of Pure & Applied Sciences* 5(2), 105-126.
- Beven, K. (2008). *Rainfall-Runoff Modelling*. London: John Wiley & Sons.
- Bhawan, J.V. (1999). Flood Control Regulations of a Multi-Reservoir System. *National Institute of Hydrology, Roorkee, India*.
- Boukhris, O., Willems, P., Vanneuville, W., Van Eerdenbrugh, K. (2008). Climate Change Impact on Hydrological Extremes in Flanders: Regional Differences. *Final report of the research project for the Flemish Government*. Belgium.
- CAS Consultants. (2006). Draft Study Report. *Study on Causes and Effects of Floods in Nyanza and Western Provinces, Tana Basin and Taita-Taveta District*. Kenya.
- Chapman, T. (1991). Comment on: Evaluation of automated techniques for base flow and recession analysis. *Water Resources Research* 27(7), 1783-1784.
- Chen, F., and Liu, C. (2012). Estimation of the Spatial Rainfall Distribution Using Inverse Distance Weighting (IDW) in the Middle of Taiwan. *Paddy Water Environment*, Springer.
- Chow, V.T., Maidment, D.R., Mays, L.W. (1988). *Applied hydrology*. New York: McGraw-Hill.
- Courant, R., and K.O. Friedrichs. (1948). *Supersonic Flow and Shock Waves*. New York: Interscience Publishers.
- Dan Roseberg and Henrik Madsen. (2004). Advanced Approaches in PDS/POT Modelling of Extreme Hydrological Events. *Hydrology: Science & Practice for the 21st Century*, Vol.1.
- De Silva, R. P., N.D.K. Dayawansa and M. D. Ratnasiri. (2007). A Comparison of Methods Used In Estimating Missing Rainfall Data. *The Journal of Agricultural Sciences* 3, 2102-2108.
- De Silva, R. P. (1997). *Spatiotemporal Hydrological Modelling with GIS for the Upper Mahaweli Catchment, Sri Lanka*. Unpublished PhD Thesis. Silsoe Campus, Cranfield University, UK,

- DHI. (2008). MIKE VIEW- A Results Presentation Tool for MOUSE, MIKE URBAN, MIKE NET and MIKE 11, *User Guide and Tutorial*. Danish Hydraulic Institute, Horsholm, Denmark.
- DHI. (2007). MIKE 11- A Modelling System for Rivers and Channels. *Reference manual*, Danish Hydraulic Institute, Horsholm, Denmark.
- Eckhardt, K. (2005). How to Construct Recursive Digital Filters For Baseflow Separation. *Hydrological Processes*, Vol. 19. pp. 507–515.
- Ghanemi, A. (2011). Climatology of the Areal Precipitation in Amman/Jordan. *International Journal of Climatology*, 31(9), 1328-1333.
- Githui, F.W. (2007). *Assessing the Impacts of Environmental Change on the Hydrology of the Nzoia Catchment, In the Lake Victoria Basin*. Unpublished PhD Thesis, VU University, Brussel.
- Gupta, R.S. (1989). *Hydrology and Hydraulic Systems*. Englewood Cliffs, New Jersey: Prentice Hall.
- JICA. (1992). *The Study on the National Water Master Plan: Final Report*. Sector Report G. Flood Control No 3, Ministry of Water Development.
- KMD. (2011). Advisory Report: Potential for Flooding in Budalangi.
- Khan, S. (1997). Decision support System for Reservoir Operation to Manage Severe Floods in Pakistan. *National Engineering Services*, Paper No.576,
- Klemes, V. (1986). Operational Testing of Hydrological Simulation Models. *Hydrological Science Journal* 31(1), 13–24.
- Krause, P., Boyle, D.P., and Base, F. (2005). Comparison of Different Efficiency Criteria for Hydrological Model Assessment. *Advanced Geosciences*, 5, 89-97.
- Madsen, H. (2000). Automatic Calibration of a Conceptual Rainfall-Runoff Model Using Multiple Objectives. *Journal of Hydrology* 235, 276-288.
- Makhanu, S. K. (2005). Workshop and Seminar on Nile Basin Capacity Building Network for River Engineering (NBCBN-RE). *Regional Power Integration in Hydropower Project*; Report for Phase I, Cairo, Egypt, 26-27.
- Mango, T. (2003). Budalangi Stakeholders Forum. *The Issue of Floods in Budalangi division*: Report for Budalangi Flood, Kenya.
- Mauricio, F.V., Willems, P. (2010). Filling Gaps and Daily Disaccumulation of Precipitation Data for Rainfall-runoff model. *Balwois Journal* 25, Ohrid, Macedonia.

- NWCPC. (2009). Flooding problem in Budalangi, Kenya.
- Nejadhashemi, A.P., Wardynski, B.J., and Munoz, J.D. (2011). Evaluating the Impacts of Land Use Changes On Hydrologic Responses in Agricultural Regions of Michigan and Wisconsin. *Hydrology and Earth System Sciences Discussions* 8, 3421-3468.
- Ngo, Madsen *et al.* (2008). Implementation and Comparison of Reservoir Operation Strategies for the Hoa Binh Reservoir, Vietnam using the Mike 11 Model. *Water Resource Management Journal* 22, Springer, 457–472.
- NBCBN. (2005). Flood management Research Cluster group II. *Flood and Catchment Management*.
- NBCBN. (2010). Flood and Drought Forecasting and Early Warning. *Hydraulic Research Institute*, Cairo, Egypt.
- Patra, K.C. (2008). *Hydrology and Water Resources Engineering*. India: Alpha Science International Ltd.
- Pircher, W. (1990). Hydrology in Mountainous Regions: Artificial Reservoirs; Water and Slopes. *194th International Association of Hydrological Sciences Conference Proceedings*, Lausanne.
- Price, R. K. (2009). Volume-Conservative Nonlinear Flood Routing. *Journal of Hydraulic Engineering* 135 (10), 838-845.
- Reddy, P. J. R. (1992). *A Textbook of Hydrology*. 2nd Ed. New Delhi: Laxmi Publications,
- Refsgaard, J. C. (2007). Hydrological Modelling and River Basin Management. Published PhD Thesis, Geological Survey of Denmark and Greenland (GEUS).
- Refsgaard, J. C., Jesper, K. (1996). Operational validation and intercomparison of different types of hydrological models. *Water Resources Research* 32 (7) 2189–2202.
- Rohan, M. B. (2009). *Quantification of Reservoir Operation-Based Losses to Floodplain Physical Processes and Impact on the Floodplain Vegetation at the Kootenai River*, unpublished PhD thesis, USA.
- Sadiq *et al.*, (2011). Satellite Remote Sensing and Hydrologic Modelling for Flood Inundation Mapping in Lake Victoria Basin: Implications for Hydrologic Prediction in Un-gauged Basins. *IEEE Transactions on Geoscience and Remote Sensing*, Vol. 49 No. 1

- Sergio, M. V., Begueria, S., Juan, L., Miguel, A. and Stepanek, P. A. (2010). Complete daily precipitation database for Northeast Spain: Reconstruction, Quality Control, and Homogeneity. *International Journal of Climatology*, Wiley 30 (8),1146-1163.
- Shamsudin, S., Hashim, N., (2002) Rainfall Runoff Simulation Using Mike11 NAM. *Journal of Civil Engineering, Malaysia* 15(2).
- Shaw, E., Beven, K.J., Chappell, N. A., and Lamb, R. (2011). *Hydrology in Practice*. 4th Ed. London, England: Spon Press,
- TAHAL. (2007). Final Report .*Consultancy on Nzoia and Yala Multipurpose Flood Protection Works Sub-component*, Kenya.
- Tawatchai, T. (1996). Control and Mitigation of Floods along Tran basin Diversion Channel of Mekong Tributaries and Nan River, Thailand. *School of Civil Engineering Journal*, Asian Institute of Technology.
- Vu Min Cat, B. (2007). Application of Mike Package to Assess Hydraulic Regimes and Flood Mapping When Construction of Thermal Power at the Mong Duong Estuary. *Vietnam Estuary Workshop*, Japan.
- (WKCDD&FMP). (2006). Feasibility Study and Design preparation of Flood Control Structures within Nzoia River basin: Request for Expression of Interest (EOI).
- Willems, P. (2004). WETSPRO: Water Engineering Time Series Processing Tool. *Methodology and User's Manual*. K.U. Leuven (Hydraulics Laboratory), Belgium.
- Willems, P. (2004). ECQ: Hydrological Extreme Value Analysis Tool. *Methodology and Users' manual*. K.U. Leuven, Belgium,
- Willems, P. (2009). A Time Series Tool To Support The Multi-Criteria Performance Evaluation of Rainfall-Runoff Models. *Science Direct Journals, Environmental Modelling & Software* 24(3), 311-321.
- Willems, P. (1998). Hydrological Applications of Extreme Value Analysis. *Hydrology In a Changing Environment*, Vol. III, 15-25, ed. H. Wheater and C. Kirby. Chichester: John Wiley & Sons.
- WMO. (2006). APFM, Flood Management Policy Series. *Environmental Aspects of Integrated flood Management*. Technical Document No.3, Geneva.
- WMO. (1994). Guide to hydrological practices, Data Acquisition and Processing, Analysis, Forecasting and other applications, 5th edition, WMO-No.168.

APPENDICES

APPENDIX A: WEATHER DATA AND RESERVOIR PARAMETERS

Table A 1: Nzoia catchment rain gauging stations and their coordinates

Station Name	Station ID	UTM Coordinates		Period of records
		Long. (°E)	Lat.(°N)	
Chorlim	8834013	700,297.78	110,585.08	1970-2009
Kitale Met	8834098	720,669.20	110,596.82	1975-2009
Elgon Downs	8834009	707,751.56	117,998.74	1970-2000
Vale Estate	8934008	713,328.02	99,533.20	1970-2009
Lugari	8934016	709,553.94	75,533.11	1970-2009
Butula	8934039	648,340.51	36,816.54	1970-2006
Butere	8934040	666,930.63	22,113.64	1970-2006
Uholo	8934059	650,234.30	22,112.20	1970-2009
Kimilili	8934060	685,504.50	86,581.97	1970-2003
Malava	8934061	703,995.30	51,644.20	1970-2009
Kaimosi	8934072	715,134.90	16,589.01	1970-2009
Kakamega	8934096	696,651.86	31,294.98	1970-2009
Kapsakwony	8934113	691,067.00	93,993.09	1970-2007
Webuye Agric.	8934119	696,642.90	68,229.73	1970-2009
Mumias	8934133	666,928.55	38,698.90	1970-2006
Bungoma W.S	8934134	672,488.50	64,462.78	1970-2009
Kadenge	8934140	668,815.70	63,024.40	1970-2005
Alupe	8934161	626,064.85	107,235.35	1975-2009
Kipkabus	8935061	661,363.84	33,169.70	1970-1987

Turbo F.S	8935076	724,473.92	71,889.40	1970-2006
Nabkoi	8935080	772,706.61	14,714.03	1970-1999
Chebororwa	8935158	763,428.60	103,213.30	1970-2009
Kaptagat	8935164	776,372.40	55,317.30	1970-1997
Turbo (New)	8935170	728,152.70	60,830.70	1970-2008
Eldoret Met.	8935181	754,097.60	58,627.80	1973-2009

(Source: KMD 2010)

Table A 2: Evaporation data for Nzoia weather stations

Station Name	Station ID	Period of Records
Kitale Met.	8834098	1975-2009
Kakamega Met	8934096	1970-2009
Butulla	8934039	1970-1986
Alupe R.S	8934161	1975-1986

(Source: KMD 2010)

Table A 3: Stream flow data (RGS) in the Nzoia basin

Station Name	ID	Longitude. (°E)	Latitude. (°N)	Water-shed Area (km ²)	Period of Records
Rwambwa	1EF01	34.090	0.123611	12,656	1975-2009
Nzoia Market	1EE01	34.225	0.177778	11,829	1963-2006
Webuye	1DA02	34.807	0.588889	8472	1949-1996
Kipkaren	1CE01	34.96	0.608	2,656	1949-2007

(Source: WARMA 2010)

Table A 4: Elevation–Area–Volume Relationships of the 3 Dam Sites

WEBUYE (34B)			KIPKAREN (35)			ANYIKO/RAMBULA(42A)		
Elevation (m)	Area (km ²)	Volume (MCM)	Elevation (m)	Area (km ²)	Volume (MCM)	Elevation (m)	Area (km ²)	Volume (MCM)
1,620	0.24	4.8	1,600	0.00	0.00	1,190	0.00	0.0
1,625	1.48	12.2	1,605	0.13	0.65	1,200	1.07	10.7
1,630	2.88	26.6	1,610	0.42	2.75	1,205	2.97	25.6
1,635	4.69	50.1	1,615	0.70	6.25	1,210	7.32	62.2
1,640	6.40	82.1	1,620	1.14	11.95	1,215	12.14	122.9

1,645	9.19	128.1	1,625	1.66	20.25	1,220	19.47	220.2
1,650	12.46	190.4	1,630	2.23	31.40	1,225	29.20	366.2
1,655	15.95	270.1	1,635	2.82	45.50	1,230	40.90	570.7
1,660	20.11	370.6	1,640	3.50	63.00	1,235	51.69	829.2
1,665	25.11	496.2	1,645	4.77	86.85			
1,670	31.29	652.6	1,650	6.18	117.75			
			1,655	7.40	154.75			

(Source: TAHAL, 2007)

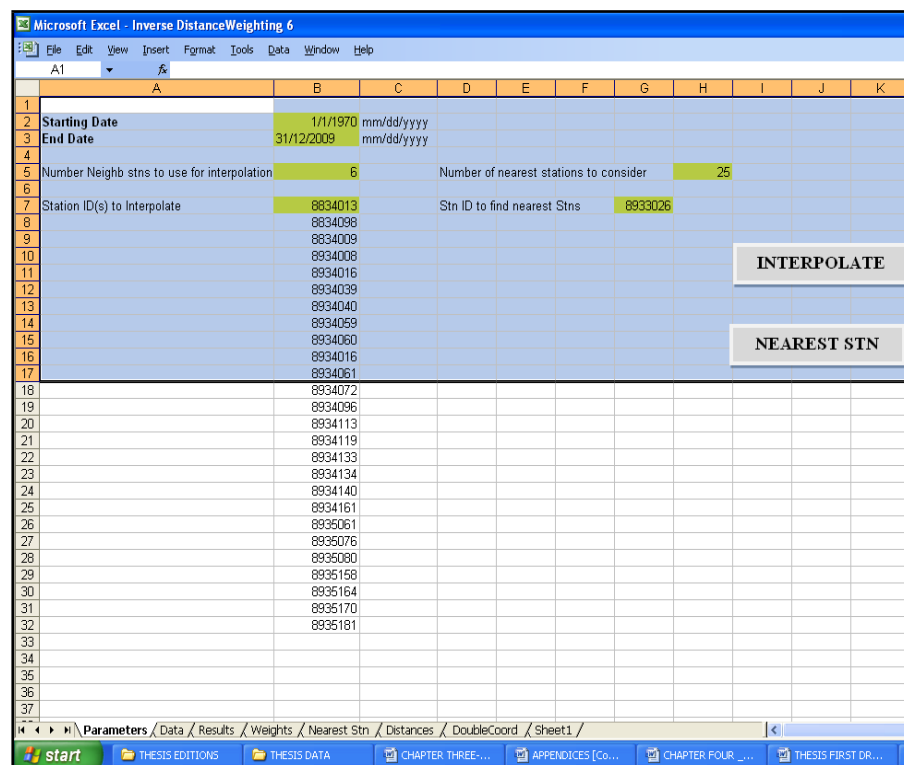


Figure A 1: IDW procedure used in gap filling daily rainfall data

APPENDIX B: THIESSEN POLYGON WEIGHTS

Table B 1: Thiessen polygon weights for Webuye (Sub basin C)

Item No.	WEBUYE (SUB BASIN C)		
	Rain gauge Station	Station ID	Thiessen Weights
1	Chebororwa	8935158	0.339
2	Kitale	8834098	0.178
3	Elgon Downs	8834009	0.077
4	Chorlim	8834013	0.092
5	Vale Estate	8934008	0.080
6	Turbo	8935076	0.080
7	Lugari	8934016	0.091
8	Kapsakwony	8934113	0.064

Table B 2: Thiessen polygon weights for Nzoia Market (Sub basin B)

Item No.	NZOIA MARKET (SUB BASIN B)		
	Rain gauge Station	Station ID	Thiessen Weights
1	Kipkabus	8935061	0.050
2	Kaptagat	8935164	0.043
3	Eldoret	8935181	0.088
4	Chebororwa	8935158	0.150
5	Kitale Met	8834098	0.087
6	Elgon Downs	8834009	0.038
7	Vale Estate	8934008	0.039
8	Turbo Met	8935076	0.051
9	Turbo Forest	8935170	0.048
10	Malava	8934061	0.052
11	Lugari	8934016	0.032
12	Kapsakwony	8934113	0.043
13	Kimilili	8934060	0.042
14	Brodrick Falls	8934119	0.047
15	Kakamega	8934096	0.056

16	Mumias Booker	8934133	0.054
17	Butula	8934039	0.015
18	Uholo	8934059	0.017
19	Chorlim	8834013	0.048

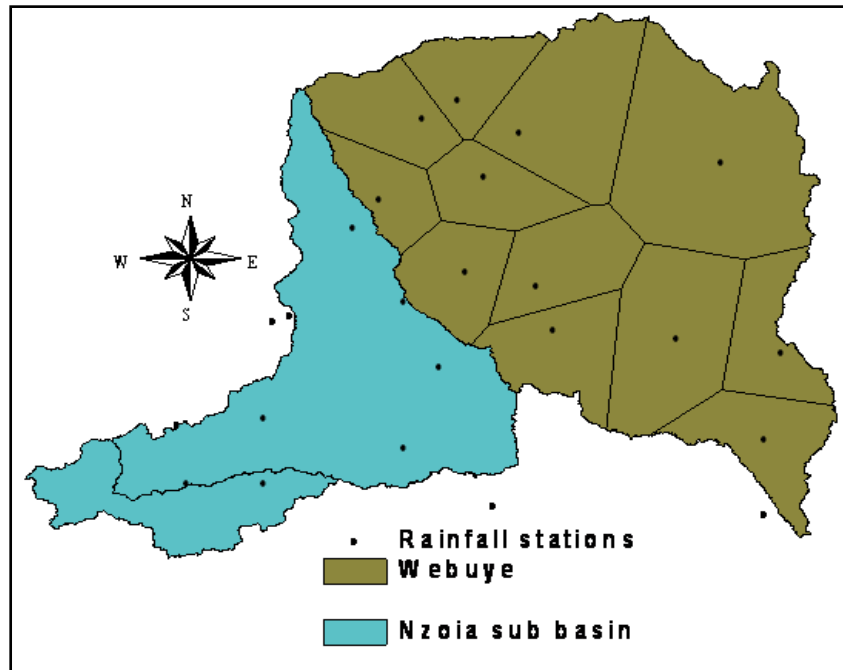


Figure B 1: Thiessen polygon map for Sub basin C

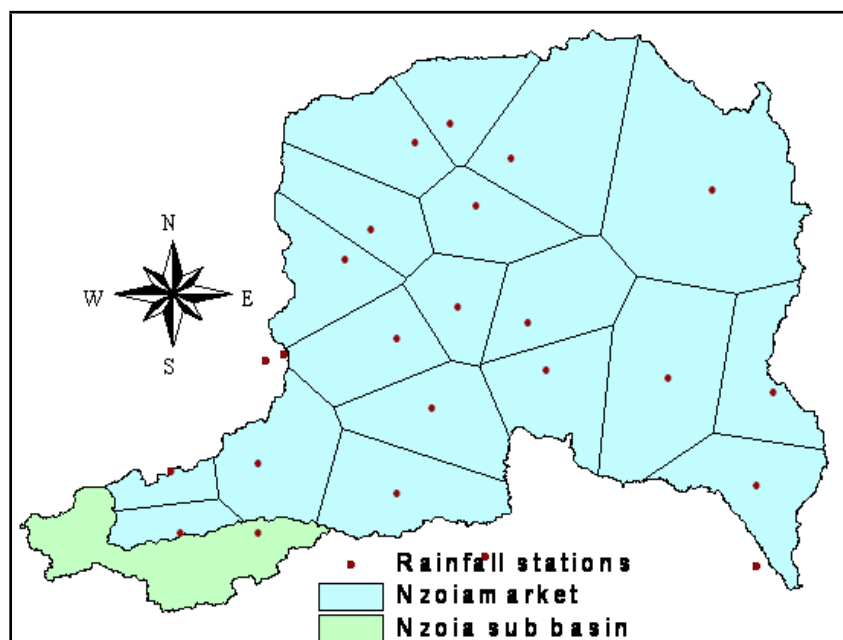


Figure B 2: Thiessen polygon map for Sub basin B

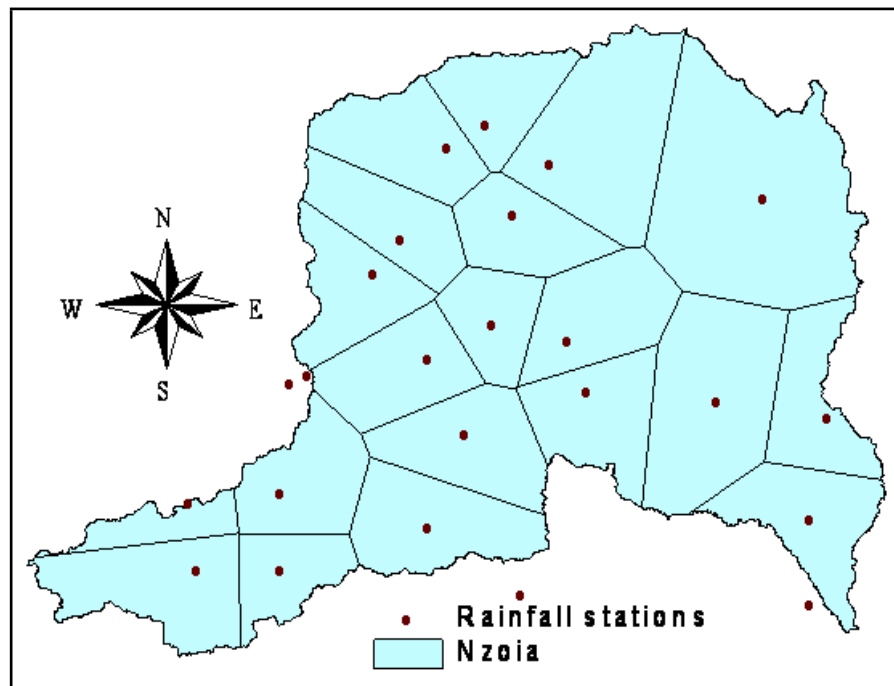


Figure B 3: Thiessen polygon map for Nzoia basin

Table B 3: Thiessen polygon weights for Nzoia Market (Sub basin B)

Item No.	River Nzoia Basin		
	Rain gauge Station	Station ID	Thiessen Weights
1	Kipkabus	8935061	0.047
2	Kaptagat	8935164	0.040
3	Chebororwa	8935158	0.140
4	Eldoret	8935181	0.082
5	Turbo Forest stn.	8935170	0.045
6	Turbo	8935076	0.048
7	Vale Estate	8934008	0.037
8	Kitale	8834098	0.082
9	Elgon Downs	8834009	0.035
10	Chorlim	8834013	0.045
11	Kapsakwony	8934113	0.040
12	Lugari	8934016	0.030
13	Malava	8934061	0.049
14	Brodrick Falls	8934119	0.044
15	Kimilili	8934060	0.040
16	Mumias Booker	8934133	0.044
17	Kakamega	8934096	0.051
18	Butere	8934040	0.029
19	Butula	8934039	0.018
20	Uholo	8934059	0.057

APPENDIX C: NAM CALIBRATION AND VALIDATION

Table C1: NAM Calibration parameters and default hypercube search space

Parameter	Unit	Lower bound	Upper bound
U_{\max}	[mm]	5	35
L_{\max}	[mm]	50	400
CQ_{OF}	[-]	0	1
$CKIF$	[hours]	200	2000
$CK12$	[hours]	3	72
TOF	[-]	0	0.9
TIF	[-]	0	0.9
TG	[-]	0	0.9
$CKBF$	[hours]	500	5000

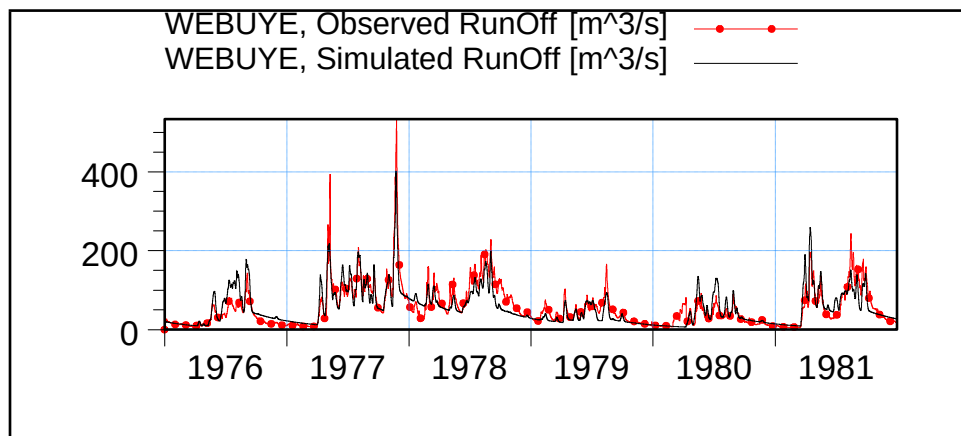


Figure C 1: Calibration hydrograph at Webuye (1DA02)

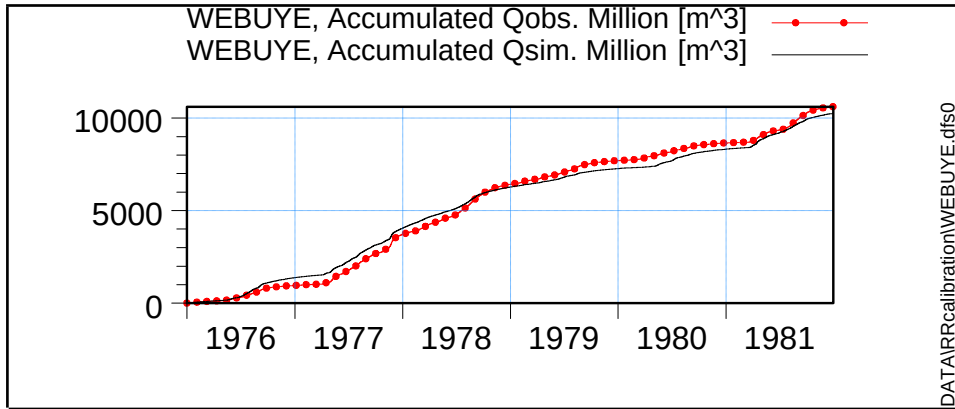


Figure C 2: Calibration cumulative volumes at Webuye (1DA02)

		Client:	NAM autocalibration	MIKE2-fo
		Project:	Results	
Parameterfile	Date:	R2=0.767, WBL= 1.8% (obs= 209mm/y, sim= 205mm/y)		
WEBUYER.r11	11/ 6/2011 13:13	Init:		

Figure C 3: Calibration result at Webuye ($R^2 = 76.7\%$)

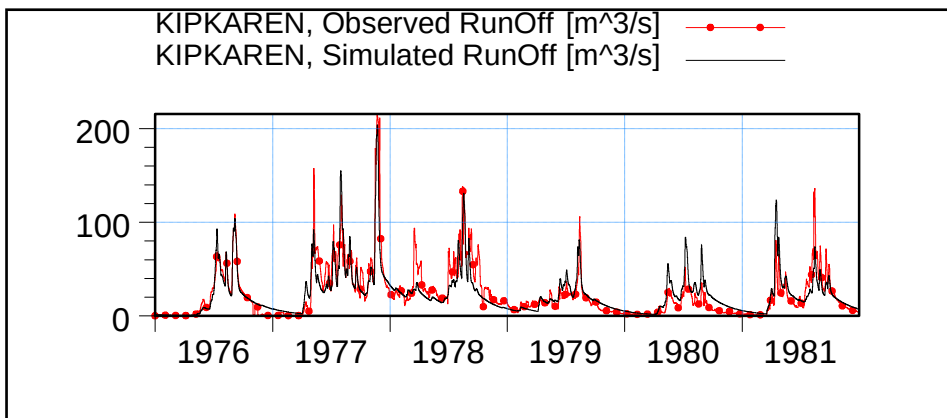


Figure C 4: Calibration hydrograph at Kipkaren (1CE01)

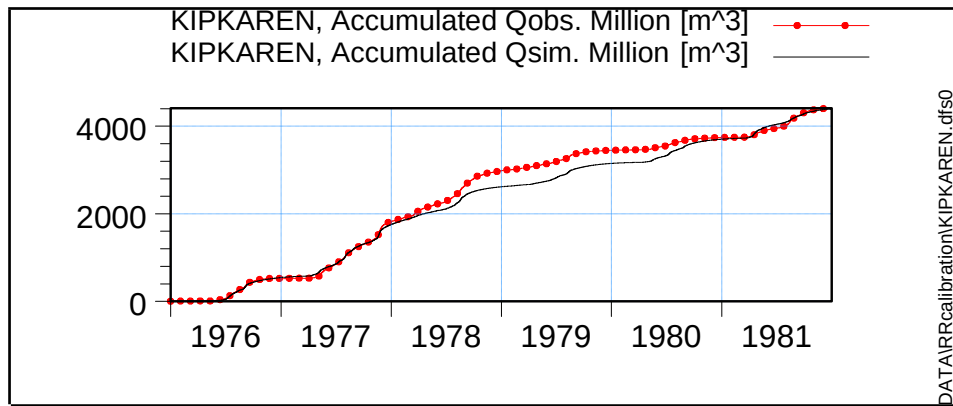


Figure C 5: Calibration cumulative volumes at Kipkaren (1CE01)

		Client: NAM autocalibration	MIKE2.0
		Project: Results	
Parameterfile KIPKAREN	Date: RRPar1.rr1111	R2=0.772, WBL= 0.3% (obs= 277mm/y, sim= 276mm/y)	
	Init:		

Figure C 6: Calibration result at 1CE01 ($R^2 = 77.2\%$)

APPENDIX D: LOCATION OF THE PROPOSED RESERVOIRS

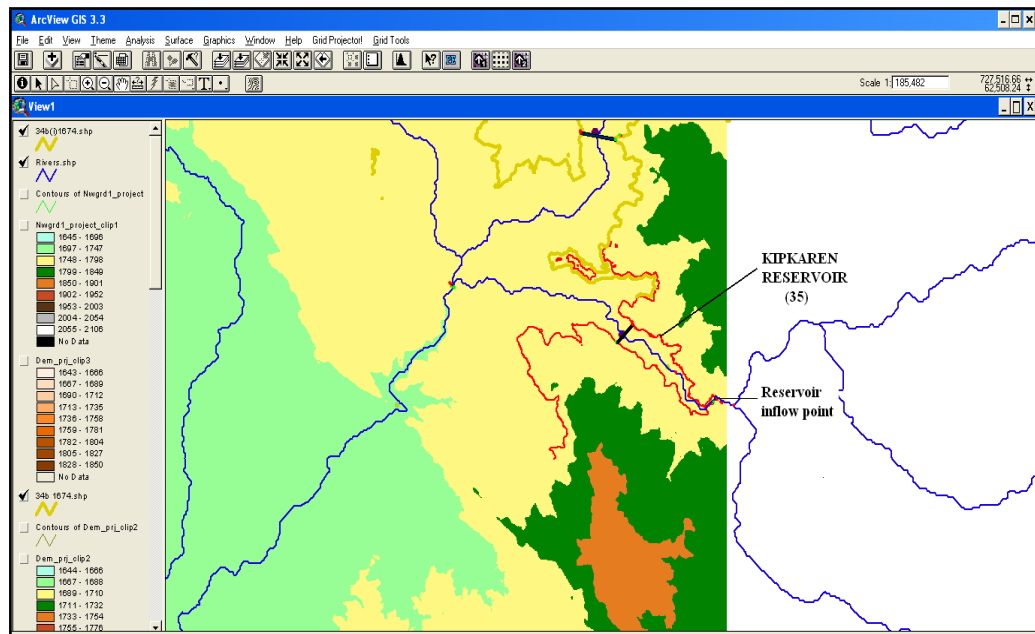


Figure D 1: Location of Kipkaren reservoir (35)

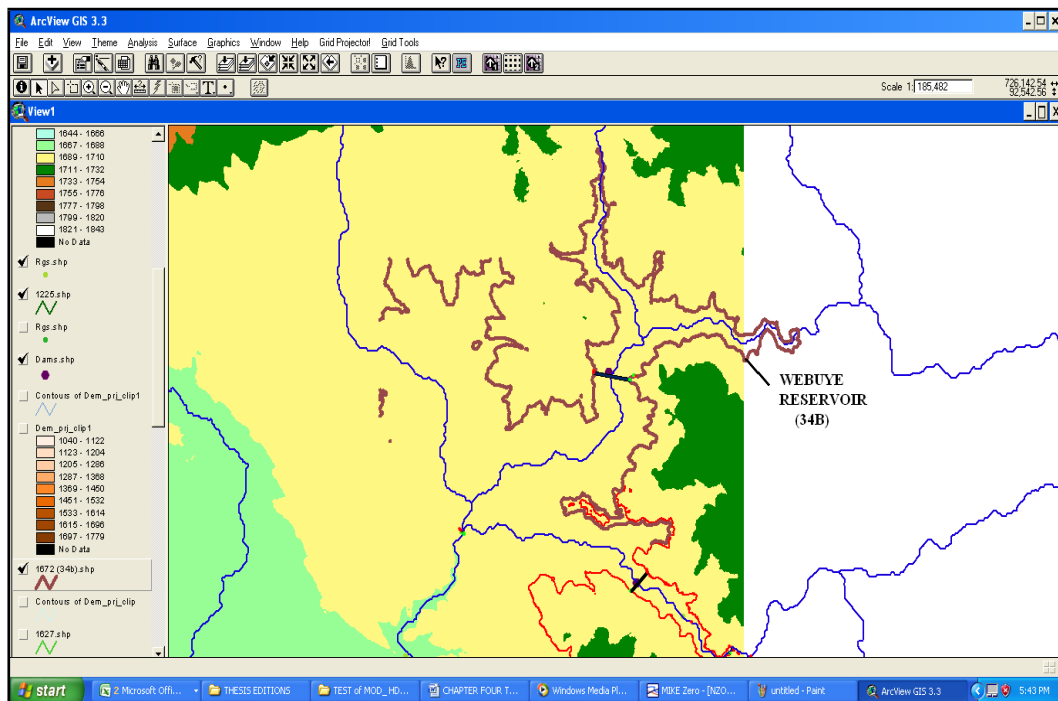


Figure D 2: Location of Webuye reservoir (34B)

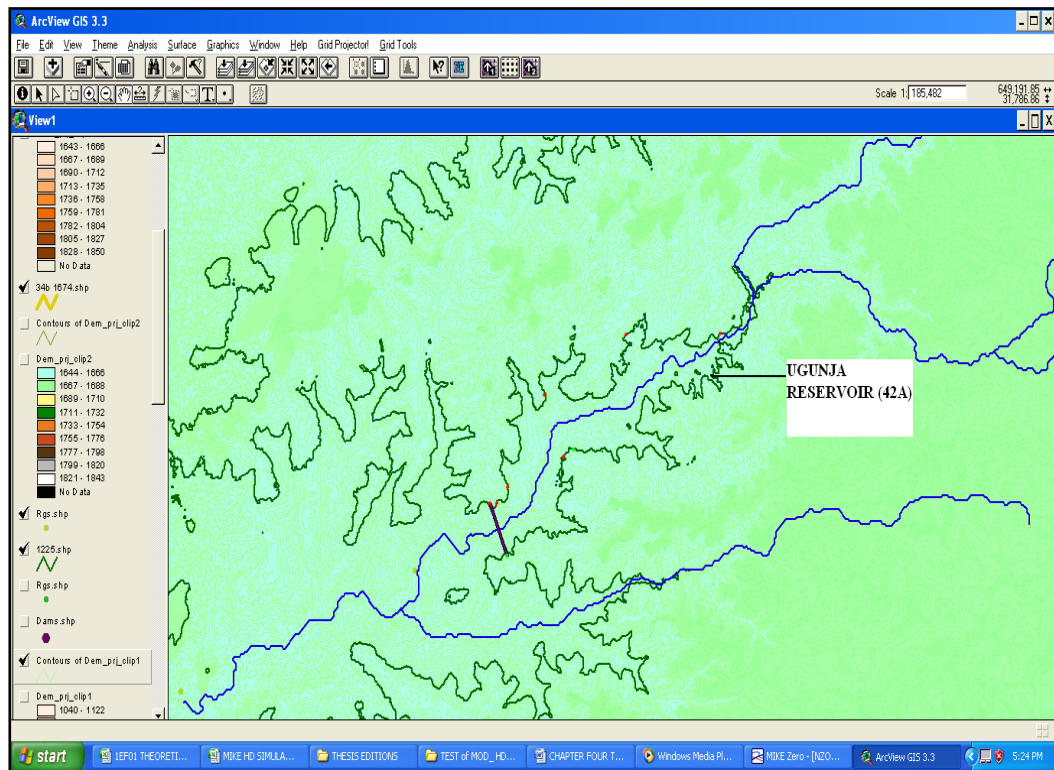


Figure D 3: Location of Anyiko/Rambula reservoir (42A)

APPENDIX E: PEAK-OVER – THRESHOLDS

Table E: Peak-Over-Threshold flows for no dams

POT results quick flow periods-No Dam			Rank No.	Ranked POT Value
Time at POT value (days)	POT value	Time at previous minimum (days)		(m ³ /s)
8	60.386	1	1	936.264
150	320.302	97	2	753.038
199	297.975	185	3	736.028
250	336.046	238	4	648.258
490	753.038	445	5	490.761
535	426.304	522	6	490.283
580	490.283	574	7	437.657
602	328.536	594	8	426.304
696	936.264	656	9	415.041
725	206.793	721	10	409.038
788	332.632	780	11	408.163
815	490.761	798	12	405.25
834	209.951	826	13	389.197
864	736.028	846	14	381.301
905	408.163	890	15	341.834
928	437.657	910	16	336.046
966	648.258	941	17	332.632
991	405.25	986	18	328.536
1007	341.834	998	19	320.302
1149	157.302	1121	20	309.701
1172	147.331	1165	21	302.519
1200	296.415	1185	22	297.975
1228	229.92	1209	23	296.415
1324	290.074	1244	24	290.074
1376	133.702	1357	25	245.703
1571	100.487	1550	26	229.92
1595	245.703	1582	27	213.285
1643	193.095	1632	28	209.951
1703	187.327	1671	29	206.793
1783	138.508	1781	30	193.095
1934	389.197	1902	31	187.327
2054	381.301	2002	32	177.422
2344	309.701	2278	33	157.812
2425	302.519	2404	34	157.302
2525	415.041	2472	35	147.331
2686	213.285	2653	36	143.307
2740	177.422	2729	37	138.508
2794	409.038	2754	38	133.702
3040	157.812	3019	39	100.487
3064	143.307	3049	40	60.386

Table E : Peak-Over-Threshold flows after implementing dam 42A

POT results quick flow periods (Regulated Dam 42A Flows)				
Time at POT value(days)	POT value	Time at previous minimum (days)	Rank	Ranked POT Values
246	291.229	1	1	319.681
494	300.873	451	2	308.845
628	303.746	523	3	308.176
693	319.681	655	4	306.309
789	231.639	779	5	305.066
865	184.747	849	6	303.746
977	305.066	890	7	303.548
1141	70.863	1119	8	300.873
1200	110.323	1192	9	291.229
1262	144.356	1222	10	283.914
1323	185.358	1306	11	265.614
1370	73.162	1362	12	248.684
1597	170.13	1558	13	231.639
1651	202.043	1634	14	219.419
1682	123.43	1672	15	202.043
1702	192.228	1691	16	192.228
1932	303.548	1901	17	185.358
1964	219.419	1953	18	184.747
2054	248.684	2001	19	170.13
2342	265.614	2278	20	169.006
2426	283.914	2355	21	148.744
2459	147.484	2449	22	148.488
2505	308.176	2477	23	147.484
2525	308.845	2519	24	144.356
2705	148.744	2652	25	123.43
2739	148.488	2729	26	110.323
2809	306.309	2752	27	106.648
2870	169.006	2865	28	100.896
3098	67.915	3051	29	73.162
3144	100.896	3118	30	70.863
3176	106.648	3169	31	67.915
3245	62.756	3239	32	62.756
3271	50.838	3265	33	50.838

Table E: Peak-Over- Threshold results after implementing dam 34B:

POT results quick flow periods				
Time at	POT value	Time at previous	Rank	Ranked POT

POT value (days)		minimum (days)		Value
147	147.627	1	1	546.81
247	238.49	167	2	416.982
467	160.653	451	3	399.891
496	399.891	481	4	348.807
581	348.807	523	5	345.822
628	275.941	615	6	326.961
693	546.81	656	7	322.211
752	169.432	745	8	298.947
807	241.17	779	9	281.295
865	184.704	848	10	275.941
958	345.822	886	11	272.96
1007	190.456	998	12	241.17
1140	88.397	1120	13	241.085
1199	103.557	1167	14	238.49
1262	132.391	1243	15	238.037
1323	230.786	1309	16	230.786
1370	69.894	1362	17	225.534
1598	162.214	1552	18	204.941
1651	202.147	1634	19	202.147
1682	116.513	1675	20	190.456
1702	171.923	1692	21	184.704
1933	298.947	1901	22	171.923
1964	225.534	1953	23	169.432
2054	326.961	2001	24	162.214
2098	238.037	2084	25	160.653
2342	241.085	2278	26	153.153
2426	272.96	2388	27	147.627
2459	142.931	2450	28	142.931
2505	281.295	2477	29	137.937
2525	322.211	2519	30	133.929
2705	137.937	2651	31	132.391
2739	133.929	2729	32	116.513
2794	416.982	2752	33	103.557
2855	204.941	2851	34	102.978
2870	153.153	2866	35	94.387
3098	65.464	3051	36	88.397
3128	94.387	3118	37	69.894
3176	102.978	3169	38	65.464
3245	57.853	3239	39	57.853
3271	46.03	3265	40	46.03

Table E: Peak-Over- Threshold flows after implementing dam 35

POT Results Quick Flow Periods- Dam 35				
Time at POT value (days)	POT value	Time at previous minimum (days)	Rank	POT Value
2	33.8	1	1	610.156
147	146.705	129	2	350.045

246	231.307	167	3	343.72
467	151.035	451	4	340.037
490	334.141	481	5	337.294
580	337.294	523	6	334.141
627	327.595	615	7	327.595
694	610.156	656	8	322.214
752	169.431	745	9	291.768
807	241.174	779	10	282.704
865	184.703	848	11	272.96
977	350.045	886	12	253.169
1007	190.457	997	13	241.174
1140	88.397	1120	14	238.038
1199	103.559	1167	15	231.307
1262	132.388	1243	16	227.809
1323	227.809	1309	17	225.534
1598	162.215	1552	18	204.939
1651	202.147	1634	19	202.147
1682	116.514	1674	20	190.457
1702	171.924	1692	21	184.703
1933	343.72	1901	22	171.924
1964	225.534	1953	23	169.431
2054	291.768	2001	24	162.215
2098	238.038	2084	25	151.035
2342	253.169	2278	26	146.705
2426	272.96	2388	27	142.932
2459	142.932	2450	28	137.942
2505	282.704	2477	29	133.929
2525	322.214	2519	30	132.388
2705	137.942	2651	31	116.514
2739	133.929	2729	32	103.559
2794	340.037	2752	33	102.977
2855	204.939	2851	34	94.385
3098	65.461	3051	35	88.397
3128	94.385	3118	36	65.461
3176	102.977	3169	37	57.855
3245	57.855	3239	38	33.8

APPENDIX F: RESERVOIR FLOWS EXTREME VALUE ANALYSIS

Appendix F (1): Extreme value analysis graphs for dam 42A regulated peak flow

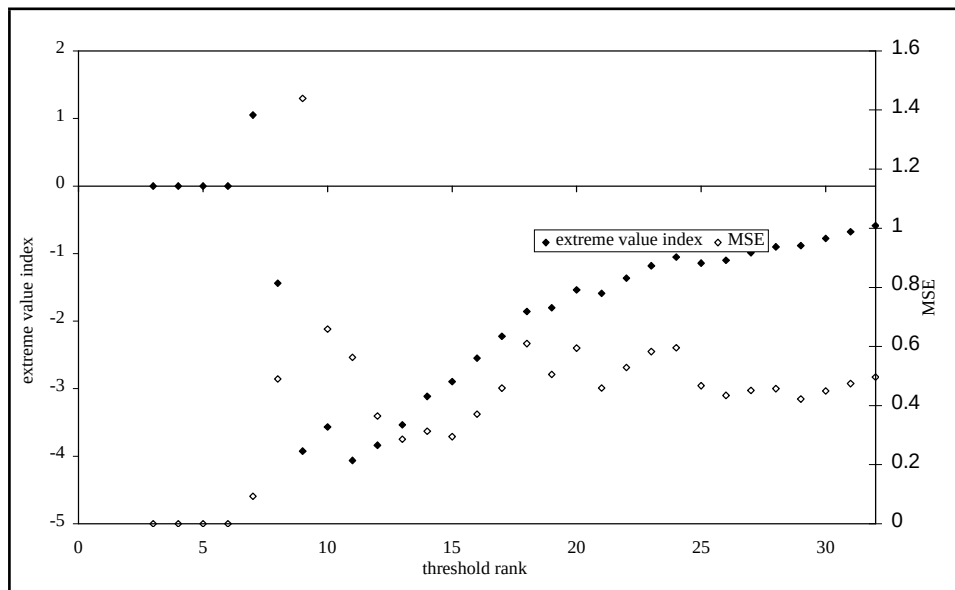


Figure F 1: UH-Slope Plot for dam 42A regulated peak flows

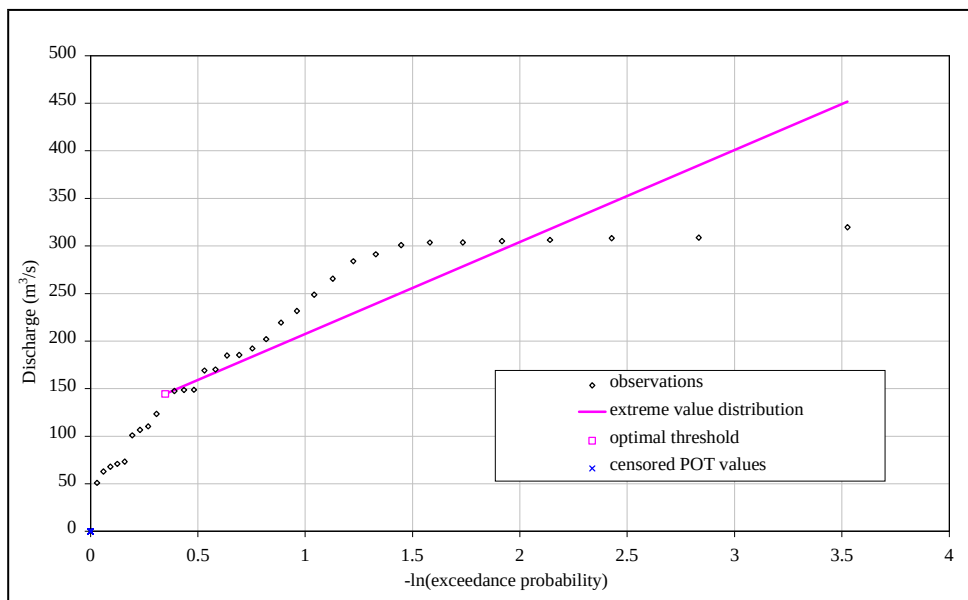


Figure F 2: Exponential Q-Q Plot for dam 42A regulated flow

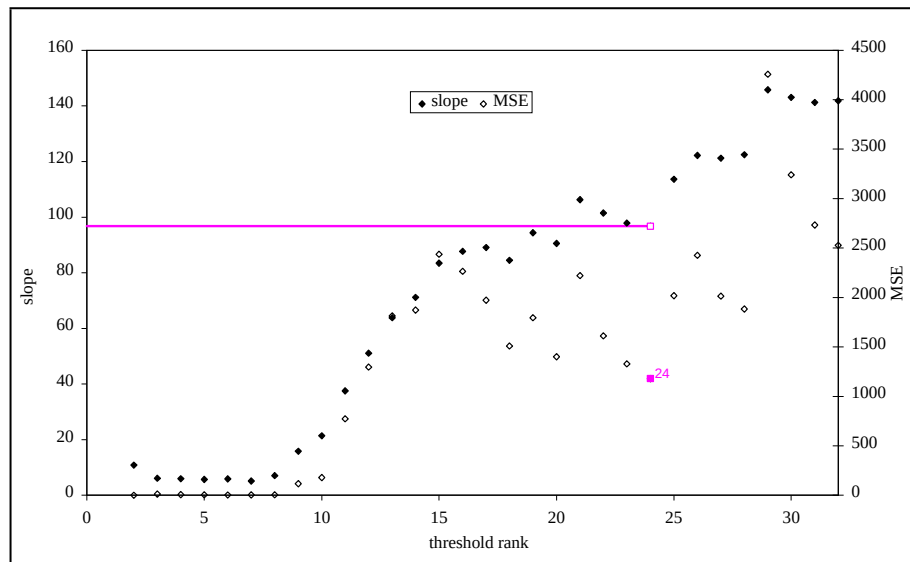


Figure F 3: Exponential Slope Q-Q Plot for dam 42A regulated flows

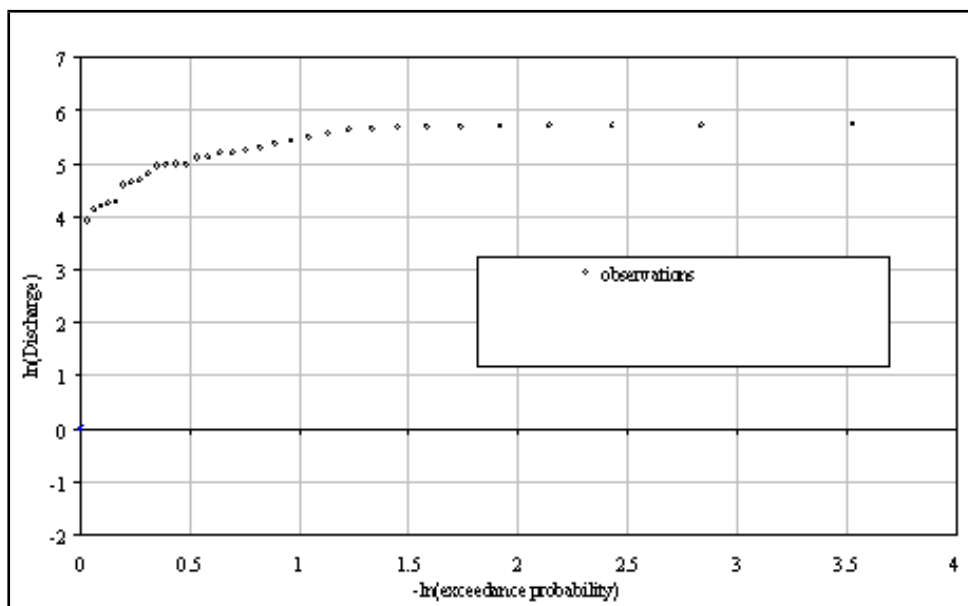


Figure F 4: Pareto Q-Q Plot for dam 42A regulated flows

Appendix F (2): Extreme Value Analysis Distribution Graphs for Dam 34B for Regulated Flows

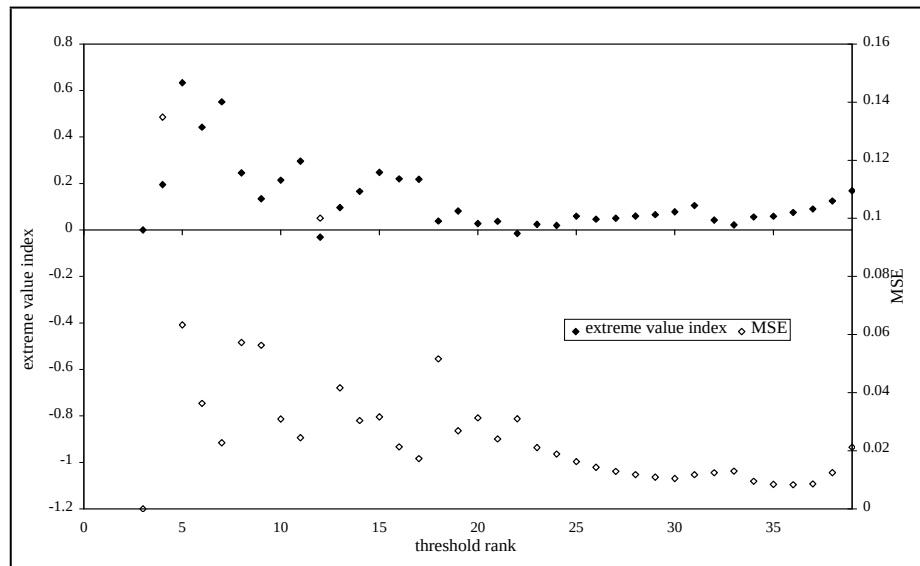


Figure F 5: Slope U-H Quantile-Quantile Plot for dam 34B regulated flows

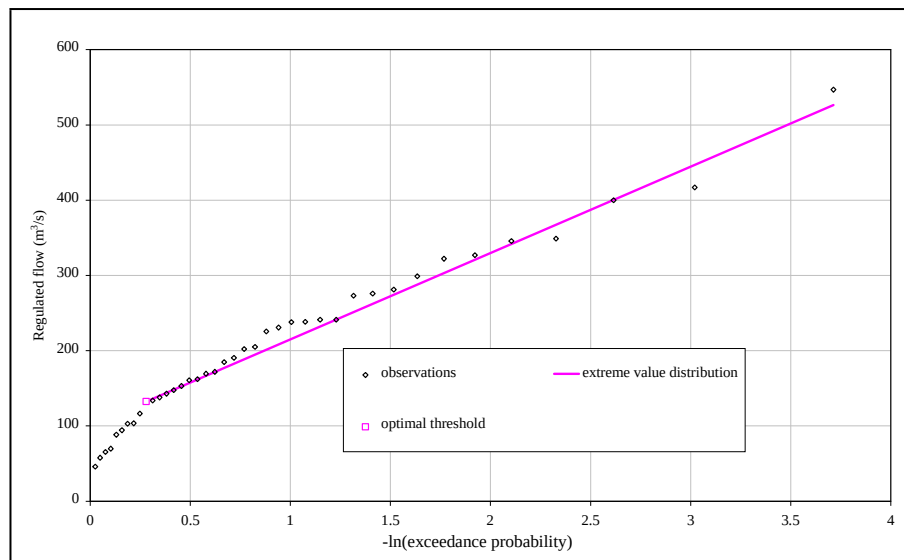


Figure F 6: Exponential Q-Q Plot for dam 34B regulated flow

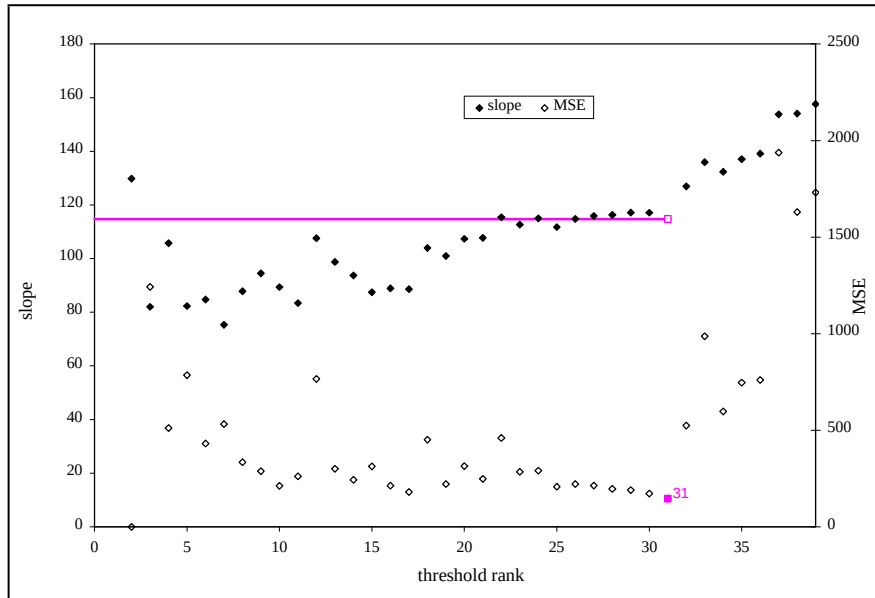


Figure F 7: Exponential Slope Q-Q Plot for Dam34B regulated flow

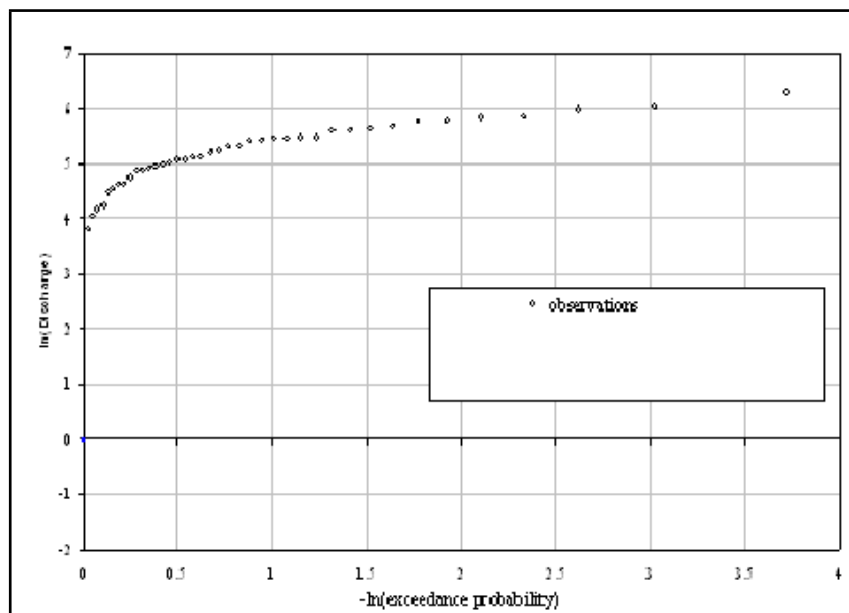


Figure F 8: Pareto Q-Q plot for Dam 34B regulated flow

Appendix F (3): Extreme Value Analysis Distribution Graphs for Dam 35

Regulated Flow

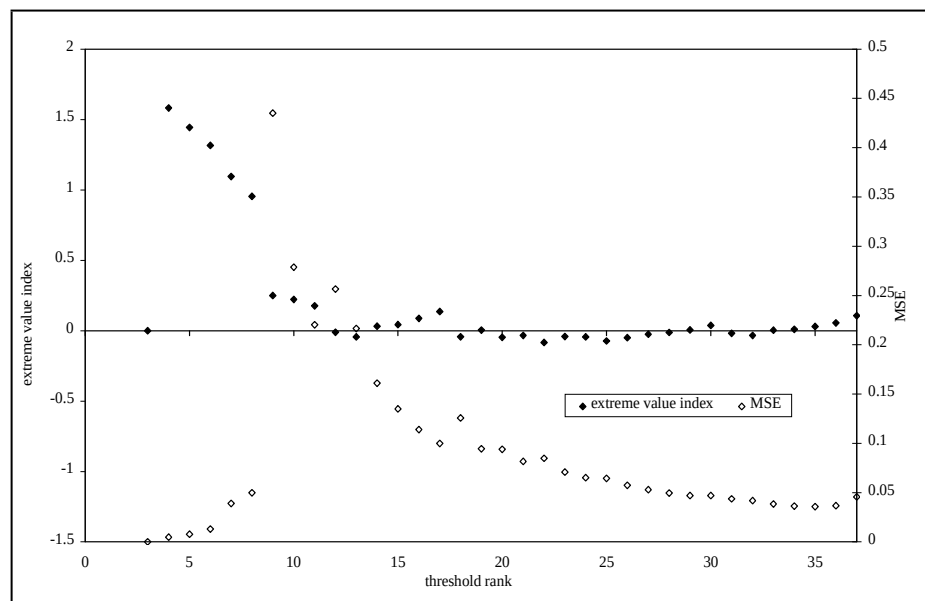


Figure F 9: U-H Slope Q-Q plot for dam 35 regulated discharge

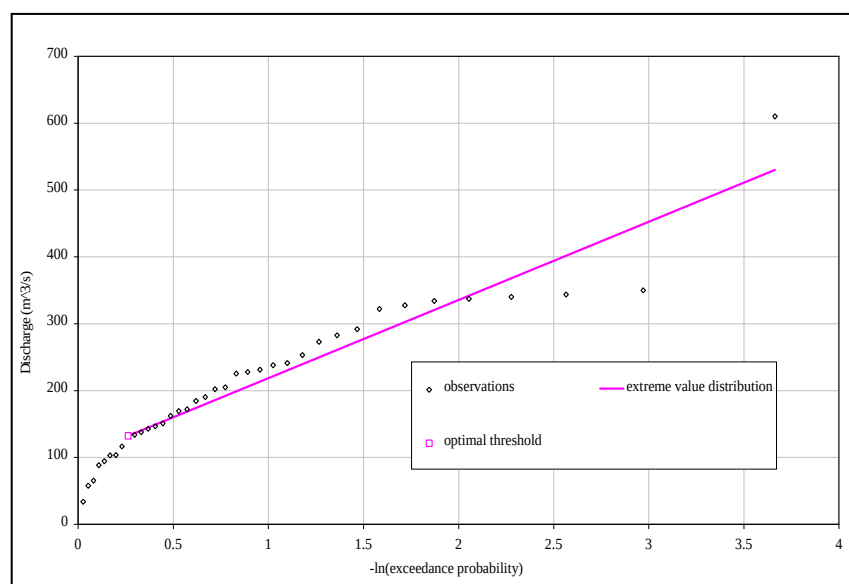


Figure F10: Exponential Q-Q plot for dam 35 regulated discharges

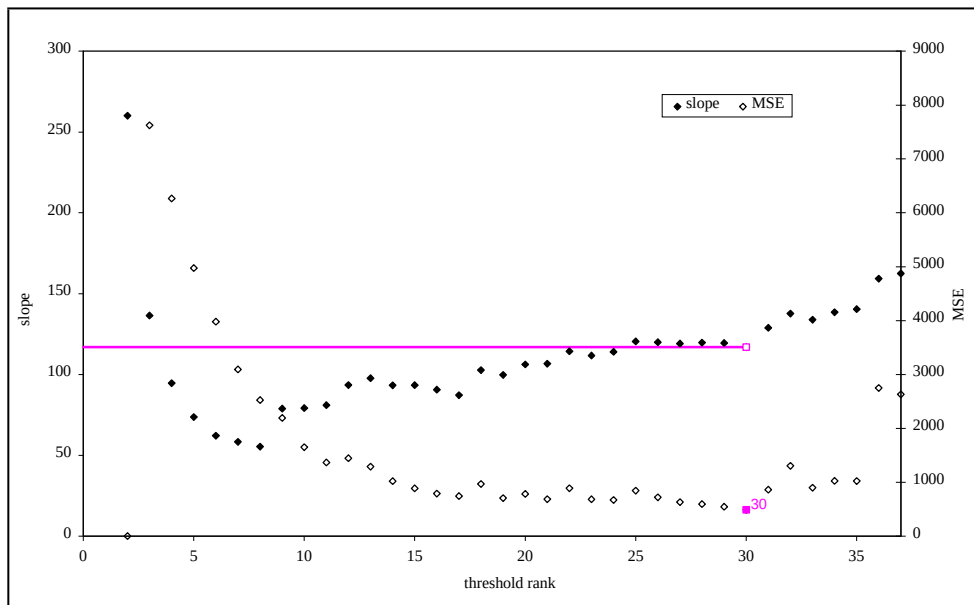


Figure F 11: Slope-Exponential Q-Q plot for dam 35 regulated discharge

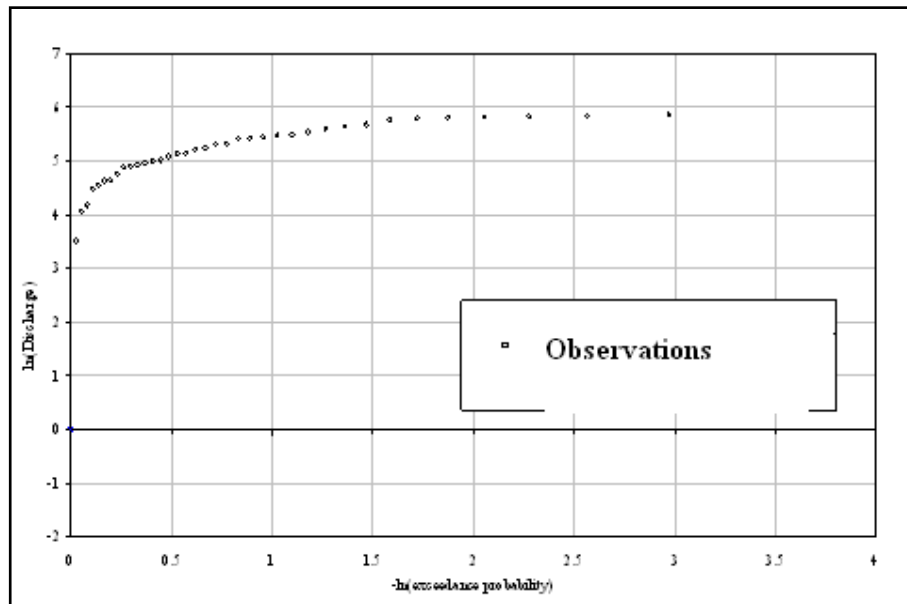


Figure F 12: Pareto distribution for simulated discharge at dam site 35

APPENDIX G: RETURN PERIOD

Table G1: Theoretical return period

Discharge (m ³ /s)	NO DAM	Dam 42A	Dam 35	Dam 34B
	Theoretical return period			
30	0.0824	0.065550332	0.124938312	0.118930602
60	0.098179545	0.091791401	0.161491048	0.154470145
90	0.116923661	0.128537277	0.208737882	0.200629824
120	0.139246341	0.17999324	0.269807545	0.260583209
150	0.165830795	0.252048021	0.348744131	0.338452218
180	0.197490664	0.352947728	0.450774901	0.439590503
210	0.235194932	0.494239542	0.582656432	0.570951526
240	0.280097575	0.692093207	0.75312205	0.741566623
270	0.333572882	0.969151528	0.973460158	0.963165928
300	0.397257519	1.357121664	1.258261764	1.250984843
330	0.473100617	1.900403762	1.626386714	1.6248115
360	0.563423431	2.661172211	2.102212606	2.11034724
390	0.670990378	3.726491011	2.717249105	2.740973629
420	0.799093653	5.21827757	3.512224537	3.56004751
450	0.951653984	7.307255193	4.539782965	4.62388187
480	1.133340631	10.23249104	5.867970329	6.005617479
510	1.349714295	14.32875547	7.584740514	7.800251458
540	1.607397307	20.06483392	9.803779747	10.13116853
570	1.914276312	28.09717573	12.67203501	13.15862397
600	2.279743647	39.3450196	16.37944501	17.09076147
630	2.714984802	55.09559332	21.17151812	22.19792345
660	3.233320767	77.15142689	27.36559019	28.83123765
690	3.850615728	108.036638	35.3718388	37.44675787
720	4.585762613	151.2857976	45.72044571	48.63681856
750	5.461261322	211.8484337	59.09670592	63.17075908
780	6.503907363	296.6554666	76.38640867	82.0478173
810	7.745611956	415.4123981	98.73449525	106.5658292
840	9.224378703	581.7100303	127.6208781	138.4104578
870	10.98546673	814.5798269	164.9584423	179.7710859
900	13.08277589	1140.671915	213.2197183	233.4913403
930	15.58049642	1597.304985	275.6006157	303.2645976
960	18.55507353	2236.737121	356.2320595	393.8879104
990	22.09754711	3132.146331	460.453544	511.5918153
1020	26.31633809	4386.005197	595.1667194	664.4686941
1050	31.34056677	6141.808064	769.2924258	863.029142
1080	37.32400465	8600.492838	994.3614405	1120.924592